Indicators of Global Climate Change 2024: annual update of key indicators of the state of the climate system and human influence

Piers M. Forster [1], Chris Smith [2,3], Tristram Walsh [4], William F. Lamb [1, 5], Robin Lamboll [6], Christophe Cassou [7, 8], Mathias Hauser [9], Zeke Hausfather [10, 11], June-Yi Lee [12, 13], Matthew D. Palmer [14, 15], Karina von Schuckmann [16], Aimée B.A. Slangen [17], Sophie Szopa [18], Blair Trewin [19], Jeongeun Yun [12], Nathan P. Gillett [20], Stuart Jenkins [4], H. Damon Matthews [21], Krishnan Raghavan [22], Aurélien Ribes [23], Joeri Rogelj [3, 6, 24], Debbie Rosen [1], Xuebin Zhang [25], Myles Allen [4, 26], Lara Aleluia Reis [27, 28], Robbie M. Andrew [29], Richard A. Betts [14, 30], Alex Borger [31], Jiddu A. Broersma [31], Samantha N. Burgess [32], Lijing Cheng [33], Pierre Friedlingstein [7, 30], Catia M. Domingues [34, 35], Marco Gambarini [27, 28], Thomas Gasser [3], Johannes Gütschow [36], Masayoshi Ishii [37], Christopher Kadow [38], John Kennedy [39], Rachel E. Killick [14], Paul B. Krummel [40], Aurélien Liné [8, 16, 41], Didier P. Monselesan [42], Colin Morice [14], Jens Mühle [43], Vaishali Naik [44], Glen P. Peters [29], Anna Pirani [45], Julia Pongratz [46, 47], Jan. C. Minx [1, 5], Matthew Rigby [48], Robert Rohde [10], Abhishek Savita [49, 50], Sonia I. Seneviratne [9], Peter Thorne [51], Christopher Wells [1], Luke M. Western [48], Guido R. van der Werf [52], Susan E. Wijffels [42, 53], Valérie Masson-Delmotte [18], Panmao Zhai [54]

1. Priestley Centre for Climate Futures, University of Leeds, Leeds, LS2 9JT, UK
2. Department of Water and Climate, Vrije Universiteit Brussel, Brussels, Belgium
3. International Institute for Applied Systems Analysis (IIASA), Vienna, Austria
4. Environmental Change Institute, University of Oxford, Oxford, UK
5. Potsdam Institute for Climate Impact Research (PIK), Member of the Leibniz Association, Potsdam, Germany
6. Centre for Environmental Policy, Imperial College London, London, UK
7. Laboratoire de Météorologie Dynamique/Institut Pierre-Simon Laplace, CNRS, Ecole Normale Supérieure/Université PSL, Paris, France
8. CECI, Université de Toulouse, CERFACS, CNRS, Toulouse, France
9. Institute for Atmospheric and Climate Science, Department of Environmental Systems Science, ETH Zurich, Zurich, Switzerland
10. Berkeley Earth, Berkeley, CA, USA
11. Stripe Inc., South San Francisco, CA, USA
12. Research Center for Climate Sciences, Pusan National University, Busan, Republic of Korea
13. Center for Climate Physics, Institute for Basic Science, Busan, Republic of Korea
14. Met Office Hadley Centre, Exeter, UK
15. School of Earth Sciences, University of Bristol, Bristol, UK
16. Mercator Ocean international, Toulouse, France

34   17. NIOZ Royal Netherlands Institute for Sea Research, Department of Estuarine and Delta Systems, Yerseke, the

35   Netherlands

36   18. Institut Pierre Simon Laplace, Laboratoire des Sciences du Climat et de l'Environnement (UMR 8212 CEA-CNRS-

37   UVSQ), Université Paris-Saclay, Gif-sur-Yvette, France

38   19. Bureau of Meteorology, Melbourne, Australia

39   20. Canadian Centre for Climate Modelling and Analysis, Environment and Climate Change Canada, Victoria, BC,

40   Canada

41   21. Concordia University, Montreal, Canada

42   22. Indian Institute of Tropical Meteorology, Pune, India

43   23. CNRM, Université de Toulouse, Météo France, CNRS, Toulouse, France

44   24. Grantham Institute for Climate Change and Environment, Imperial College London, United Kingdom

45   25. Pacific Climate Impacts Consortium, University of Victoria, Victoria, Canada

46   26. Atmospheric, Oceanic and Planetary Physics, Department of Physics, University of Oxford, UK

47   27. CMCC Foundation, Euro-Mediterranean Center on Climate Change, Lecce, Italy

48   28. RFF-CMCC, European Institute on Economics and the Environment, Milan, Italy

49   29. CICERO Center for International Climate Research, Oslo, Norway

50   30. Global Systems Institute, Science and Economy, University of Exeter, Exeter, UK

51   31. Climate Change Tracker, Data for Action Foundation, Amsterdam, the Netherlands

52   32. European Centre for Medium-Range Weather Forecasts, ECMWF, Reading, United Kingdom

53   33. State Key Laboratory of Earth System Numerical Modeling and Application, Institute of Atmospheric Physics,

54   Chinese Academy of Sciences, Beijing, China

55   34. Marine Physics and Ocean Climate, National Oceanography Centre, Southampton, UK

56   35. Environmental Business Unit, CSIRO, Hobart, Australia

57   36. Climate Resource, Melbourne, Australia

58   37. Meteorological Research Institute, Tsukuba, Japan

59   38. German Climate Computing Center, Hamburg, Germany (DKRZ)

60   39. No affiliation, Verdun, France

61   40. CSIRO Environment, Aspendale, Australia

62   41. Institut de Mécanique des Fluides de Toulouse, Université de Toulouse, INP, CNRS, Toulouse, France

63   42. CSIRO, Environment Research Unit, Climate Intelligence, Climate variability and hazards, Hobart, Tasmania,

64   Australia

65   43. Scripps Institution of Oceanography, University of California San Diego, La Jolla, CA, USA

66   44. NOAA Geophysical Fluid Dynamics Laboratory, Princeton, NJ, USA

67   45. Euro-Mediterranean Center on Climate Change (CMCC), Venice, Italy; Università Cà Foscari,Venice, Italy

68   46. Ludwig-Maximilians-Universität München, München, Germany

69   47. Max Planck Institute for Meteorology, Hamburg, Germany

70   48. School of Chemistry, University of Bristol, Bristol, United Kingdom

71   49. Centre for Atmospheric Sciences, Indian Institute of Technology Delhi, Delhi, India

72   50. Department of Atmospheric Sciences, Rosenstiel School of Marine, Atmospheric and Earth Science, Miami, USA

73   51. ICARUS Climate Research Centre, Maynooth University, Maynooth, Ireland

74   52. Wageningen University and Research, Wageningen, The Netherlands

75   53. Physical Oceanography, Woods Hole Oceanographic Institution, Woods Hole, Massachusetts, USA

76   54. Chinese Academy of Meteorological Sciences, Beijing, China

77

78   *Correspondence to*: Piers. M. Forster (p.m.forster@leeds.ac.uk)

79

80   **Abstract.**

81   In a rapidly changing climate, evidence-based decision-making benefits from up-to-date and timely information. Here

82   we compile monitoring datasets (published here, https://doi.org/10.5281/zenodo.15327155 Smith et al., 2025a) to

83   produce updated estimates for key indicators of the state of the climate system: net emissions of greenhouse gases and

84   short-lived climate forcers, greenhouse gas concentrations, radiative forcing, the Earth's energy imbalance, surface

85   temperature changes, warming attributed to human activities, the remaining carbon budget, and estimates of global

86   temperature extremes. This year, we additionally include indicators for sea-level rise and land precipitation change.

87   We follow methods as closely as possible to those used in the IPCC Sixth Assessment Report (AR6) Working Group

88   One (WGI) report.

89

90   The indicators show that human activities are increasing the Earth's energy imbalance and driving faster sea-level rise

91   compared to the AR6 assessment. For the 2015–2024 decade average, observed warming relative to 1850-1900 was

92   1.24 [1.11 to 1.35] °C, of which 1.23 [1.0 to 1.5] °C was human-induced. The 2024 observed record in global surface

93   temperature (1.52 °C best estimate) is well above the best estimate of human-caused warming (1.36°C). However, the

94   2024 observed warming can still be regarded as a typical year, considering the human induced warming level and the

95   state of internal variability associated with the phase of El Niño and Atlantic variability. Human-induced warming has

96   been increasing at a rate that is unprecedented in the instrumental record, reaching 0.27 [0.2 - 0.4] °C per decade over

97   2015-2024. This high rate of warming is caused by a combination of greenhouse gas emissions being at an all-time

98   high of 53.6 ± 5.2 GtCO$_2$e per year over the last decade (2014-2023), as well as reductions in the strength of aerosol

99   cooling. Despite this, there is evidence that the rate of increase in CO$_2$ emissions over the last decade has slowed

100   compared to the 2000s, and depending on societal choices, a continued series of these annual updates over the critical

101   2020s decade could track decreases or increases in the rate of the climatic changes presented here.

1 Introduction

IPCC AR6 provided an assessment of human influence on key indicators of the state of climate grounded in available data at the time of publication. The preparation for the next IPCC report, the Seventh Assessment Report (AR7), has started and the assessment is due in around 5 years. Given the speed of recent change, and the need for updated climate knowledge to inform evidence-based decision-making, the Indicators of Global Climate Change (IGCC) was initiated to provide policymakers with annual updates of the latest scientific understanding on the state of selected critical indicators of the climate system and where possible of the quantified human influence upon these.

This third annual update follows broadly the format of last year (Forster et al., 2024), focusing on indicators related to heating of the climate system, building from greenhouse gas emissions towards estimates of human-induced warming and the remaining carbon budget. Fig. 1 presents an overview of the aspects assessed and their interlinkages from cause (emissions) through effect (changes in physical indicators) to Climatic Impact-Drivers. It also provides a visual roadmap as to the structure of remaining sections in this paper to guide the reader.
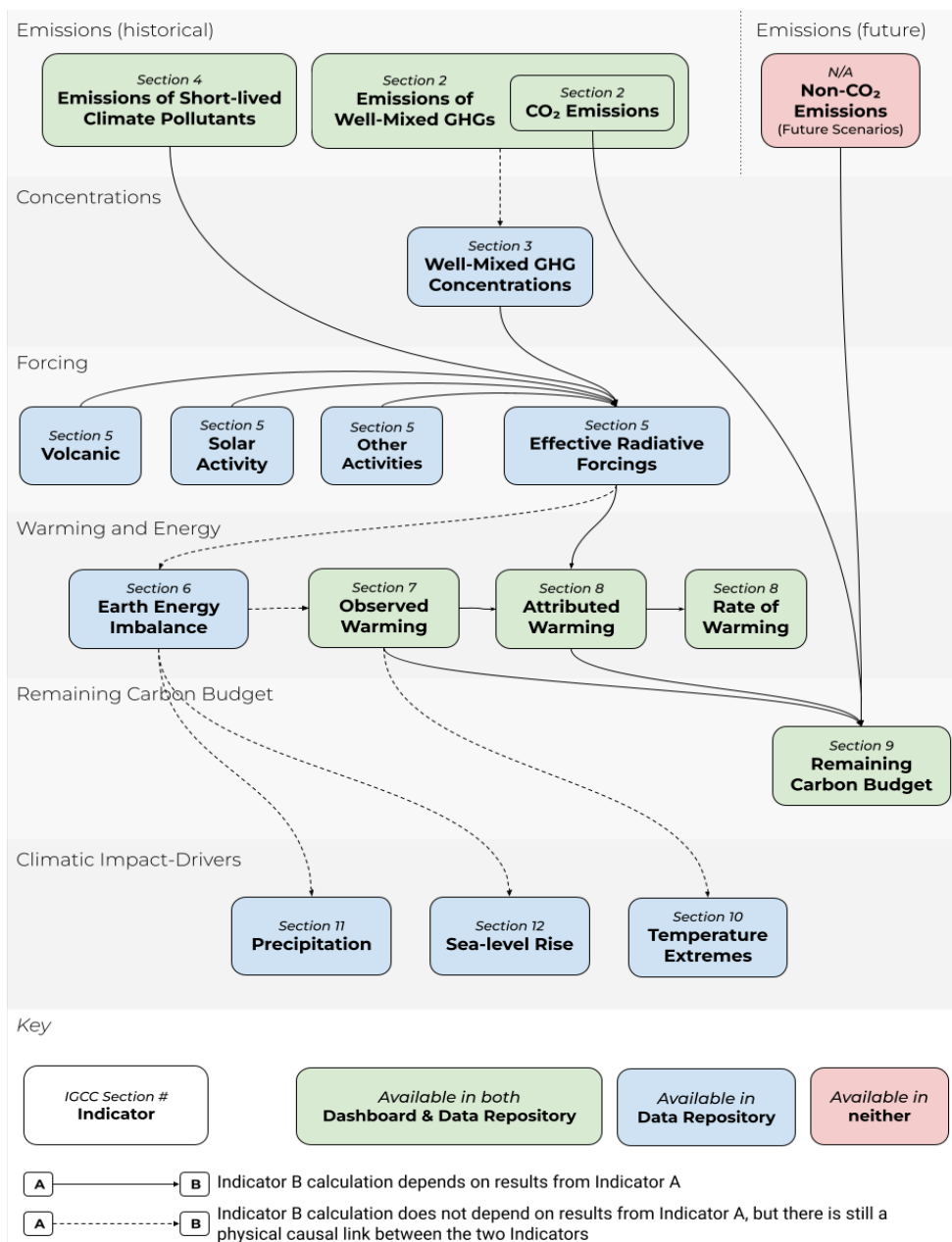
Figure 1 The flow chart of data production from emissions to human induced warming, the remaining carbon budget, and changes to Climatic Impact-Drivers, illustrating both the rationale and workflow within the paper production.

The update is based on methodologies assessed by the IPCC Sixth Assessment Report (AR6) of the physical science basis of climate change (Working Group One (WGI) report; IPCC, 2021a) as well as Chap. 2 of the WGIII report

120   (Dhakal et al., 2022) and is aligned with the efforts initiated in AR6 to implement FAIR (Findable, Accessible,
121   Interoperable, Reusable) principles for reproducibility and reusability (Pirani et al., 2022; Iturbide et al., 2022). IPCC
122   reports make a much wider assessment of the science and methodologies – we do not attempt to reproduce the
123   comprehensive nature of these IPCC assessments here. We also do not consider adopting fundamentally different
124   approaches to AR6. Rather, our aim is to rigorously track both climate system change and evolving methodological
125   improvements between IPCC report cycles, thereby increasing transparency and consistency in between successive
126   reports.

127

128   The update is organised as follows: greenhouse gas (GHG) emissions (Sect. 2), greenhouse gas concentrations (Sect.
129   3) and emissions of short-lived climate forcers (Sect. 4) are used to develop updated estimates of effective radiative
130   forcing (Sect. 5). The Earth energy imbalance (Sect. 6) and observations of global surface temperature change (Sect.
131   7) are key global indicators of a warming world. The contributions to global surface temperature change from human
132   and natural influences are formally attributed in Sect. 8, which tracks the level and rate of human-induced warming.
133   Sect. 9 updates the remaining carbon budget for policy-relevant temperature thresholds. Sect. 10 gives an example of
134   global-scale indicators associated with climate extremes of maximum land surface temperatures and Sect. 11 shows
135   land-surface precipitation trends traceable to AR6, a new addition to this year's update. Sect. 12 presents updated
136   estimates of global mean sea-level rise, also a new addition. Code and data availability are given in Sect. 13, and
137   conclusions are presented in Sect. 14. Data are available at https://doi.org/10.5281/zenodo.15327155 (Smith et al.,
138   2025a).

139

140   **2 Greenhouse gas emissions**

141   Historic GHG emissions from human activity were assessed in both AR6 WGI and WGIII. Chapter 5 of WGI assessed
142   CO_2 and CH_4 emissions in the context of the carbon cycle (Canadell et al., 2021). Chapter 2 of WGIII, published one
143   year later (Dhakal et al., 2022), assessed the sectoral sources of emissions and gave the most up-to-date understanding
144   of the current level of emissions. This section bases its methods and data on those employed in this WGIII chapter.

145   **2.1 Methods of estimating greenhouse gas emissions changes**

146   Like in AR6 WGIII, net GHG emissions in this paper refer to releases of GHGs from anthropogenic sources minus
147   removals by anthropogenic sinks, for the set of GHGs outlined in the United Nations Framework Convention on
148   Climate Change (UNFCCC). These include: CO_2 emissions from fossil fuels and industry (CO_2-FFI); net CO_2
149   emissions from land use, land-use change and forestry (CO_2-LULUCF); CH_4 emissions; N_2O emissions; and
150   fluorinated gas (F-gas) emissions comprising hydrofluorocarbons (HFCs), perfluorocarbons (PFCs), sulphur
151   hexafluoride (SF_6) and nitrogen trifluoride (NF_3) - hereafter the "UNFCCC F-gases".

152

153   Despite an extensive literature on GHG emissions, there remains important differences in reporting conventions and
154   system boundaries between assessments. These differences relate to three underlying issues: (1) emissions data sets
155   vary in their coverage of sources and sectors; (2) there are different approaches to determining the 'anthropogenic'
156   component of LULUCF emissions and removals; and (3) the Paris Agreement does not cover all relevant sources of
157   emissions (Lamb et al., 2025).

158

159   Concerning the first issue, there are several possible emissions datasets to draw from, each with varying coverage and
160   update schedules. Emissions data are gathered by countries and submitted to the UNFCCC in the form of national
161   inventory reports and common reporting tables. However, these "national inventories" are generally incomplete and
162   are not kept up to date for all countries. Emissions reporting therefore often relies on "third-party" datasets compiled
163   by research organisations, including: the Global Carbon Budget (GCB; Friedlingstein et al., 2024); the Emissions
164   Database for Global Atmospheric Research (EDGAR; Crippa et al., 2023); the Potsdam Real-time Integrated Model
165   for probabilistic Assessment of emissions Paths (PRIMAP-hist; Gütschow et al., 2016; Gütschow et al., 2025)[1]; the
166   Community Emissions Data System (CEDS; Hoesly et al., 2018; Hoesly and Smith, 2024); and the Global Fire
167   Emissions Database (GFED; van der Werf et al., 2017). As detailed below, for various reasons not all these datasets
168   were employed in this update.

169

170   Concerning the second issue, there are varying conventions used to quantify CO_2-LULUCF fluxes. These include the
171   use of bookkeeping models and aggregated national inventory reporting (Pongratz et al., 2021), which differ in terms
172   of their applied system boundaries and definitions, and in particular how they treat "indirect anthropogenic effects"
173   such as the influence of increased atmospheric CO_2 on vegetation growth. As such, the CO_2-LULUCF emissions
174   estimates generated using bookkeeping models versus national inventories are not directly comparable and differ by
175   about 7.5GtCO2yr-1 (2013-2022 average), but there are now methods to "translate" between these two approaches
176   (Friedlingstein et al., 2022; Grassi et al., 2023; Schwingshackl et al., 2022). Assessments also differ with respect to
177   biomass fire emissions and to what extent components of these are treated as anthropogenic (Lamb et al., 2025).

178

179   Finally, two categories of emissions are not directly covered by the Paris Agreement but might be considered
180   depending on the objectives of an assessment. These include the Ozone Depleting Substances (hereafter the "ODS F-
181   gases") comprising halons, chlorofluorocarbons (CFCs) and hydrochlorofluorocarbons (HCFCs). The ODS F-gases
182   were initially controlled under the Montreal Protocol and its amendments and are therefore not included in national
183   inventories submitted to the UNFCCC, nor in many third-party emissions datasets - in contrast to the UNFCCC F-
184   gases. Another important omission is the cement carbonation sink. To date this has also been excluded from national

---

[1] PRIMAP is a synthetic dataset that includes two time-series: PRIMAP Hist-TP, which is compiled from other underlying products such as EDGAR; and PRIMAP Hist-CR, which prioritises data from national inventories but gap-fills these where necessary.

185 reporting under the UNFCCC, but plans for a new chapter covering these removals in the IPCC Task Force on National

186 Greenhouse Gas Inventory Guidelines indicates a pathway for its eventual inclusion (IPCC, 2025).

187

188 The IPCC AR6 WGIII addressed these issues as follows. Total net GHG emissions were calculated as the sum of CO_2-

189 FFI, CH_4, N_2O and UNFCCC F-gases from EDGAR (version 6, with a fast-track methodology applied for the final

190 year of data - 2019), and net CO_2-LULUCF emissions from the GCB (the 2020 version; Friedlingstein et al., 2020).

191 Net CO_2-LULUCF emissions followed the GCB convention and were derived from the average of three bookkeeping

192 models (Hansis et al., 2015; Houghton and Nassikas, 2017; Gasser et al., 2020). "Indirect anthropogenic effects" on

193 the terrestrial carbon fluxes were therefore excluded from totals (i.e., they were treated as part of the natural land sink).

194 Further, the GCB methodology (and thus reporting in IPCC AR6 WGIII) includes CO_2 emissions from deforestation

195 and forest degradation fires, but excludes those from wildfires, which are classified as natural even if climate change

196 affects their intensity and frequency. Similarly, the EDGAR dataset used in AR6 includes some non-CO_2 biomass fire

197 emissions in the agricultural sector, but otherwise excludes those from wildfires. Sources not covered by inventories

198 or the Paris Agreement (ODS F-gases and cement carbonation) were also excluded. Together these choices ensured

199 consistency with the Integrated Assessment Model (IAM) benchmarks reported in WGIII and were closely focused

200 on direct anthropogenic emissions under the UNFCCC, reflecting the importance of human-driven technology and

201 policy options in shaping the future climate response.

202

203 The analysis presented here continues to provide an "WGIII update" estimate that tracks the same system boundary

204 and compilation of GHGs as in AR6 WGIII, albeit with some differences in the selected data sources. As in previous

205 years, we use GCB data for CO_2-FFI. We also continue to use GCB for CO_2-LULUCF, which has now been updated

206 to use the average of four (rather than three) bookkeeping models (BLUE by Hansis et al., 2015; H&C by Houghton

207 and Castanho, 2023; OSCAR by Gasser et al., 2020; LUCE by Qin et al., 2024). We use PRIMAP Hist-TP data for

208 CH_4 and N_2O, and inversions of atmospheric concentrations tracked by NOAA and AGAGE with best-estimate

209 lifetimes for UNFCCC F-gas emissions based on analysis in the subsequent Section 3 (Lan et al., 2025; Dutton et al.,

210 2024; Prinn et al., 2018). We follow the same approach for estimating uncertainties and CO_2-equivalent emissions as

211 in AR6, as described in the Supplement.

212

213 In addition to the WGIII update, we provide two further estimates that provide clarity and comparison to other

214 assessment approaches. This reflects the fact that other decision criteria for tracking emissions are possible. First, in

215 cases where assessments prioritise calculating the best estimate of fluxes to the atmosphere, it would be important to

216 include ODS F-gases, cement carbonation and all non-CO_2 biomass fire emissions, including those from wildfires.

217 Indeed, these are included in this article in subsequent assessments of concentration change (including compounds

218 formed in the atmosphere as ozone), effective radiative forcing, human-induced warming, carbon budgets and climate

219 impacts, in line with the WGI assessment. We therefore provide an "IPCC update + additional sources and sinks"

220 estimate that shows the change implied by including these three components in the global total. Second, the IPCC

Earth System
Open Access Science
Data Discussions

221   AR7 report outline foresees the tracking of "inventory-aligned" emissions that are consistent with national reporting.

222   Full alignment between emissions inventories and WGIII emissions consistent with IAM benchmarks is essential for

223   an accurate assessment and stocktake of the Nationally Determined Contributions (NDCs) and pathways to net-zero

224   emissions (Grassi et al., 2021; Gidden et al., 2023; Allen et al., 2025). We therefore provide an "Inventory-aligned"

225   estimate that follows the inventory approach to accounting for LULUCF emissions, while also integrating the latest

226   national inventory data from the Common Reporting Tables. The data sources associated with these additional

227   estimates are detailed in Table S1 in the Supplement.

228

229   We expect to see differences between the three estimates, most notably between the "WGIII update" and "Inventory-

230   aligned" estimates. As discussed above, these differ conceptually in their treatment of the LULUCF sector. However,

231   national inventory reporting can also differ from third-party datasets in terms of underlying methods: in some

232   countries, investments into statistical infrastructures have enabled the use of more precise emissions factors in

233   inventories to estimate fluxes according to local or national conditions, while in others this may not be the case. In

234   contrast, third-party datasets often use globally consistent emissions factors. Notably, the PRIMAP Hist-CR dataset,

235   which is here used to represent national inventories, has significantly lower total CH_4 emissions relative to other

236   datasets reported here, as well as the global atmospheric inversion estimates evaluated in this paper. A substantive

237   body of literature has found that, on average, national inventories tend to underestimate CH_4 compared to inversions

238   (Deng et al., 2022; Tibrewal et al., 2024; Janardanan et al., 2024; Scarpelli et al., 2022).

239   **2.2 Updated greenhouse gas emissions**

240   Updated GHG emission estimates following the WGIII assessment are presented in Fig. 2 and Table 1. Total global

241   GHG emissions were $55.1 \pm 5.1\,GtCO_2e$ in 2023. Of this total, CO_2-FFI contributed $37.8 \pm 3.0\,GtCO_2$, CO_2-LULUCF

242   contributed $3.6 \pm 2.5\,GtCO_2$, CH_4 contributed $9.2 \pm 2.7\,GtCO_2e$, N_2O contributed $2.9 \pm 1.7\,GtCO_2e$ and F-gas

243   emissions contributed $1.6 \pm 0.5\,GtCO_2e$.

244

245   Initial projections for 2024 indicate that CO_2 emissions from fossil fuels and industry increased to 38.2 ± 3.0, and CO_2

246   emissions from land-use change increased to $4.2 \pm 2.8\,GtCO_2$ (Friedlingstein et al., 2024; Deng et al., 2024). The

247   significant increase in land-use change emissions is connected to high emissions from tropical deforestation and

248   degradation fires in the aftermath of the El Niño with droughts in South America continuing since 2023. Synchronous

249   large fires occurred in North America, where the record-breaking Canadian fires of 2023 were followed by another

250   well above average year in 2024, but are attributable to climate variability and climate change, and not anthropogenic

251   land-use change (Friedlingstein et al., 2024).

252

253   Average annual GHG emissions for the decade 2014–2023 were $53.6 \pm 5.2\,GtCO_2e$. Average decadal GHG emissions

254   have increased steadily since the 1970s across all major groups of GHGs, driven primarily by increasing CO_2

255   emissions from fossil fuel and industry but also rising emissions of CH_4 and N_2O. Emissions of UNFCCC F-gases

Earth System
Science
Data

256 have grown more rapidly than other GHG, but from low levels. Both the magnitude and trend of CO_2 emissions from

257 land-use change remain highly uncertain, with the latest data indicating an average net flux between 4–5 $GtCO_2$ yr^{-1}

258 for the past few decades.

259

260 The fossil fuel share of global GHG emissions was approximately 70% in 2023 (GWP100 weighted), based on the

261 EDGAR v9 dataset (Crippa et al., 2023) and net land-use CO_2 emissions from the Global Carbon Budget

262 (Friedlingstein et al. 2024). The remaining share of non-fossil fuel emissions are mostly from land-use change,

263 agriculture, cement production, waste and F-gas emissions.

264

265 Different emissions assessment approaches are shown in Fig. 3. Increasing the scope of the WGIII update to include

266 ODS F-gases, cement carbonation, and CH_4 and N_2O from biomass burning results in emissions of 56.6 ± 5.2 GtCO2e

267 yr^{-1} in 2023, or a total change of $+1.5$ GtCO2e yr^{-1}. ODS F-gas emissions have declined substantially since the 1990s

268 under the Montreal Protocol and its amendments, reaching 1.4 GtCO2e yr^{-1} in 2023, with a stalling rate of reduction

269 in the past decade. The cement carbonation sink has steadily increased alongside cement production to reach -0.8

270 GtCO2e yr^{-1} in 2023. Biomass fire emissions have a more variable trend and 2023 was a relatively extreme year at 1

271 GtCO2e yr^{-1}, compared to an average of 0.7 GtCO2e yr^{-1} in the preceding decade.

272

273 Emissions according to national inventories were 47.1 ± 4.7 GtCO2e yr^{-1} in 2023, or 7.9 GtCO2e yr^{-1} lower than the

274 WGIII update (Fig. 3). The main reason is due to diverging estimates of net LULUCF emissions, which according to

275 inventory accounts were on average 7.5 $GtCO_2$ lower over the past decade (2014-2023). Additional differences result

276 from a lower estimate of Energy, Industrial Process, Agriculture and Waste emissions in inventories (-1.5 GtCO2e

277 yr^{-1}), particularly for CH_4 (-0.7 GtCO2e yr^{-1}).

278

279 Emerging literature, published after AR6 suggests that increases in atmospheric CH_4 concentrations may also be

280 driven by methane emissions from wetland changes resulting from climate change and variability (e.g. Basu et al.,

281 2022; Hardy et al., 2023; Peng et al., 2022; Nisbet et al., 2023; Zhang et al., 2023). There is also a possible effect from

282 CO_2 fertilisation (Feron et al., 2024; Hu et al., 2023). The latest global methane budget estimates indirect

283 anthropogenic CH_4 fluxes from wetlands and freshwater bodies of approximately 2.4 GtCO2e yr^{-1} (Saunois et al.,

284 2024). Such emissions are not captured in the WGIII estimate here as they are not a direct emission from human

285 activity, but rather a feedback induced by a changing climate, yet they will contribute to GHG concentration rise,

286 forcing and energy budget changes discussed in the next sections. They will become more important to properly

287 account for in future years. Note that these indirect CH_4 emissions are not used to determine the effective radiative

288 forcing in Sect. 5.

289
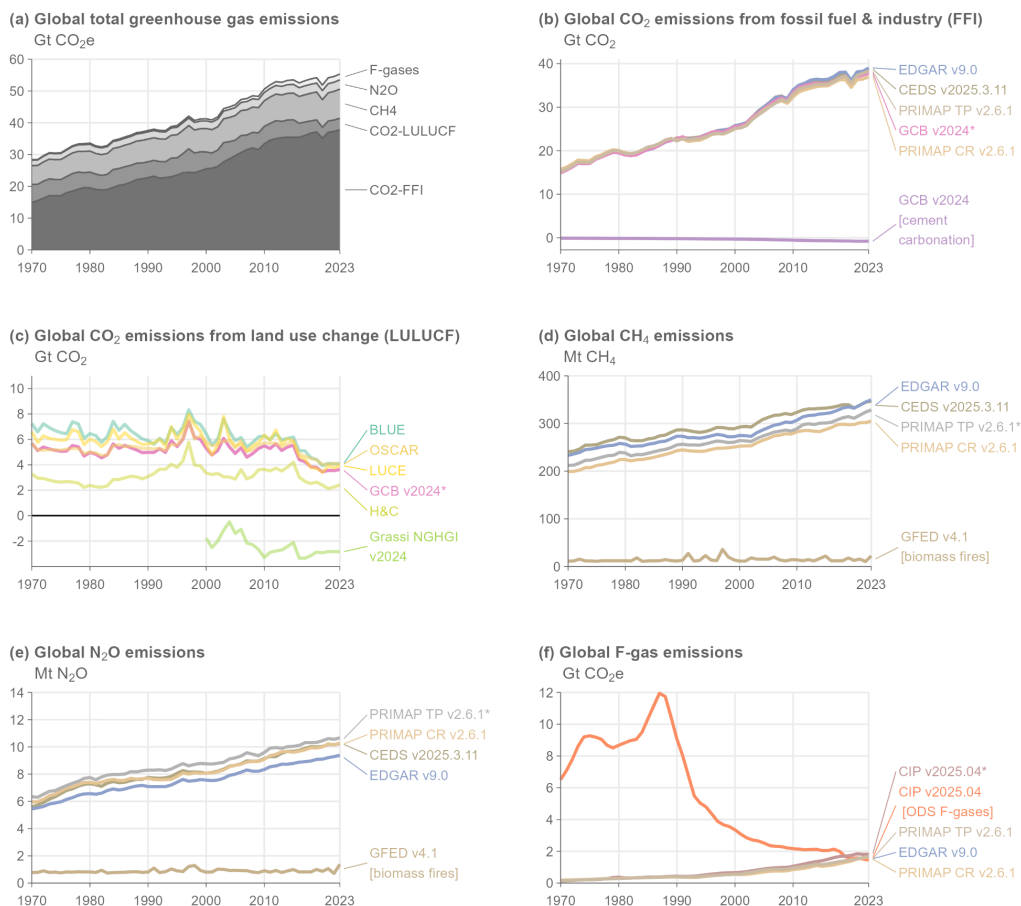
Figure 2 Annual global anthropogenic GHG emissions by source, 1970–2023. Refer to Sect. 2.1 and Table S1 for a list of datasets. Datasets with an asterisk (*) indicate the sources used to compile global total greenhouse gas emissions following the WGIII assessment in (a). CO₂-equivalent emissions in (a) and (f) are calculated using GWP100 from the AR6 WGI Chap. 7 (Forster et al., 2021). F-gas emissions in (a) comprise only UNFCCC F-gas emissions (see Sect. 2.1 for a list of species). F-gas emissions in (f) refer to UNFCCC F-gases, except for "CIP v2024.04 [ODS F-gases]". Some of the major depicted differences between datasets (e.g. between GCB v2024 and Grassi NGHGI v2024 in panel c) are due to varying system boundaries, rather than underlying uncertainties in activity levels or emissions factors.

Earth System
Science
Data

299 **Table 1 Global anthropogenic greenhouse gas emissions by source and decade following the WGIII assessment. All numbers**
300 **refer to decadal averages, except for annual estimates in 2023 and 2024. CO_2-equivalent emissions are calculated using**
301 **GWP100 from AR6 WGI Chap. 7 (Forster et al., 2021). Projections of non-CO_2 GHG emissions in 2024 remain unavailable**
302 **at the time of publication. Uncertainties are ±8 % for CO_2-FFI, ±70 % for CO_2-LULUCF, ±30 % for CH_4 and F-gases, and**
303 **±60 % for N_2O, corresponding to a 90 % confidence interval.**

| Units: $GtCO_2e$	1970-1979	1980-1989	1990-1999	2000-2009	2010-2019	2014-2023	2023	2024 (projection)
GHG	30.9±4.5	34.6±4.6	39.3±5.1	45.1±5.1	52.9±5.4	53.6±5.2	55.1±5.1	
CO_2-FFI	17.3±1.4	20.3±1.6	23.6±1.9	28.9±2.3	35.4±2.8	36.3±2.9	37.8±3.0	38.2±3.0
CO_2-LULUCF	5.2±3.7	5.1±3.6	5.7±4.0	5.2±3.6	4.9±3.4	4.1±2.9	3.6±2.5	4.2±2.8
CH_4	6.3±1.9	6.7±2	7.2±2.2	7.7±2.3	8.4±2.5	8.7±2.6	9.2±2.7	
N_2O	1.9±1.1	2.2±1.3	2.3±1.4	2.5±1.5	2.7±1.6	2.8±1.7	2.9±1.7	
UNFCCC F-gases	0.2±0.01	0.4±0.1	0.5±0.2	0.8±0.3	1.4±0.4	1.6±0.5	1.6±0.5	

304
305
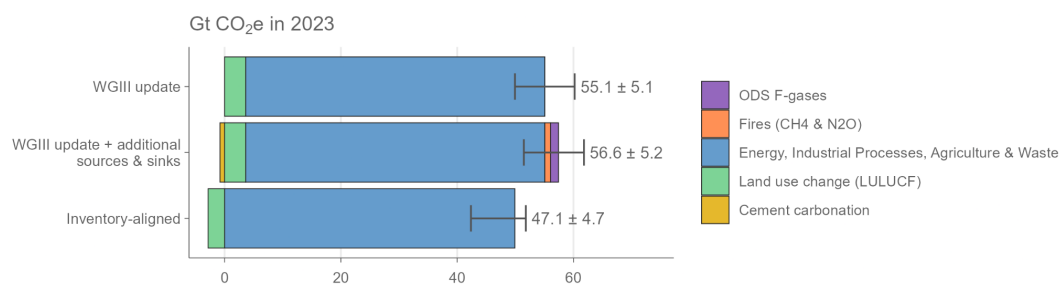
306
307 **Figure 3 Annual global anthropogenic greenhouse gas emissions by assessment convention in 2023. Refer to Table 1 for a**
308 **list of underlying datasets. Differences between conventions are primarily due to differences in system boundaries (Lamb**
309 **et al., 2025). Uncertainties are ±8 % for CO_2-FFI, ±70 % for CO_2-LULUCF, ±30 % for CH_4 and F-gases, and ±60 % for**
310 **N_2O, corresponding to a 90 % confidence interval.**

Earth System
Open Access
Science
Data
Discussions

3 Well-mixed greenhouse gas concentrations

As in Forster et al. (2024), we report best-estimate global mean concentrations for 52 well-mixed GHGs. These concentrations are updated to 2024. CO_2 mixing ratios were taken from the NOAA Global Monitoring Laboratory (GML) and are updated here through 2024 (Lan et al., 2025a). As in Forster et al. (2023, 2024), CO_2 is reported on the WMO-CO_2-X2019 scale, which differs from the WMO-CO_2-X2007 scale used in AR6 with WMO-CO_2-X2019 being around 0.18 ppm higher than WMO-CO_2-X2007 in recent years. For consistency with WMO-CO_2-X2019, the AR6 CO_2 concentrations that make up the 1750 to 1978 period in the IGCC dataset (before recent NOAA updates) have been converted to the WMO-CO_2-X2019 scale. Other GHG records were compiled from NOAA and AGAGE global networks or extrapolated from literature. An average of NOAA and AGAGE data, updated through 2024, were used for N_2O, CH_4, CFC-11, CFC-12, CCl_4, HCFC-22, HFC-134a, and HFC-125 (Lan et al., 2025; Dutton et al., 2024; Prinn et al., 2018), which, along with CO_2, account for over 97% of the ERF from well-mixed GHGs. Several other species also use means from the NOAA and AGAGE networks, where the NOAA data is updated to 2024 from the values given in the BAMS State of the Climate Report (Dunn et al., 2024) and AGAGE data up until 2022 is available; for 2023 and 2024, an offset to the NOAA data was applied which was equal to the mean difference between the NOAA and AGAGE datasets over the recent past. In cases where no updated information is available, global estimates were extrapolated from Vimont et al. (2022), Western et al. (2023, 2024), or other literature and scaled to be consistent with those reported in AR6. Some extrapolations are based on data from the mid-2010s (Droste et al., 2020; Laube et al., 2014; Simmonds et al., 2017; Vollmer et al., 2018), but have an imperceptible effect on the total ERF assessed in Sect. 5, and are included to maintain consistency with AR6. Mixing ratio uncertainties for 2024 are assumed to be like 2019, and we adopt the same uncertainties as assessed in AR6 WGI.

Fig. 4 shows recent GHG concentrations and their changes. Table S2 in the Supplement shows specific updated concentrations for all the GHGs considered. The global surface mean concentrations of CO_2, CH_4 and N_2O in 2024 were 422.8 [±0.4] parts per million (ppm), 1929.7 [±3.3] parts per billion (ppb) and 337.9 [±0.4] ppb, respectively. Concentrations of all three major GHGs have increased since 2019, with CO_2 increasing by 12.7 ppm, CH_4 by 63.3 ppb, and N_2O by 5.8 ppb. Increases since 2019 are consistent with those from the CSIRO network (Francey et al., 1999), which are 13.0 ppm, 61.9 ppb, and 6.0 ppb for CO_2, CH_4, and N_2O, respectively. With few exceptions, concentrations of ozone-depleting substances, such as CFC-11 and CFC-12, continue to decline, while those of replacement compounds (HFCs) have increased. HFC-134a, for example, has increased 25% since 2019 from 107.6 to 134.7 parts per trillion (ppt). Aggregated across all gases, PFCs have increased from 109.7 to an estimated 117.4 ppt CF_4-eq from 2019 to 2024, HFCs from 237 to 312 ppt HFC-134a-eq, while ozone depleting gases have declined from 1032 to 996 ppt CFC-12-eq. Mixing ratio equivalents are determined by the radiative efficiencies of each GHG from Hodnebrog et al. (2020).
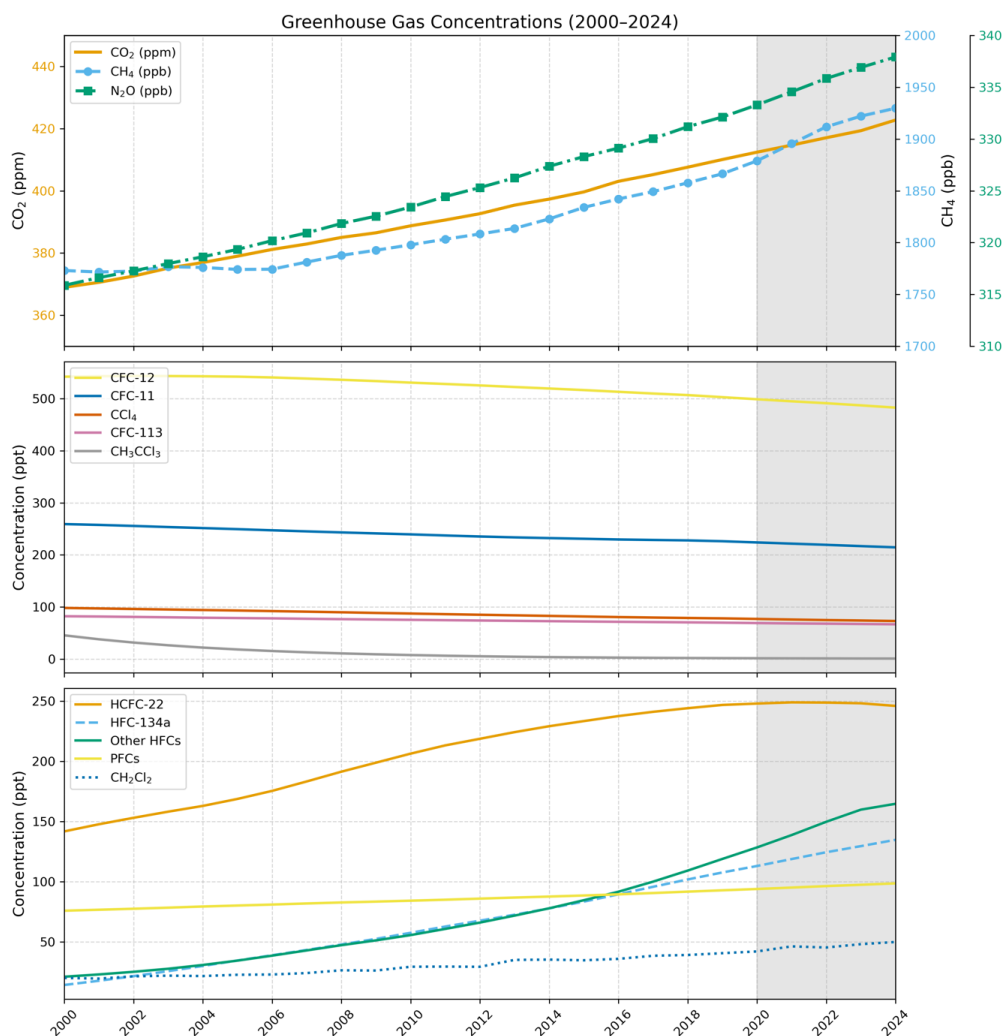
Figure 4 Atmospheric concentrations of a set of well mixed greenhouse gases over 2000-2024. The grey shaded region represents continuing changes since AR6. Note the different vertical scales.

Ozone and other non-methane SLCFs are not well-mixed in the atmosphere and are thus discussed separately (in Section 4). For this reason, the warming impact of ozone, the third most important GHG (in terms of current contribution to warming) is not included in the contribution of well-mixed GHGs to observed warming, consistently with AR6. Note that change in methane concentration affects ozone, but this indirect effect is not accounted for in the estimate of the warming due to the evolution of in well mixed GHG concentrations.

4 Non-methane short-lived climate forcers

Chapter 6 of WGI assessed emissions in the context of understanding the climate and air quality impacts of SLCFs (Szopa et al., 2021). Methane is a SLCF but also a well mixed GHG and is discussed in Sections 2 and 3. Trends in SLCFs emissions are spatially heterogeneous (Szopa et al., 2021), with strong shifts in the locations of reductions and increases over the decade 2010–2019 (Hodnebrog et al., 2024). Concentrations of non-methane SLCFs are heterogeneously distributed in the atmosphere and the observation networks are too sparse to report globally averaged concentrations. Typically, a combination of satellite data, where available, and global models and reanalysis are relied upon for producing global-scale distributions. In the case of models, production of near-real time information relies upon the availability of near-real time updates to SLCF emissions which are still challenging. Little information, whether from observations from local monitoring networks, satellite data or from global model reanalysis, is released in near real time.

In addition to GHG emissions, we provide an update of anthropogenic emissions of non-methane SLCFs (SO_2, black carbon (BC), organic carbon (OC), NOx, volatile organic compounds (VOCs), CO and NH_3). Data are presented in Table 2 and the evolution of SLCF emission estimates from the AR6 to this study is presented in Sect. S4 of the Supplement. Consistency between emission trends and concentrations is considered whenever feasible. HFCs, whatever their lifetimes, were considered in Sect. 2.2.

Sectoral emissions of SLCFs are derived from two sources: CEDS, which was used in the AR6 and in CMIP6 to assess historical evolution of atmospheric composition and that has been updated since then, and the Copernicus Atmosphere Monitoring Service (CAMS). The most recent release of the CEDS anthropogenic emissions dataset (Hoesly et al., 2025) covers the 1750-2023 period (Hoesly et al., 2018; Hoesly and Smith, 2024). Since 2023, CAMS has released regular updates of their global emission dataset (Soulie et al., 2023). For the year 2024, we apply, for each compound, the trend in emission from the CAMS dataset to the 2023 CEDS emission. The CAMS dataset is essentially based on the EDGARv6/v7 emissions as well as on CEDS, so CEDS and CAMS are not entirely independent. The temporal extension is based on evolution of drivers of emissions (energy consumption, production rates) and trends in technologies that affect the emissions factors (e.g. fleet renewal and abatement systems) (Denier van der Gon et al., 2023).

The CAMS v6.2 emission dataset (ECCAD, 2025) indicates a decrease in global anthropogenic emissions of the primary SLCFs (NOx, CO, NMVOCs, SO_2, BC and OC) since the COVID hiatus in emissions, except for NH_3, whose emissions are steadily increasing. SLCF emissions from biomass burning are taken from GFED (van der Werf et al., 2017) with small fires (GFED4.1s) updated to 2024 (following AR6 WGIII (Dhakal et al., 2022)). Estimates from GFED for 2017 to 2024 are provisional and will be updated with GFED5 in future datasets which will provide substantially higher emissions for most species. The estimate of global carbon emissions due to wildfires in 2024 is slightly lower than in 2023 (both were higher than average fire years). These lower overall

390   carbon emissions in 2024 hide an increase in CO_2 emissions (accompanied by an increase in NOx emissions) but a

391   decrease in CH_4 and CO emissions accompanied by a decrease in carbonaceous aerosols and NMVOC emissions.

392

393   The decrease of global NOx emissions, despite very heterogeneous regional trends (Szopa et al., 2021), is confirmed

394   by global NO_2 satellite observations from OMI (tropospheric NO_2 column from OMI visualised through the

395   Giovanni system, Acker and Leptoukh, 2007). The trends in global CO concentration are less clear. Surface data

396   from MOPITT and AIRS show a slight increase over the last three years. CO does not result solely from CO

397   emissions but also from VOC including methane oxidation which can explain differences in trends between

398   emissions and concentrations.

399

400   Overall, the trends in emissions were similar (see Supplement Sect. S4) over the 2020-23 period in the most recent

401   CEDS dataset to our previous estimate (Forster et al., 2024) but with a lower post COVID rebound for NOx and SO_2.

402   Regarding SO_2, the CEDS datasets (v2024_04_01 used in Forster et al., 2024 and v2025_03_18 used here) account

403   for the introduction of strict fuel sulphur controls brought in by the International Maritime Organization in January

404   2020. Total SO_2 emissions in 2019 were 80.9 $TgSO_2$ (Table 2). The SO_2 emissions from international shipping

405   declined by 8.4 $TgSO_2$ from 10.4 $TgSO_2$ in 2019 to 2.0 $TgSO_2$ in 2020, which is close to the expected 8.5 $TgSO_2$

406   reduction estimated by the International Maritime Organization. This decrease was estimated at 7.4 $TgSO_2$ in the

407   previous CEDS version used in Forster et al. (2024). More generally, the reduction pace of the global SO_2 emission

408   over the last ten years corresponds to that of the first ten years of the SSP scenarios assuming strong air pollution

409   control (SSP1 and SSP5).

410

411   Using our combined estimate of GFED, and CEDS (with a 2024 extrapolation based on CAMS), emissions of all

412   SLCFs were reduced in 2022 relative to 2019, but rebounded in 2023 and then slightly decreased in 2024 (relative to

413   2023) for all compounds except NOx whose increase is partly driven by increased emissions from biomass burning

414   (Table 2 and Supplement Sect. S4). 2023 was a record year for emissions of organic carbon (driven again by a very

415   active biomass burning season) and ammonia (driven by a steady background increase in agricultural sources, plus a

416   contribution from biomass burning). Fires can be worsened by climate change, because of increased fire prone weather

417   conditions (Burton et al., 2024). Strictly speaking, such fires should be considered as feedbacks and not be included

418   in anthropogenic forcings. However, we choose to include fires in our tracking, as historical biomass burning

419   emissions inventories have previously been consistently treated as an anthropogenic forcing (for example in CMIP6),

420   though this assumption may need to be revisited in the future (see also discussion in Sect. 5). This differs from the

421   treatment of accounting for CO_2 and CH_4 emissions at present (Sect. 2.2), where we do not include natural emissions

422   in the inventories. As described in Sect. 5, this treatment of all biomass burning emissions as a forcing has implications

423   for several categories of anthropogenic radiative forcing.

424

425 **Table 2 Emissions of the major SLCFs in 1750, 2019, and 2024 from a combination of CEDS and GFED. Emissions of**
426 **SO_2+SO_4 use SO_2 molecular weights. Emissions of NO_x use NO_2 molecular weights. VOCs are for the total mass.**

427

Compound	SLCF emissions (Tg yr^{-1})				
	1750	2019 (WGI for ERF estimates)	2019 (updated)	2023 (updated)	2024 (updated)
Sulphur dioxide (SO_2) + sulfate (SO_4^{2-})	2.8	84.2	80.9	72.7	71.2
Black carbon (BC)	2.1	7.5	7.3	7.6	7.5
Organic carbon (OC)	15.5	34.2	33.0	41.0	36.1
Ammonia (NH_3)	6.6	67.6	66.3	72.7	70.6
Oxides of nitrogen (NO_x)	19.4	141.7	133.6	128.4	130.4
Volatile organic compounds (VOCs)	60.9	217.3	204.8	224.1	212.7
Carbon monoxide (CO)	348.4	853.8	816.1	896.0	845.3

428
429

430 Uncertainties associated with these emission estimates are difficult to quantify. From the non-biomass-burning sectors
431 they are estimated to be smallest for SO_2 (±14 %), largest for black carbon (BC) (a factor of 2) and intermediate for
432 other species (Smith et al., 2011; Bond et al., 2013; Hoesly et al., 2018). Relative uncertainties are also likely to
433 increase both backwards in time (Hoesly et al., 2018) and again in the most recent years. Future updates of CEDS are
434 expected to include uncertainties (Hoesly et al., 2018).

435

436 **5 Effective radiative forcing (ERF)**

437 ERFs were principally assessed in Chap. 7 of AR6 WGI (Forster et al., 2021), which focussed on assessing ERF from
438 changes in atmospheric concentrations; it also supported estimates of ERF in Chap. 6 that attributed forcing to specific

439   precursor emissions (Szopa et al., 2021) and generated the time history of ERF shown in AR6 WGI Fig. 2.10 and

440   discussed in Chap. 2 (Gulev et al., 2021).

441

442   The ERF calculation follows the methodology used in AR6 WGI (Smith et al., 2021) as updated by Forster et al.

443   (2024) and described in the Supplement Sect. S5). One methodological update is incorporated in IGCC 2024 for the

444   ERF from land use surface reflection and irrigation (Supplement Sect. S5.4). For each category of forcing, a 100,000-

445   member probabilistic Monte Carlo ensemble is sampled to span the assessed uncertainty range in each forcing.

446   Uncertainties account for systematic, structured random and random components. All uncertainties are reported as

447   5 %–95 % ranges and provided in square brackets. The methods are all detailed in the Supplement, Sect. S5.

448

449   The summary results for the anthropogenic constituents of ERF and solar irradiance in 2024 relative to 1750 are shown

450   in Fig. 5a. In Table 3 these are summarised alongside the equivalent ERFs from AR6 (1750–2019) and last year's

451   Climate Indicators update (1750-2023). Fig. 5b shows the time evolution of ERF from 1750 to 2024.

452

453   **Table 3 Contributions to anthropogenic effective radiative forcing (ERF) for 1750–2024 assessed in this section. Data is for**

454   **single year estimates unless specified. All values are in watts per square metre (W m^{-2}), and 5 %–95 % ranges are in square**

455   **brackets. As a comparison, the equivalent assessments from AR6 (1750–2019) and last year's Climate Indicators (1750-**

456   **2023) are shown. Solar ERF is included and unchanged from AR6, based on the most recent solar cycle (2009–2019), thus**

457   **differing from the single-year estimate in Fig. 5a. Volcanic ERF is excluded due to the sporadic nature of eruptions.**

Forcer	1750-2019 [W m^{-2}] (AR6)	1750-2023 [W m^{-2}] (Forster et al., 2024)	1750-2024 [W m^{-2}]	Reason for change since last year
CO_2	2.16 [1.90 to 2.41]	2.28 [2.01 to 2.56]	2.33 [2.05 to 2.61]	Increases in GHG concentrations resulting from increases in emissions
CH_4	0.54 [0.43 to 0.65]	0.56 [0.45 to 0.68]	0.57 [0.45 to 0.68]	
N_2O	0.21 [0.18 to 0.24]	0.22 [0.19 to 0.26]	0.23 [0.20 to 0.26]	
Halogenated GHGs	0.41 [0.33 to 0.49]	0.41 [0.33 to 0.49]	0.41 [0.33 to 0.49]	
Ozone	0.47 [0.24 to 0.71]	0.51 [0.25 to 0.76]	0.50 [0.25 to 0.75]	
Stratospheric water vapour	0.05 [0.00 to 0.10]	0.05 [0.00 to 0.10]	0.05 [0.00 to 0.11]	
Aerosol-radiation interactions	-0.22 [-0.47 to +0.04]	-0.26 [-0.50 to -0.03]	-0.22 [-0.44 to +0.01]	Decrease in most aerosol and aerosol precursor emissions (Table 2)
Aerosol-cloud interactions	-0.84 [-1.45 to -0.25]	-0.91 [-1.80 to -0.27]	-0.85 [-1.65 to -0.25]	

Land use (surface albedo changes and effects of irrigation)	-0.20 [-0.30 to -0.10]	-0.20 [-0.31 to -0.10]	-0.19 [-0.30 to -0.05]	Separation of albedo and irrigation components; updated data source and methodology
Light-absorbing particles on snow and ice	0.08 [0.00 to 0.18]	0.08 [0.00 to 0.17]	0.08 [0.00 to 0.19]	
Contrails and contrail-induced cirrus	0.06 [0.02 to 0.10]	0.05 [0.02 to 0.09]	0.06 [0.02 to 0.10]	
Total anthropogenic	2.72 [1.96 to 3.48]	2.79 [1.78 to 3.61]	2.97 [2.05 to 3.76]	Increasing positive GHG forcing and decreasing negative aerosol forcing
Solar irradiance	0.01 [-0.06 to 0.08]	0.01 [-0.06 to 0.08]	0.01 [-0.06 to 0.08]	

458

459
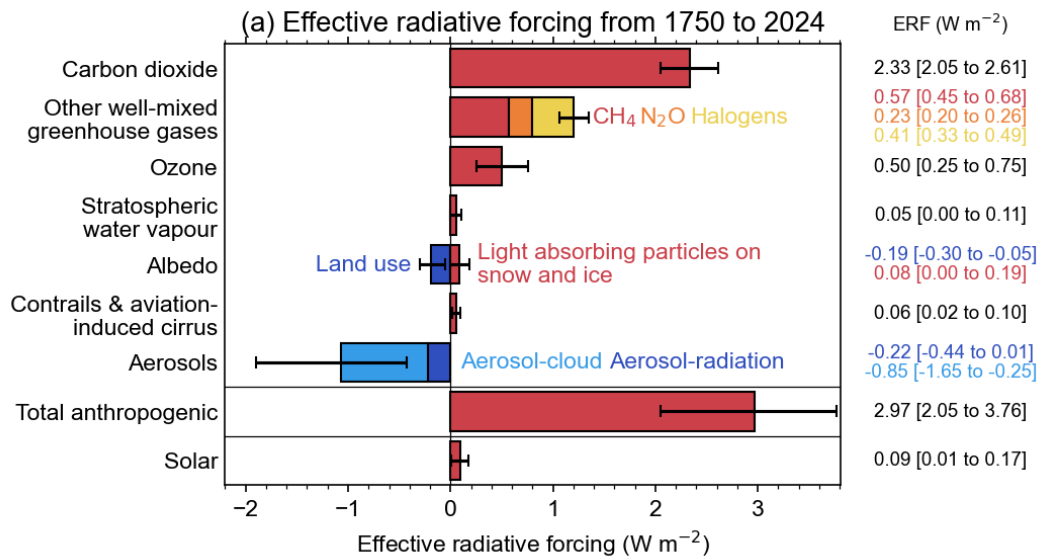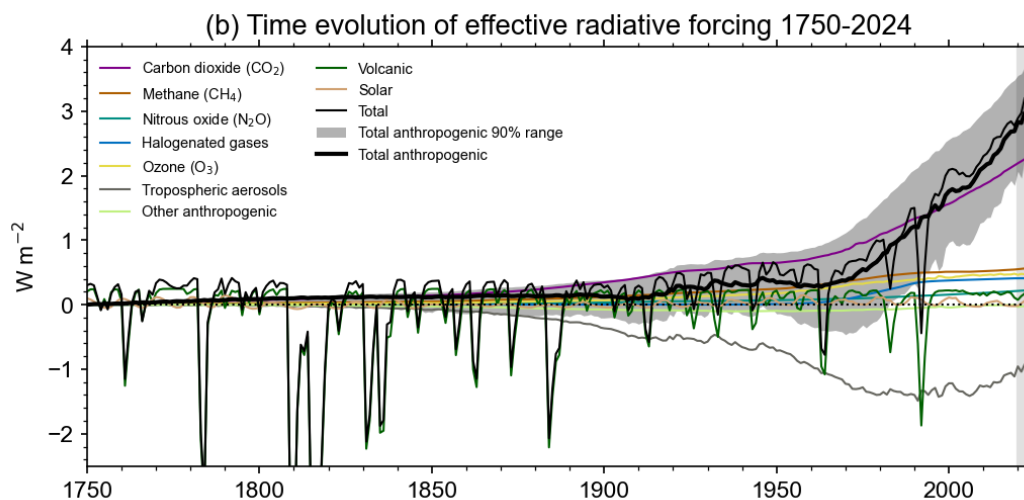
Figure 5 Effective radiative forcing (ERF) from 1750–2024. (a) 1750–2024 change in ERF, showing best estimates (bars) and 5 %–95 % uncertainty ranges (lines) from major anthropogenic components to ERF, total anthropogenic ERF and solar forcing. Note that solar forcing in 2024 is a single-year estimate and hence differs from Table 3. (b) Time evolution of ERF from 1750 to 2024. Best estimates from major anthropogenic categories are shown along with solar and volcanic forcing (thin coloured lines), total (thin black line), and anthropogenic total (thick black line). The 5 %–95 % uncertainty in the anthropogenic forcing is shown by grey shading.

Total anthropogenic ERF has increased to 2.97 [2.05 to 3.76] $W\,m^{-2}$ in 2024 relative to 1750, compared to 2.72 [1.96 to 3.48] $W\,m^{-2}$ for 2019 relative to 1750 in AR6. The ERF has increased considerably from the 2023 estimate of 2.79 [1.79 to 3.61] $W\,m^{-2}$. 2023 was a year associated with high biomass burning aerosol which resulted in a stronger negative aerosol forcing than recent trends. Biomass burning was also high in 2024, but lower than 2023 levels. Sulphur emissions from shipping have declined since 2020, weakening the aerosol ERF and adding around +0.1 $W\,m^{-2}$ over 2020 to 2024 (see Sect. 7.2 and Supplement Sects. S5 and S7). The approach of including all biomass burning aerosols is consistent with reporting ERF based on concentration increase of GHGs independent of whether CO_2 and CH_4 are caused by anthropogenic emissions or a smaller part is caused by any feedbacks such as from biomass burning fires or wetlands. Changes in mineral dust and sea salt are not easily relatable to human activity and are not included in the ERF of aerosols.

The ERF from well-mixed GHGs is 3.54 [3.22 to 3.85] $W\,m^{-2}$ for 1750–2024, of which 2.33 $W\,m^{-2}$ is from CO_2, 0.57 $W\,m^{-2}$ from CH_4, 0.23 $W\,m^{-2}$ from N_2O and 0.41 $W\,m^{-2}$ from halogenated gases. This is an increase of around 7% from 3.32 [3.03 to 3.61] $W\,m^{-2}$ for 1750–2019 in AR6. ERFs from CO_2, CH_4 and N_2O have all increased since the AR6 WG1 assessment for 1750–2019, owing to increases in atmospheric concentrations.

20

The total aerosol ERF (sum of the ERF from aerosol–radiation interactions (ERFari) and aerosol–cloud interactions (ERFaci)) for 1750–2024 is -1.07 [-1.90 to -0.43] W m^{-2} compared to -1.18 [-2.10 to -0.49] W m^{-2} for 1750–2023 (Forster et al., 2024) and -1.06 [-1.71 to -0.41] W m^{-2} assessed for 1750–2019 in AR6 WGI. Attributing year-to-year trends to aerosol forcing is problematic due to the variability in biomass burning emissions. Increasing biomass burning emissions since AR6 have been mostly offset by a decrease in emissions from energy and industrial sectors, leading to best estimates of ERFari and ERFaci that are virtually unchanged from the 1750–2019 AR6 assessment to the 1750–2024 determination here (Table 3).

Ozone ERF is determined to be 0.50 [0.25 to 0.75] W m^{-2} for 1750–2024, slightly higher than the AR6 assessment of 0.47 [0.24 to 0.71] W m^{-2} for 1750–2019. This is due to the increase in emissions of some of its precursors (CO, VOC, CH_4), but this result is highly uncertain since consolidated ozone trends are not yet released. Stratospheric water vapour from methane oxidation is unchanged (to two decimal places) since AR6. ERF from light-absorbing particles on snow and ice being 0.08 [0.00 to 0.19] W m^{-2} for 1750–2024, like AR6. We determine from provisional data that aviation activity in 2024 has returned to pre-COVID levels (IATA, 2024). Therefore, ERF from contrails and contrail-induced cirrus is the same as in AR6, at 0.06 [0.02 to 0.10] W m^{-2} in 2024. The methodology to determine land-use ERF has been updated (Sect. S5.4) but this forcing has a similar best estimate to 2023 and AR6, with a wider uncertainty range that accounts for the separate assessment of irrigation forcing.

The headline assessment of solar ERF has not been re-assessed, at 0.01 [-0.06 to $+0.08$] W m^{-2} from pre-industrial to the 2009–2019 solar cycle mean (Table 3). Separate to the assessment of solar forcing over complete solar cycles, we provide a single-year solar ERF for 2024 of $+0.09$ [$+0.01$ to $+0.17$] W m^{-2} (Fig. 5a). This is higher than the single-year estimate of solar ERF for 2019 (a solar minimum) of -0.02 [-0.08 to 0.06] W m^{-2}.

Volcanic ERF is included in the overall time series (Fig. 5b) but following IPCC convention we do not provide a single-year estimate for 2024 given the sporadic nature of volcanoes. Alongside the time series of stratospheric aerosol optical depth derived from proxies and satellite products, for 2022–2024 we include the stratospheric water vapour contribution from the Hunga Tonga-Hunga Ha'apai (HTHH) eruption derived from Microwave Limb Sounder (MLS) data. We estimate a net positive (positive forcing from stratospheric water vapour more than outweighing negative forcing from stratospheric aerosols) forcing through 2024, though note that other studies find the net HTHH forcing to be negative (Gupta et al., 2025) or close to zero (Schoeberl et al., 2024).

6 Earth energy imbalance (EEI)

EEI, assessed in Chap. 7 of AR6 WGI (Forster et al., 2021), provides a measure of accumulated surplus energy (heating) in the climate system, and is hence an essential indicator to monitor the current and future status of global

518   warming. It represents the difference between the radiative forcing acting to warm the climate, and Earth's radiative

519   response, which acts to oppose this warming. Under stable climate conditions, i.e., in the absence of anthropogenic

520   climate forcing, this difference would be balanced over interdecadal time scales. Since at least 1970 there has been a

521   persistent imbalance in the energy flows that has led to excess energy being absorbed by the climate system (Forster

522   et al., 2021). On annual and longer timescales, the global Earth heat inventory changes associated with EEI are

523   dominated by the changes in global ocean heat content (OHC), which accounts for about 90 % of global heating since

524   the 1970s (Forster et al., 2021). This planetary heating results in changes in all components of the Earth system such

525   as sea-level rise, ocean warming, ice loss, rises in temperature and water vapor in the atmosphere, changes in ocean

526   and atmospheric circulation, continental warming and permafrost thawing (e.g. Cheng et al., 2022; von Schuckmann

527   et al., 2023a), with adverse impacts for ecosystems and human systems (Douville et al., 2021; IPCC, 2022).

528

529   On decadal timescales, changes in global surface temperatures (Sect. 5) can become decoupled from EEI by ocean

530   heat rearrangement processes (e.g. Palmer and McNeall, 2014; Allison et al., 2020). Therefore, the increase in the

531   Earth heat inventory arguably provides a more robust indicator of the rate of global change on interannual-to-decadal

532   timescales (Cheng et al., 2019; Forster et al., 2021; von Schuckmann et al., 2023a). AR6 WGI found increased

533   confidence in the assessment of change in the Earth heat inventory compared to previous IPCC reports due to

534   observational advances and joint closure of the energy and global sea level budgets (Forster et al., 2021; Fox-Kemper

535   et al., 2021).

536

537   AR6 estimated that EEI increased from 0.50 [0.32–0.69] $\mathrm{W\,m^{-2}}$ during the period 1971–2006 to 0.79 [0.52–

538   1.06] $\mathrm{W\,m^{-2}}$ during the period 2006–2018 (Forster et al., 2021). The contributions to increases in the Earth heat

539   inventory throughout 1971–2018 remained stable: 91 % for the full-depth ocean, 5 % for the land, 3 % for the

540   cryosphere and about 1 % for the atmosphere (Forster et al., 2021). Two recent studies demonstrated independently

541   and consistently that since 1960, the rate of warming of the world ocean is increasing at a relatively consistent pace

542   of 0.15 ± 0.05 $\mathrm{W\,m^{-2}}$ per decade (Minière et al., 2023; Storto and Yang, 2024), while the rate of warming for the land,

543   cryosphere, and atmosphere has been increasing at rate of 0.013 ± 0.003 $\mathrm{W\,m^{-2}}$ per decade (Minière et al., 2023).

544   The increase in EEI over the last several decades (Fig. 6) has also been reported by Cheng et al. (2019), von

545   Schuckmann et al. (2020, 2023a), Loeb et al. (2021), Hakuba et al. (2021), Kramer et al. (2021), Raghuraman et al.

546   (2021) and Minère et al. (2023). The observed increase in EEI over the most recent period (i.e. past 2 decades) are

547   helping to drive exceptionally warm conditions (Sect. 7; Minobe et al., 2025). The increase in has been linked to rising

548   concentrations of well-mixed GHGs and recent reductions in aerosol emissions (Sect. 5; Raghuraman et al., 2021;

549   Kramer et al., 2021; Hansen et al., 2023), and to an increase in absorbed solar radiation associated with decreased

550   reflection by clouds and sea-ice and a decrease in outgoing longwave radiation (OLR) due to increases in trace gases

551   and water vapor (Loeb et al., 2021; Goesling et al., 2025).

552

553   We carry out an update to the AR6 estimate of changes in the Earth heat inventory based on updated observational

554   time series for the period 1971–2020 (Table 4 and Fig. 6). Time series of heating associated with loss of ice and

555   warming of the atmosphere and continental land surface are obtained from the recent Global Climate Observing

556   System (GCOS) initiative (von Schuckmann et al., 2023b; Adusumilli et al., 2022; Cuesta-Valero et al., 2023;

557   Vanderkelen and Thiery, 2022; Nitzbon et al., 2022; Kirchengast et al., 2022). We use the original AR6 time series

558   ensemble OHC time series for the period 1971–2018 and then an updated five-member ensemble for the period 2019–

559   2024. We "splice" the two sets of time series by adding an offset as needed to ensure that the 2018 values are identical.

560   The AR6 heating rates and uncertainties for the ocean below 2000 m are assumed to be constant throughout the period.

561   The time evolution of the Earth heat inventory is determined as a simple summation of time series of atmospheric

562   heating; continental land heating; heating of the cryosphere; and heating of the ocean over three depth layers: 0–700,

563   700–2000 and below 2000 m (Fig. 6a). While von Schuckmann et al. (2023a) have also quantified heating of

564   permafrost and inland lakes and reservoirs, these additional terms are small and not included here for consistency with

565   AR6 (Forster et al., 2021).

566
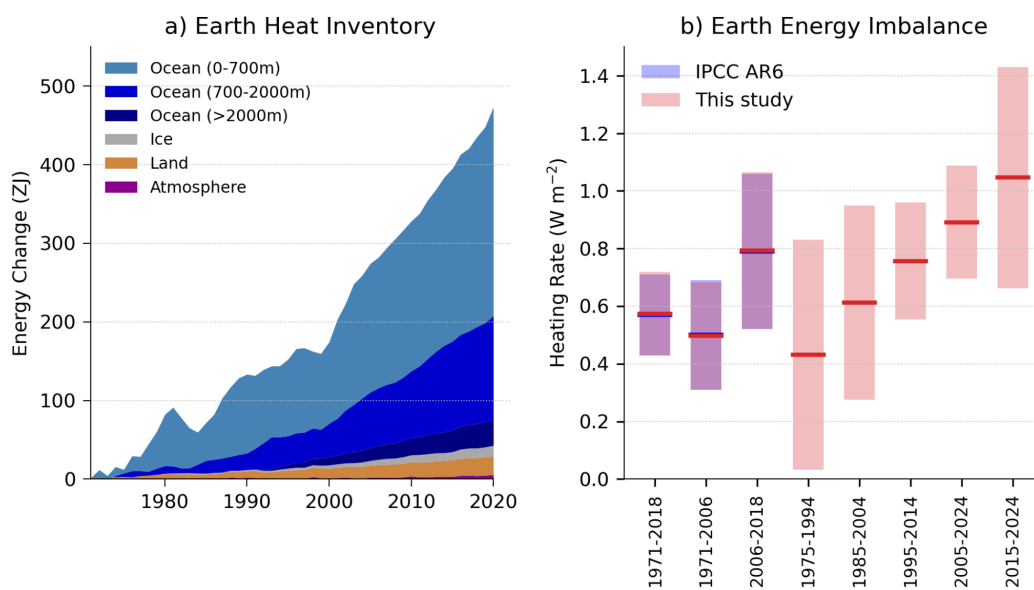
567

568 **Figure 6 (a) Observed changes in the Earth heat inventory for the period 1971–2020, with component contributions as**
569 **indicated in the figure legend. (b) Estimates of the Earth energy imbalance for the IPCC AR6 assessment periods, for**
570 **consecutive 20-year periods and the most recent decade. Shaded regions indicate the *very likely* range (90 % to 100 %**
571 **probability). Data use and approach are based on the AR6 methods and further described in Supplement Sect. S6. For the**
572 **IPCC AR6 periods our assessment closely matches that in AR6. Note the periods in our assessment overlap with different**
573 **IPCC AR6 periods.**

574 In our updated analysis, we find successive increases in EEI for each 20-year period since 1975, with an estimated
575 value of 0.43 [0.03 to 0.83] $\mathrm{W\,m^{-2}}$ during 1975–1994 that more than doubled to 0.89 [0.7 to 1.09] $\mathrm{W\,m^{-2}}$ during
576 2005–2024 (Fig. 6b). In addition, there is some evidence that the warming signal is propagating into the deeper ocean
577 over time, as seen by a robust increase of ocean warming in the 700-2000m depth layer since the 1990s (von
578 Schuckmann et al., 2020; 2023; Cheng et al., 2019, 2022). The model simulations qualitatively agree with the
579 observational evidence (e.g. Gleckler et al., 2016; Cheng et al., 2019), further suggesting that more than half of the
580 OHC increase since the late 1800s occurs after the 1990s.

581

582 The update of the AR6 assessment periods to end in 2024 results in systematic increases of EEI: 0.68 $\mathrm{W\,m^{-2}}$ during
583 1977–2024 compared to 0.57 $\mathrm{W\,m^{-2}}$ during 1971–2018; and 0.99 $\mathrm{W\,m^{-2}}$ during 2012–2024 compared to 0.79 $\mathrm{W\,m^{-2}}$
584 2006–2018 (Table 4). The trend and interannual variability of EEI can largely be explained by a combination of
585 surface temperature changes and radiative forcing (Hodnebrog et al., 2024). However, there was a jump in 2023 and
586 2024 which is still being investigated (see Sect. 7.2), but which is also discussed in the light of recent exceptional
587 extreme climate conditions (Minobe et al., 2025).

588

589 **Table 4 Estimates of the Earth energy imbalance (EEI) for AR6 and the present study.**

Time Period	Earth energy imbalance (W m^{-2}). Square brackets [show 90% confidence intervals].	
	IPCC AR6	**This Study**
1971-2018	0.57 [0.43 to 0.72]	0.57 [0.43 to 0.72]
1971-2006	0.50 [0.32 to 0.69]	0.50 [0.31 to 0.68]
2006-2018	0.79 [0.52 to 1.06]	0.79 [0.52 to 1.07]
1977-2024	-	0.68 [0.52 to 0.85]

2012-2024	-	0.99 [0.70 to 1.28]

590

7 Observed surface temperature change

7.1 Change since 1850-1900

AR6 WGI Chap. 2 assessed the 2001–2020 globally averaged surface temperature change above an 1850–1900 baseline to be 0.99 [0.84 to 1.10] °C and 1.09 [0.95 to 1.20] °C for 2011–2020 (Gulev et al., 2021). Updated estimates to 2013-2022 of 1.15 [1.00–1.25] °C were given in AR6 SYR (Lee et al., 2023), matching the estimate in Forster et al. (2023).

There are choices around the methods used to aggregate surface temperatures into a global average, how to correct for systematic errors in measurements, methods of infilling missing data, and whether surface measurements or atmospheric temperatures just above the surface are used. These choices, and others, affect temperature change estimates and contribute to their uncertainty (IPCC AR6 WGI Chap. 2, Cross Chap. Box 2.3, Gulev et al., 2021). The methods chosen here closely follow AR6 WGI and are presented in the Supplement Sect. S7. Confidence intervals are taken from AR6 as only one of the employed datasets regularly updates ensembles (see Supplement Sect. S7).

Based on the updates available as of March 2025, the change in global surface temperature from 1850–1900 to 2015–2024 is presented in Fig. 7. These data, using the same underlying datasets (with some version changes: see Supplement Sect. S7) and methodology as AR6, estimate 1.24 [1.11–1.35] °C of warming, an increase of 0.15 °C within four years from the 2011–2020 value reported in AR6 WGI (Table 5), or 0.14 °C from the 2011–2020 value in the most recent dataset version. The decade 2015-2024 was 0.31 °C warmer than the previous decade (2005–2014). These changes, although amplified somewhat by the exceptionally warm years in 2023 and 2024, are broadly consistent with typical warming rates over the last few decades, which were assessed in AR6 as 0.76 °C over the 1980–2020 period (using ordinary-least-square linear trends) or 0.019 °C per year (Gulev et al., 2021). They are also broadly consistent with projected warming rates from 2001–2020 to 2021–2040 reported in AR6, which have a very likely range between 0.016 °C per year and 0.036 °C per year under SSP2-4.5 (Lee et al., 2021, their Table 4.5), and with human-induced warming rates discussed in Sect. 8.4.

Land temperatures have increased by 1.79 [1.56–2.03] °C from 1850-1900 to 2015-2024, and ocean temperatures by 1.02 [0.81-1.13] °C over the same period, implying that most land areas have already experienced more than 1.5 °C of warming from the 1850–1900 period. As was the case for the periods reported in AR6, the ratio of observed land

620   to ocean warming is in the vicinity of 1.75, somewhat higher than the ratio of 1.5 [1.4–1.7] projected by the end of the

621   century in CMIP6 models (AR6, their Table 4.2 and Section 4.5.1.1.1). The additional observed warming since 2020

622   in the most recent dataset versions (0.21 °C for land, 0.13 °C for ocean) has a ratio within the CMIP6 projections

623   range.

624

625   **Table 5 Estimates of global surface temperature change from 1850–1900 [*very likely* (90 %–100 % probability) ranges] for**

626   **IPCC AR6 and the present study.**

Time period	Temperature change from 1850-1900 (°C)	
	IPCC AR6 (as reported)	This study
Global, most recent 10 years	1.09 [0.95 to 1.20] (to 2011-2020)	1.24 [1.11 to 1.35] (to 2015-2024)
Global, most recent 20 years	0.99 [0.84 to 1.10] (to 2001-2020)	1.09 [0.93 to 1.20] (to 2005-2024)
Land, most recent 10 years	1.59 [1.34 to 1.83] (to 2011-2020)	1.79 [1.56 to 2.03] (to 2015-2024)
Ocean, most recent 10 years	0.88 [0.68 to 1.01] (to 2011-2020)	1.02 [0.81 to 1.13] (to 2015-2024)

627

Earth System
Science
Data

Open Access

Discussions

628
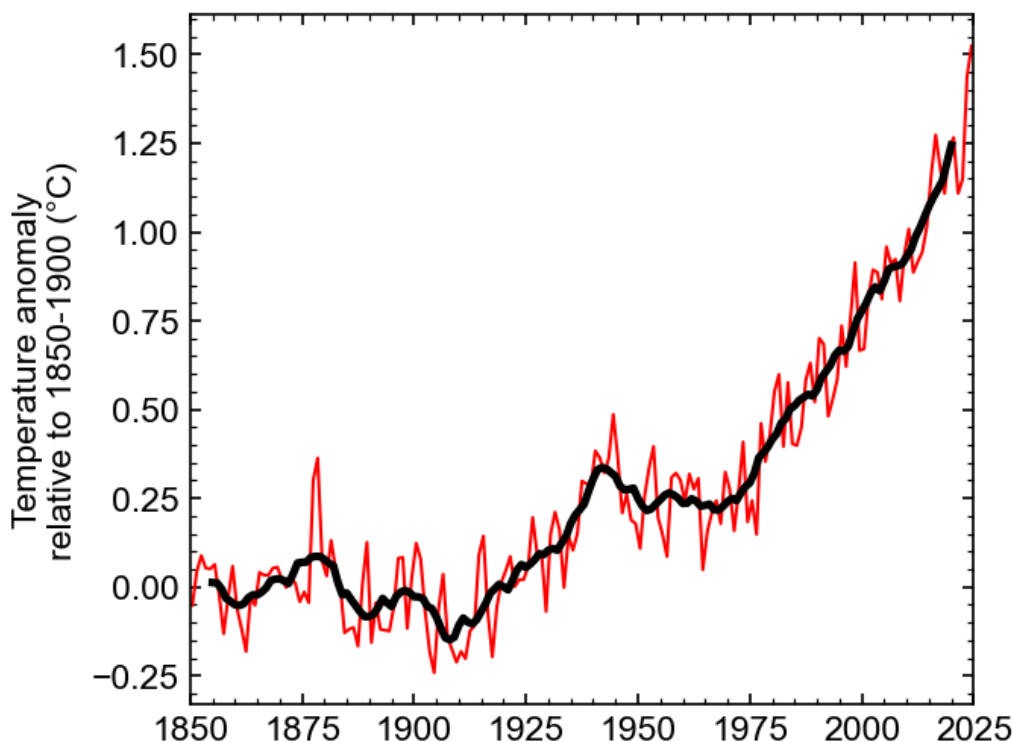
Figure 7 Annual (thin line) and decadal (thick line) means of global surface temperature (expressed as a change from the 1850–1900 reference period). Temperatures are based on an average of four datasets following AR6, see Supplement Sect. S7 for details.

7.2 2023-2024 global mean temperature -anomalies

At the time, 2023 set a new global annual-mean surface temperature change record, with a best estimate of 1.44 °C, beating 2016 by 0.16 °C. 2024 surpassed this, reaching a best estimate of 1.52 °C; 2024, becoming the first calendar year since preindustrial likely exceeding 1.5 °C (Fig. 7). Natural drivers and internal variability are expected to modulate human-caused warming at interannual-to-decadal timescales. 2024 is assessed to be 0.16 °C warmer than the updated human-induced value (Table 6) while 2022 was 0.06 °C colder. These values are not inconsistent with AR6, which estimated the effect of internal variability in any single year be +/- 0.25 °C based on CMIP6 models, nor with the lower estimated ranges (+/- 0.17 °C) when calculated from observational products (Trewin, 2022).

The probability of seeing an observed temperature of 1.52 °C in 2024 considering a human-induced warming equal to 1.36 °C is about 1 chance out of 6 (Fig. 8a). The methodology to calculate this probability consists in comparing the GSAT observed anomaly to those expected from CMIP6 models following the framework adopted in AR6 in Chapter

644   3 (Eyring et al., 2021) for decadal trends and adapted here for interannual time scale issues. The same probability but

645   conditional to the fact that 2024 followed an El Niño year and that the Atlantic Multidecadal Variability (AMV) was

646   in a positive phase (Supplement Sect. S7), rises to 1 chance out of 2. 2024 can therefore be treated as a "normal" year,

647   i.e. very much expected at the actual human-caused global warming level when the internal modes of variability are

648   taken into account and when assessed from a very large number of simulations from large ensembles. Based on the

649   same calculation, we estimate that a year as warm as 2023 would occur once in 4 years at human-induced warming

650   equal to 1.31 °C (Fig. 8b). It drops to 1-in-14 [10-20, CI 5-95%] year event, i.e. a rare-to-exceptional event, when

651   considering that 2023 followed a La Nina year and despite persistent positive AMV. Within such a framework, 2022,

652   that was colder than human-induced warming, could be interpreted as a normal/expected year considering that 2021

653   was a La Nina year and AMV positive (Fig. 8c).

654

655

656

GSAT interannual anomalies distribution from CMIP6 (15 models) for evolutive anthropogically-forced warming (ANT_GWL) and conditional to the combined phases of OND [yr-1] ENSO and AMV modes of variability

657

Earth System
Science
Data
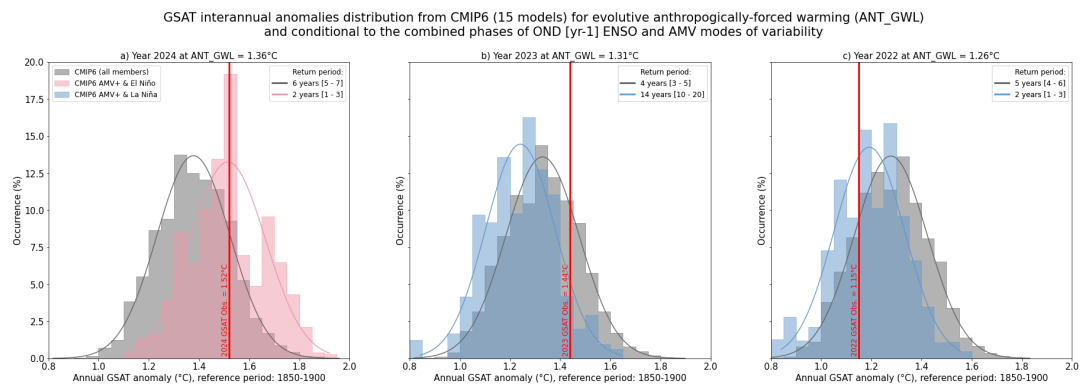
Figure 8 a) Gray histograms of global surface air temperature (GSAT) interannual anomalies estimated from 15 CMIP6 models extracted from all available SSP scenarios (~700 members) at anthropogenic global warming levels (ANT_GWL) corresponding to a) 2024, b) 2023, c) 2022. The red vertical bar stands for the observational consolidated GSAT annual anomalies (Sect. 7.1). The return period of the observed annual GSAT event estimated from the CMIP6 distribution is provided (upper-corner). Associated [5-95%] likely range is assessed through bootstrapping. Interannual anomalies are obtained following Trewin (2022) method over 10-yr sliding windows. Only models providing large-ensembles (n members >5) and having at least one member whose interannual variance of GSAT is compatible with observational estimates, are selected. Colored histograms stand for the same distribution but conditional to the combined phase of El Nino Southern Oscillation (ENSO) and Atlantic Multidecadal Variability (AMV). SST Anomalies for the modes of variability are calculated from the residual of SST obtained after removing the modelled forced response estimated as model ensemble mean. A year is considered as an El Nino/La Nina year if the (October-December) Oceanic Nino Index (ONI) index of the previous year is greater/lower than one standard deviation. A year is considered as an AMV+ year if the annual North Atlantic average SST is greater than one standard deviation. Light pink represents years when ONI and AMV are concomitantly positive and light-blue when ONI is negative.

The increase in global temperature between 2022 and 2023 and in particular in global sea surface temperature is exceptional based on model estimates accounting for projected known human and natural forcings plus internal variability (Rantanen and Laaksonen, 2024; Terhaar et al., 2025, Cattiaux et al., 2024). The La Niña-to-El Niño sequence is of key importance and has been likely reinforced by enhanced energy uptake due to multi-year persistence in the preceding La Niña. The temporal synchronicity between the modes of variability in all basins is hypothesized to have played a role in the jump (Minobe et al., 2025) with the North Atlantic being record warm (Guinaldo et al., 2025) and the austral sea ice extent being record low (Purish and Doddridge, 2023).

Possible specific causes beyond internal variability, many of which are already accounted for in the estimated human-induced warming level, have been postulated e.g.: International Maritime Organization rules on shipping fuel sulphur content that came into force in January 202l; the eruption of Hunga Tonga Hunga Ha'apai in January 2022 and other subsequent smaller volcanic activity; and a faster-than-expected onset of Solar Cycle 25 (see Supplement Section S7 for details and references). A key diagnostic of these changes including both external forcing and internal variability was the exceptional magnitude of the net energy increase into the Earth system from mid-2022 to mid-2023, driven in large part by the reduced reflectance and greater absorption of solar radiation (Hodnebrog et al., 2024; Goessling et al., 2024; Minobe et al. 2025), which may be influenced by cloud feedbacks (Tselioudis et al., 2024) as well as surface reflectance and atmospheric composition change (see also Sect. 6).

Our analysis, detailed in Supplement Sect. S7, makes use of estimates of variability and radiative forcing contributions and their uncertainty based on Sect 5. and the published literature. It shows that the increase in 2023 and 2024 compared to previous years could be explained by a combination of factors. In summary, our analyses show that, although the relative weight between the physical processes in explaining the high surface temperatures remain to be

695   better quantified, the 2023 and 2024 observed temperatures are not inconsistent with the level of human induced
696   warming assessed next, in Sect. 8.
697

8 Human contribution to surface temperature change

699   Human-induced warming, also known as anthropogenic warming, refers to the component of observed global surface
700   temperature increase attributable to both the direct and indirect effects of human activities, which are typically grouped
701   as follows: well-mixed GHGs (consisting of CO_2, CH_4, N_2O and F-gases) and other human forcings (consisting of
702   aerosol–radiation interaction, aerosol–cloud interaction, black carbon on snow, contrails, ozone, stratospheric H_2O
703   and land use) (Eyring et al., 2021). The remaining contributors to total warming are natural: consisting of both natural
704   forcings (such as solar and volcanic activity) and internal variability of the climate system (such as variability related
705   to El Niño/La Nina events).
706

707   An assessment of human-induced warming was provided in two reports within the IPCC's Sixth Assessment cycle:
708   first in SR1.5 in 2018 [Chap. 1 Sect. 1.2.1.3 and Fig. 1.2 (Allen et al., 2018), summarised in the Summary for
709   Policymakers (SPM) Sect. A.1 and Fig. SPM.1 (IPCC, 2018)] and second in AR6 in 2021 [WGI Chap. 3 Sect. 3.3.1.1.2
710   and Fig. 3.8 (Eyring et al., 2021), summarised in the WGI Summary for Policymakers (SPM) Sect. A.1.3 and Fig.
711   SPM.2 (IPCC, 2021b)], and quoted again without any updates in SYR [Sect. 2.1.1 and Fig. 2.1 (IPCC,2023a) and
712   SYR Summary for Policymakers (SPM) Sect. A.1.2. (IPCC 2023b)].

8.1 Warming period definitions in the IPCC Sixth Assessment cycle

714   Temperature increases are defined relative to a baseline; IPCC assessments typically use the 1850–1900 average
715   temperature as a proxy for the climate in pre-industrial times, referred to as the period before 1750, even though a
716   small amount of warming likely occurred over 1750-1850 (see AR6 WGI Cross Chapter Box 1.2). Temperatures in
717   the IPCC were reported as either GMST or GSAT, see Supplement Sect. 8.1 for details.
718

719   Tracking progress towards the long-term global goal to limit warming, in line with the Paris Agreement, requires the
720   assessment of both what the current level of global surface temperatures are and whether a level of global warming,
721   such as 1.5 °C, is being reached. Definitions for these were not specified in the Paris Agreement, and several ways of
722   tracking levels of global warming are in use; here we focus on those adopted within AR6. When determining whether
723   warming thresholds have been passed, both AR6 and SR1.5 adopted definitions that depend on future warming; in
724   practice, levels of current warming were therefore reported in AR6 and SR1.5 using additional definitions that
725   circumvented the need to wait for observations of the future climate, as described next. AR6 defined crossing-time for
726   a level of global warming as the midpoint of the first 20-year period during which the average *observed* warming for
727   that period exceeds that level of warming (see AR6 WGI Chapter 2 Box 2.3) (the level of warming for a given year
728   defined in this way is therefore not known until 10 years after that year). AR6 therefore reported current levels of both

729   *observed* and *human-induced* warming as their averages over just the most recent 10 years (which gives warming that

730   lags by only 5 years instead of 10 years) (see AR6 WGI Chapter 3 their Sect. 3.3.1.1.2); we refer to this definition as

731   the "AR6 decade-average" warming. SR1.5 defined the level of warming in a given year as the average *human-induced*

732   warming, in GMST, of a 30-year period centred on that year; when the given year is the *current* year, SR1.5 specified

733   that the future 15 years (required for the mean) are revealed by extrapolating the multidecadal trend (see SR1.5 Chapter

734   1, their Sect. 1.2.1); we refer to this definition as the "SR1.5 trend-based" warming. If the multidecadal trend is

735   interpreted as being linear (which it has been very close to over recent decades), this definition of current warming is

736   equivalent to the end-point of the trend line through the most recent 15 years of human-induced warming, and therefore

737   provides a definition of warming for the current year that depends only on historical warming. This interpretation

738   produces results that in recent years have been identical (or extremely close) to the current annual mean value of

739   human-induced warming (see results in Sect. 8.2, and Supplement Sect. S8.3), so in practice the attribution assessment

740   in SR1.5 was based not on the trend-based definition, but on the simple annual-year attributed warming; we refer to

741   this definition as the "SR1.5 annual-mean" warming. A diagram of these three definitions is given in Supplement Fig.

742   S11.

743

8.2 Updated assessment approach of human-induced warming to date

745   This paper provides an update of the AR6 WGI and SR1.5 human-induced warming assessments including, for

746   completeness, all three definitions (AR6 decade-average, SR1.5 trend-based, and SR1.5 annual-mean). The 2024

747   updates in this paper follow the same methods and process as the 2022 and 2023 updates provided in Forster et al.

748   (2023, 2024). Global mean surface temperature (GMST) is adopted as the definition of global surface temperature

749   (see Supplement Sect. S8.1). The three attribution methods used in AR6 are retained: the Global Warming Index

750   (GWI) (building on Haustein et al., 2017), regularised optimal fingerprinting (ROF) (as in Gillett et al., 2021) and

751   kriging for climate change (KCC) (Ribes et al., 2021). Details of each method, their different uses in SR1.5 and AR6,

752   and any methodological changes, are provided in Supplement Sect. S8.2; method-specific results are also provided in

753   Supplement Sect. S8.3. The overall estimate of attributed global warming for each definition (decade-average, trend-

754   based, and annual-mean), is based on a multi-method assessment of the three attribution methods (GWI, KCC, ROF);

755   the best estimate is given as the 0.01 °C-precision mean of the 50th percentiles from each method, and the *likely* range

756   is given as the smallest 0.1 °C-precision range that envelops the 5th to 95th percentile ranges of each method. This

757   assessment approach is identical to last year's update (Forster et al. (2024)); it is directly traceable to and fully

758   consistent with the assessment approach in AR6, though it has been lightly extended in ways that are explained in

759   Supplement Sect. S8.4.

760

761 Results are summarised in Table 6 and Fig. 9. Method-specific contributions to the assessment results, along with time

762 series, are given in the Supplement, Sect. S8.3. Where results reported in GSAT differ from those reported in GMST

763 (see Supplement Sect. S8.1), the additional GSAT results are given in Supplement Sect. S8.3.

764
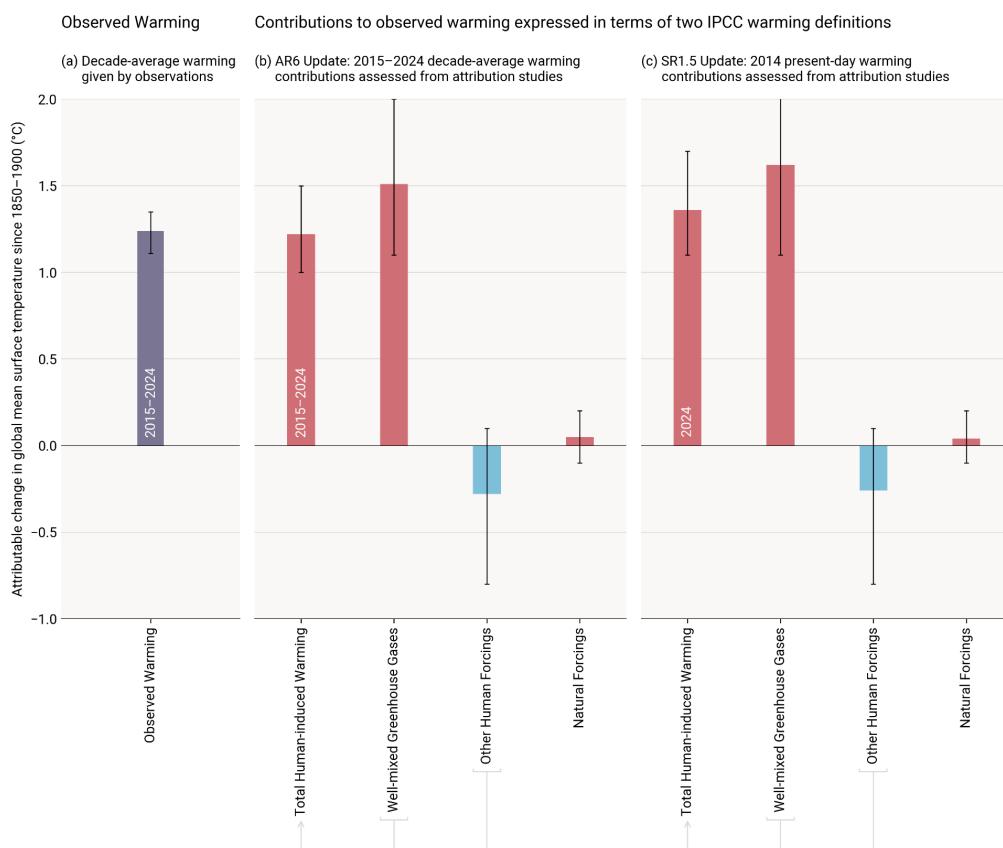
765

766 **Figure 9 Updated assessed contributions to observed warming relative to 1850–1900; see AR6 WGI SPM.2. Results for all**
767 **time periods in this figure are calculated using updated datasets and methods. The 2015–2024 average and 2024 results are**
768 **this year's updated assessments for AR6 and SR1.5, respectively. Panel (a) shows updated observed global warming from**
769 **Sect. 7, expressed as total global mean surface temperature (GMST), due to both anthropogenic and natural influences.**
770 **Whiskers give the "*very likely*" range. Panels (b) and (c) show updated assessed contributions to warming, expressed as**
771 **global mean surface temperature (GMST), from natural forcings and total human-induced forcings, which in turn consist**
772 **of contributions from well-mixed GHGs and other human forcings. Whiskers give the "*likely*" range. Changes to warming**
773 **levels since the IPCC sixth assessment cycle are depicted in Supplement Fig. S10.**

774 **Table 6 Updates to assessments in the IPCC 6th assessment cycle of warming attributable to multiple influences. Estimates**
775 **of warming attributable to multiple influences, in °C, relative to the 1850–1900 baseline period. Results are given as best**
776 **estimates, with the *likely* range in brackets, and reported as global mean surface temperature (GMST). Results from the**
777 **IPCC 6th assessment cycle, for both AR6 and SR1.5, are quoted in columns labelled (i) and are compared with repeat**
778 **calculations in columns labelled (ii) for the same period using the updated methods and datasets to see how methodological**
779 **and dataset updates alone would change previous assessments. Assessments for the updated periods are reported in columns**
780 **labelled (iii). * Updated GMST observations, quoted from Sect. 7 of this update, are marked with an asterisk, with "*very***
781 ***likely*" ranges given in brackets. ** In AR6 WGI, best-estimate values were not provided for warming attributable to well-**
782 **mixed GHGs, other human forcings and natural forcings (though they did receive a "*likely*" range); for comparison, best**
783 **estimates (marked with two asterisks) have been retrospectively calculated in an identical way to the best estimate that AR6**
784 **provided for anthropogenic warming (see discussion in Supplement Sect. S8.4.1). *** The SR1.5 assessment drew only on**
785 **GWI rounded to 0.1°C precision, whereas the repeat and updated calculations use the updated multi-method assessment**
786 **approach.**

Estimates of warming attributable to multiple influences, in °C, relative to the 1850–1900 baseline period					
Results are given as best estimates, with the *likely* range in brackets, and reported as Global Mean Surface Temperature (GMST).					
Definition ➡	**(a) IPCC AR6 Attributable Warming Update**			**(b) IPCC SR1.5 Attributable Warming Update**	
	Value for decade (average of previous 10-year period)			*Value for single year (30-year mean centred on current year)*	
Period ➡	**(i) 2010-2019** *Quoted from AR6 Chapter 3 Sect. 3.3.1.1.2 Table 3.1*	**(ii) 2010-2019** *Repeat calculation using the updated methods and datasets*	**(iii) 2015-2024** *Updated value using updated methods and datasets*	**(i) 2017** *Quoted from SR1.5 Chapter 1 Sect. 1.2.1.3*	**(ii) 2017** *Repeat calculation using the updated methods and datasets*	**(iii) 2024** *Updated value using updated methods and datasets*
Observed	1.06 [0.92 to 1.17]	1.07 [0.89 to 1.22] *	1.24 [1.11 to 1.35] *	-	-	1.52
Anthropogenic	1.07 [0.8 to 1.3]	1.09 [0.9 to 1.3]	1.22 [1.0 to 1.5]	1.0 [0.8 to 1.2] ***	1.13 [0.9 to 1.3]	1.36 [1.1 to 1.7]
Well-mixed GHGs	1.40** [1.0 to 2.0]	1.40 [1.0 to 1.9]	1.51 [1.1 to 2.0]	N/A	1.45 [1.0 to 1.9]	1.62 [1.1 to 2.1]
Other human forcings	-0.32** [-0.8 to 0.0]	-0.30 [-0.8 to 0.0]	-0.28 [-0.8 to 0.1]	N/A	-0.31 [-0.8 to 0.1]	-0.26 [-0.8 to 0.1]
Natural forcings	0.03** [-0.1 to 0.1]	0.05 [-0.1 to 0.2]	0.05 [-0.1 to 0.2]	N/A	0.05 [-0.1 to 0.2]	0.04 [-0.1 to 0.2]

Note: Period row header shows "Component ⬇" in the left column.

787

788   The repeat calculations for attributable warming in 2010–2019 exhibit good correspondence with the results in AR6
789   WGI for the same period (see also Supplement, Sect. S8). The repeat calculation for the level of attributable
790   anthropogenic warming in 2017 is about 0.1 °C larger than the estimate provided in SR1.5 for the same period,
791   resulting from changes in methods and observational data (see AR6 WGI Chapter 2 Box 2.3). The updated results for
792   warming contributions in 2024 are higher than in 2017 due also to 7 additional years of increasing anthropogenic
793   forcing. Note also that the SR1.5 assessment only used the GWI method, whereas these annual updates apply the full
794   AR6 multi-method assessment (see Supplement Sect. S8.4 for details and rationale).

795

796   In this 2025 update, we assess the 2015–2024 decade average human induced-warming at 1.22 [1.0 to 1.5] °C, which
797   is 0.15°C above the AR6 assessment for 2010–2019. The single year average human-induced warming is assessed to
798   be 1.36 [1.1 to 1.7] °C in 2024 relative to 1850–1900. In general, these forced warming levels have evolved steadily
799   and predictably in line with the current warming rate within uncertainty. The uncertainty range for the single-year
800   level of anthropogenic warming already included 1.5 °C in previous years' assessments, and for the first time this year
801   also lies at the edge of the uncertainty range for the (lagged) decade mean definition. The single-year anthropogenic
802   warming best estimate is well below the observed best estimate for 2024 (1.52 °C, see Sect. 7), but note that the best
803   estimate and lower uncertainty for observed warming lies within the uncertainty for single-year anthropogenic
804   warming from each of the three attribution methods (see Supplement Table S5), whereas the upper uncertainty range
805   of observed warming lies above the range for anthropogenic warming for the two attribution methods that fully exclude
806   internal variability.

807

808   The best estimates for decade-average and single-year human-induced warming are 0.04 °C and 0.05 °C respectively
809   above the value estimated in the previous update for the year 2023 (Forster et al., 2024), but should not be interpreted
810   as a substantive increase in the rate of forced anthropogenic warming, as the rate increase is well within uncertainty
811   ranges (Sect. 8.3).

812

813   AR6 found that, averaged for the 2010–2019 period, essentially all observed global surface temperature change was
814   human-induced, with solar and volcanic drivers and internal climate variability making a negligible contribution. This
815   conclusion remains the same for the 2015–2024 period. Generally, whatever methodology is used, on a global scale,
816   the best estimate of the current level of human-induced warming is (within small uncertainties) similar to the observed
817   global surface temperature change (Table 6).

818

819   **8.3 Rate of human-induced global warming**

820   Estimates of the human-induced warming rate follow the same methodology as in the previous year's update (a rolling
821   10-year linear trend in attributed anthropogenic warming). A full description of the approach can be found in the

822   Supplement Sect. S8.5. The rate of increase in attributed anthropogenic warming over time is distinct from the rate of

823   increase in the observed global surface temperature, which is also affected by internal variability such as El Niño and

824   natural forcings such as volcanic activity (see discussions in Sect. 7.2). The rate of anthropogenic warming we estimate

825   here is driven by the rate of change of anthropogenic ERF (Sect. 5), with variations in the climate forcing trend over

826   time correlating with variations in the rate of attributed warming (Fig. 10).

827

828

829
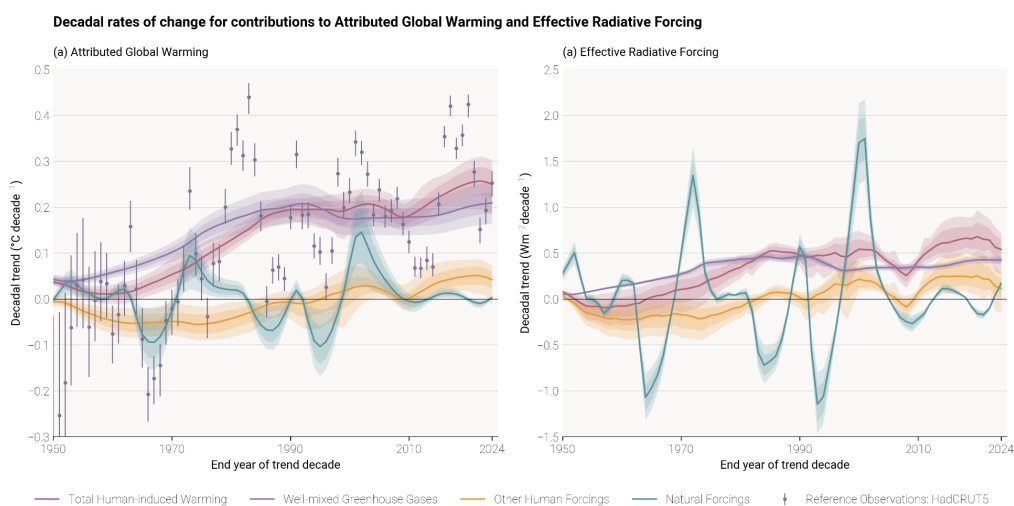
Figure 10 Rates of (a) attributable warming (global mean surface temperature (GMST)) and (b) effective radiative forcing.
The attributable warming rate time-series are calculated using the Global Warming Index method with full ensemble
uncertainty. The observed GMST rates included for reference are also calculated with uncertainty from the HadCRUT5
ensemble, and, for consistency with the attributed warming rates, do not include standard regression error, which, for
observed warming, would increase the size of the error bars. The effective radiative forcing rates are calculated using a
representative 1000-member ensemble of the forcings provided in Sect. 5 of this paper. The depicted rates are the decadal
rates, with the end year of the decade in question being the value given on the time axis.

837

838   Estimates for the trend derived from the three warming attribution methodologies are presented in Table 7, with results

839   for individual attribution methods detailed in the Supplement Table S6. The GWI (based on observed warming and

840   forcing) and KCC (based on CMIP simulations) methodologies report results that are in close agreement, while

841   estimates derived with the ROF method (also based on CMIP simulations) are more strongly influenced by residual

842   internal variability that remains in the anthropogenic warming signal due to the limitations in size of the CMIP

843   ensemble. The median result is presented at 0.01 °C/decade precision for the overall multi-method rate of warming

844   assessment.

845

846   An overall best estimate attributed rate of human-induced warming of 0.27 °C/decade is found for the decade 2015–

847   2024. This increased rate relative to the 0.2 °C/decade AR6 assessment is broken down in the following way: (i) 0.03

848   °C/decade from changing the rounding precision (updating the AR6 2010-2019 warming rate assessment from 0.2 to

849   0.23 °C/decade), (ii) 0.03 °C/decade is due to methodological and dataset updates (updating the 2010–2019 warming

850   rate from 0.23 °C/decade to 0.26 °C/decade; including the effect of adding 5 additional observed years to the attribution

851   over the entire historical period), and (iii) 0.01 °C/decade due to a real increase in rate for the 2015–2024 period since

852   the 2010–2019 period (updating 0.26 °C/decade for 2010–2019 to 0.27 °C/decade for 2015–2024), consistent with

853   increased GHG emissions over the last decade. The spread of rates across the three attribution methods remains similar

854   to their spread in AR6, and previous updates of this work, and hence does not support a decrease in the headline

855   uncertainty range. However, as previous assessments suggested, we update the uncertainty range for the rate of human-

856   induced warming from [0.1–0.3] °C/decade in AR6 to [0.2–0.4] °C/decade to better reflect the closer agreement of

857   the 5% floors and the larger spread in the 95% ceilings of the three methods, and higher rate from the ROF method.

858   The rate of human-induced warming for the 2015-2024 decade is concluded to be 0.27 °C/decade with a range of

859   [0.2–0.4] °C/decade). This agrees with the decadal trend in observed warming of 0.26 °C per decade (also calculated

860   as a linear trend through 10-year periods - see Sect. 7.1). It is important to note, however, that internal variability leads

861   to the decadal rates of observed warming being far less stable than for anthropogenic warming, and the very close

862   correspondence between the two this year is somewhat incidental (see Fig. 10).

863

864   **Table 7 Updates to the IPCC AR6 rate of human-induced warming. Results for each method are given in the Supplement**
865   **Table S6; assessment results are given as a best estimate with *likely* range in brackets. Results from AR6 WGI (Ch.3 Sect.**
866   **3.3.1.1.2 Table 3.1) are quoted in column (i), and compared with a repeat calculation using the updated methods and**
867   **datasets in column (ii), and finally updated for the 2015-2024 period in column (iii). The AR6 assessment result was identical**
868   **to the SR1.5 assessment result, though the latter was based on a different set of studies and timeframes. * Note that for**
869   **clarity and ease of comparison with this year's updated assessment, in the assessed rate in column (i) both quotes the**
870   **assessment from AR6 and retrospectively applies the median approach adopted in this paper. The observed rates are**
871   **calculated using the multi-dataset observed temperature dataset from Sect. 7; no ensemble is available for this, hence the**
872   **absence of an uncertainty range.**

Estimates of anthropogenic warming rate, in °C per decade			
Results are given as best estimates, with brackets giving the *likely* range for the assessments, and 5-95% uncertainty for the individual methods			
Definition ➡	**IPCC AR6 Anthropogenic Warming Rate Update** *Linear trend in anthropogenic warming over the trailing 10-year period*		
Period ➡	**(i) 2010-2019** *Quoted from AR6 Chapter 3 Sect. 3.3.1.1.2 Table 3.1*	**(ii) 2010-2019** *Repeat calculation using the updated methods and datasets*	**(iii) 2015-2024** *Updated value using updated methods and datasets*
Anthropogenic Warming Rate Assessment	Quoted from AR6: 0.2 [0.1 to 0.3] Using the median approach: 0.23 [0.1 to 0.3] *	0.26 [0.2 to 0.4]	0.27 [0.2 to 0.4]
Observed		0.37	0.26

873

874

9 Remaining Carbon Budget

AR5 (IPCC, 2013) assessed that long-term global surface temperature increase caused by CO_2 emissions is close to linearly proportional to the total amount of cumulative CO_2 emissions (Collins et al., 2013). The most recent AR6 report reaffirmed this assessment and highlights that this near-linear relationship also holds between cumulative CO_2 emissions and maximum global surface temperature increase caused by CO_2 (Canadell et al., 2021). This near-linear relationship implies that for keeping global warming below a specified temperature level, one can estimate the total amount of CO_2 that can ever be emitted. When expressed relative to a recent reference period, this is referred to as the remaining carbon budget (Rogelj et al., 2018).

AR6 assessed the remaining carbon budget (RCB) in Chap. 5 of its WGI report (Canadell et al., 2021) for warming limits ranging from 1.3 to 2.4 °C relative to the 1850-1900 period (see Table 5.8 in Canadell et al., 2021). A selection of these (1.5, 1.7, and 2 °C) were also reported in its Summary for Policymakers (Table SPM.2, IPCC, 2021b). These RCB values are updated in this section using the same method as last year (Forster et al., 2024). Data for four warming limits (1.5, 1.6, 1.7 and 2 °C) are included in Table 8 while figures for more values are included in the Supplement Sect. S9.

The RCB is estimated by application of the WGI AR6 method described in Rogelj et al. (2019), which involves the combination of the assessment of five factors: (i) the amount of human-induced warming for the most recent decade (given in Sect. 8), (ii) the transient climate response to cumulative emissions of CO_2 (TCRE), which quantifies the linear proportionality between cumulative CO_2 emissions and CO_2-induced warming (iii) the zero emissions commitment (ZEC), representing the expected amount of additional (at present unrealized) warming caused by past CO_2 emissions (iv) the temperature contribution of future non-CO_2 emissions and (v) an adjustment term for Earth system feedbacks that are otherwise not captured through the other factors. AR6 WGI reassessed all five terms (Canadell et al., 2021). Lamboll et al. (2023) further considered the temperature contribution of non-CO_2 emissions and integrated different uncertainties, while Rogelj and Lamboll (2024) clarified the reductions in non-CO_2 emissions that are assumed in the RCB estimation.

The RCB for 1.5, 1.6, 1.7 and 2 °C warming levels is re-assessed based on the most recent available data. Estimated RCBs are reported in Table 8. They are expressed relative to the start of 2025 for estimates based on the 2015–2024 human-induced warming update (Sect. 8). Based on the variation in non-CO_2 emissions across the scenarios in AR6 WGIII scenario database, the estimated RCB values can be higher or lower by around 200 $GtCO_2$ depending on how successful non-CO_2 emissions reductions are (Lamboll et al., 2023; Rogelj and Lamboll, 2024). Notably, RCB estimates consider the subset of non-CO_2 emission scenarios in the AR6 WGIII database that are aligned with a global transition to net zero CO_2 emissions (Lamboll et al., 2023; Rogelj and Lamboll, 2024). These estimates assume median reductions in non-CO_2 emissions between 2020–2050 of CH_4 (about 50 %), N_2O (about 20 %) and SO_2 (about 80 %) (see Supplement, Sect. S9 and Table S7 and (Rogelj and Lamboll, 2024)). If these non-CO_2 GHG emission reductions

911 are not achieved, the RCB for all temperature targets would be smaller than the values reported here in Table 8 (see

912 Lamboll et al., 2023, Rogelj and Lamboll, 2024).

913

914 Compared to RCB values reported in AR6, our estimates here are smaller owing to several factors. First, AR6 budgets

915 were expressed from 2020 onwards, and approximately 200 $GtCO_2$ have been emitted between 2020 and 2024.

916 Second, we use updated physical models of non-CO_2 forcing which lead to an increased estimate of the importance of

917 aerosols that are expected to decline with time in low emissions pathways (Rogelj et al., 2014; Rogelj and Lamboll,

918 2024). This decreased negative forcing from aerosols is expected to cause additional net non-CO_2 warming because

919 more non-CO_2 GHG warming is being unmasked and this decreases the RCB (Lamboll et al., 2023) by slightly over

920 100 $GtCO_2$. There was also a small reduction in the budget (about 10 $GtCO_2$) from using the newer AR6 scenario set.

921 Finally, the updated warming estimate reported in Sect. 8 is slightly increased due to the high observed temperatures

922 in the last few years, which resulted in a further reduction of the budget by around 40 $GtCO_2$, relative to values reported

923 in last year's assessment (Forster et al. 2024). This gives a total reduction in RCB values estimated from the beginning

924 of 2025 of ~370 $GtCO_2$ compared to the values from 2020 reported in AR6.

925

926 **Table 8 Updated estimates of the remaining carbon budget for 1.5, 1.6, 1.7 and 2.0 °C, for five levels of likelihood,**

927 **considering only uncertainty in TCRE. Estimates are expressed relative to the start of 2024. The probability includes only**

928 **the uncertainty in how the Earth immediately responds to CO_2 emissions (TCRE), not long-term committed warming or**

929 **uncertainty in the climate response to other non-CO_2 emissions. All values are rounded to the nearest 10 $GtCO_2$. Additional**

930 **values can be found in the Supplement Tables S7 and S8.**

Temperature (°C)	Estimated remaining carbon budgets from the beginning of 2025 ($GtCO_2$)				
Avoidance probability:	17%	33%	50%	67%	83%
1.5	320	200	130	80	30
1.6	620	420	310	240	160
1.7	910	640	490	390	290
2.0	1790	1310	1050	870	690

931

932 This year's update of the 1.5 °C budget uses the historical warming level for the 2015-2024 period of 1.24 °C, with

933 0.11 °C future contribution of non-CO_2 warming. Assuming a median TCRE estimate of 0.45 °C per 1000 $GtCO_2$ this

934 gives around 340 $GtCO_2$ from the midpoint of the period, from which we subtract around 210 $GtCO_2$ (204 $GtCO_2$ that

935 were already emitted from the middle until the end of the 2015-2024 period, and 7 $GtCO_2$ that represents the median

936   estimate of the impact of Earth systems feedbacks such as permafrost feedback that would otherwise not be covered).
937   The same method is used to calculate budgets for the other warming levels.

938   The values in Table 8 are all greater than zero, implying that we have not yet emitted the amount of CO_2 that would
939   commit us to these levels of warming. However, including the uncertainty in ZEC (as in the Supplement Table S8),
940   non-CO_2 emission and forcing uncertainty, and underrepresented Earth-system feedbacks results in negative RCB
941   estimates for limiting warming to low temperature limits with high likelihood. A negative RCB for a specific
942   temperature limit would mean that the world is already committed to this amount of warming, and that net negative
943   emissions would therefore be required to return to the temperature limit after a period of overshoot. The assumption
944   behind such a calculation is that we can treat the warming impact of positive and negative net emissions as
945   approximately symmetric. While the claim of symmetry is likely valid for small emissions values, some model studies
946   have shown that it holds less well for reversal of larger emissions (Canadell et al., 2021, Zickfeld et al., 2021,
947   Vakilifard et al., 2022, Pelz et al., 2025) As such, larger exceedances of the RCB for a particular temperature target
948   would decrease the likelihood that the temperature target could still be achieved by an equivalent amount of net
949   negative emissions.

950   Note that the 50 % RCB estimate of 130 GtCO$_2$ would be be exhausted in a little more than 3 years if global CO_2
951   emissions remain at 2024 levels (42 GtCO$_2$/yr, see Table 1). This is not expected to correspond exactly to the time
952   that 1.5 °C global warming level is reached due to uncertainty associated with committed warming from past CO_2
953   emissions (the ZEC) as well as ongoing warming and cooling contributions from non-CO_2 emissions. For comparison,
954   our estimate of 2024 anthropogenic warming (1.36 °C) and the recent rate of increase (0.27 °C/decade) would suggest
955   that continued emissions at current levels would cause human-induced global warming to reach 1.5°C in
956   approximately 5 years.

10 Indicator of climate and weather extremes: land average maximum temperatures

958   Changes in climate and weather extremes are among the most visible effects of human-induced climate change. Within
959   AR6 WGI, a full chapter was dedicated to the assessment of past and projected changes in extremes on continents
960   (Seneviratne et al., 2021), and the chapter on ocean, cryosphere and sea level changes also provided assessments on
961   changes in marine heatwaves (Fox-Kemper et al., 2021). Global indicators related to climate extremes include
962   averaged changes in climate extremes, for example, the mean increase of annual minimum and maximum temperatures
963   on land (AR6 WGI Chap. 11, Fig. 11.2, Seneviratne et al., 2021) or the area affected by certain types of extremes
964   (AR6 WGI Chap. 11, Box 11.1, Fig. 1, Seneviratne et al., 2021; Sippel et al., 2015).

966   The presented climate indicator for changes in temperature extremes consists of land average maximum temperatures
967   for any single day in a year (TXx) (excluding Antarctica). Fig. 11 updates the land mean TXx shown in Forster et al.
968   (2023, 2024), originally based on Fig. 11.2 from Seneviratne et al. (2021). Three datasets are analyzed: HadEX3
969   (Dunn et al., 2020), Berkeley Earth Surface Temperature (building off Rohde et al., 2013), and the fifth-generation

970   ECMWF atmospheric reanalysis of the global climate (ERA5; Hersbach et al., 2020). HadEX3 is static and has not

971   received any updates. Berkeley Earth has been extended and updated compared to Forster et al. (2024), resulting in

972   TXx differences for most years (less than 0.1°C), and now includes data for 2023. Of the three datasets, only ERA5

973   covers the whole of 2024 at the present time. TXx is calculated by averaging the annual maximum temperature over

974   all available land grid points (excluding Antarctica) and then converted to anomalies with respect to a base period of

975   1961–1990. To express the TXx as anomalies with respect to 1850–1900, we add an offset of 0.51 °C to all three

976   datasets. See Supplement Sect. S10 for details on the data selection, averaging and offset computation.

Land average annual maximum temperature anomaly

977
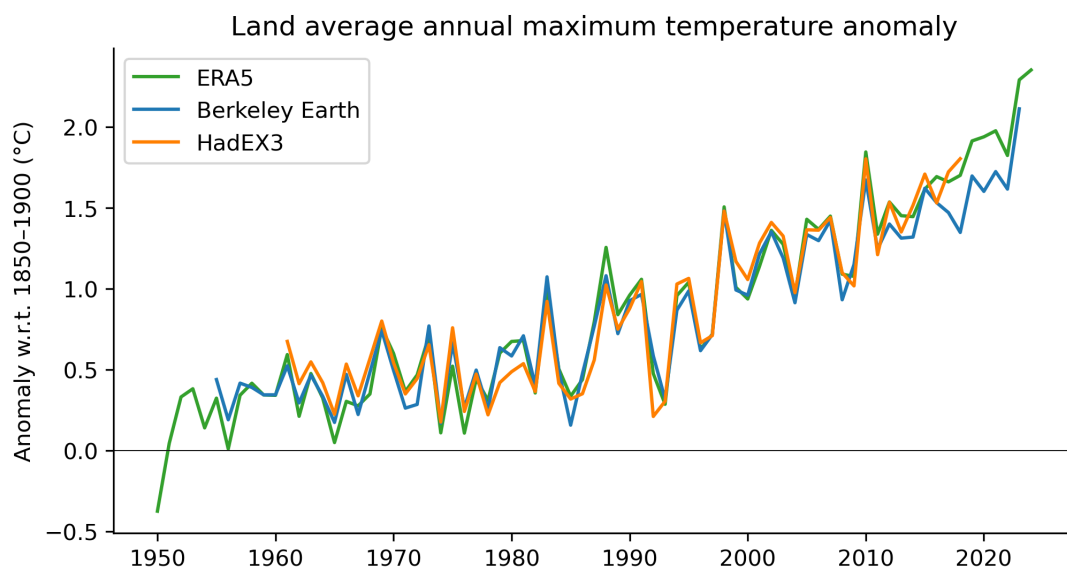
Figure 11 Time series of observed temperature anomalies for land average annual maximum temperature (TXx) for ERA5
(1950–2024), Berkeley Earth (1955–2023) and HadEX3 (1961–2018), with respect to 1850–1900. The datasets have different
spatial coverage and are not coverage-matched. All anomalies are calculated relative to 1961–1990, and an offset of 0.51 °C
is added to obtain TXx values relative to 1850–1900. Note that while the HadEX3 numbers are the same as shown in
Seneviratne et al. (2021) Fig. 11.2, these numbers were not specifically assessed.

983

984   Our climate has warmed rapidly in the last few decades (Sect. 7), which also manifests in changes in the occurrence

985   and intensity of climate and weather extremes. From about 1980 onwards, all datasets point to a strong TXx increase,

986   which coincides with the transition from global dimming, associated with aerosol increases, to brightening, associated

987   with aerosol decreases (Wild et al., 2005, Sect. 4). The ERA5 based TXx warming estimate w.r.t. 1850–1900 for 2024

988   is at 2.35 °C; an increase of 0.05 °C compared to 2023, and thus even warmer than the previous record in 2023. On

989   longer time scales, land average TXx has warmed 0.49 °C in the past 10 years (comparing the decades 2015–2024 to

990   2005–2014) and 1.90 °C with respect to pre-industrial conditions (Table 9). Since the offset relative to our pre-

991   industrial baseline period is calculated over 1961–1990, temperature anomalies align by construction over this period

992   but can diverge afterwards.

993

Table 9 Anomalies of land average annual maximum temperature (TXx) for recent decades based on HadEX3, Berkeley Earth, and ERA5, with respect to 1850–1900. All anomalies are calculated relative to 1961–1990, and an offset of 0.51 °C is added to obtain TXx values relative to 1850–1900.

	HadEX3	Berkeley Earth	ERA5
2000–2009	1.23	1.18	1.21
2005–2014	1.37	1.31	1.4
2009–2018	1.52	1.41	1.54
2011–2020	-	1.45	1.63
2013–2022	-	1.52	1.72
2014–2023	-	1.6	1.81
2015–2024	-	-	1.9

997

11 Global land precipitation

Anthropogenic radiative forcings modify the Earth's energy budget and subsequently drive substantial and widespread changes in the global water cycle including precipitation, evaporation, atmospheric moisture, and runoff (Forster et al., 2021, Douville et al., 2021; Gulev et al. 2021). AR6 Chapter 8 assessed that human-caused climate change has driven detectable changes in the global water cycle since the mid-20th century with high confidence, including an overall increase in atmospheric moisture (7% per 1 °C of warming), precipitation intensity (1-3% per 1 °C of warming) and increased terrestrial evapotranspiration (Douville et al., 2021).

In AR6, global land precipitation was highlighted as one of the large-scale indicators of climate change rather than global precipitation since land precipitation has greater societal relevance and in situ precipitation records over land extend back to the early to mid-20th century quasi-globally except Antarctica and parts of Africa and South America (Gulev et al., 2021; Lee et al., 2021; Douville et al., 2021). AR6 assessed that global land precipitation has likely increased since the middle of the 20th century with a faster increase since the 1980s with large interannual variability and regional heterogeneity. The observed Northern Hemispheric land summer monsoon precipitation experienced a significant decline during 1901-2014, which has been attributed to the dominant influence of anthropogenic aerosols (Cao et al., 2022). Here, we include an update of global land precipitation change since AR6 (i.e., from 2020 to 2024).

Figure 12 shows annual global land precipitation anomaly relative to 1991-2020, following the current WMO climatology reference, obtained from GPCC V2020 (Schamm et al., 2014), CRU TS 4.08 (Harris et al., 2020), GPCP V.2.3 (Adler et al., 2018), and GHCN V4 (Menne et al., 2018) observed datasets. There is little consistency among

1018   datasets due to differences in input data, completeness of records, period of covered, and the gridding procedures

1019   applied (Sun et al., 2018; Nogueira, 2020). While the globally averaged land surface specific humidity has

1020   continuously increased (Dunn et al., 2024), global land precipitation has exhibited considerable interannual to

1021   interdecadal variability (Fig, 12). There was a positive anomaly in global land precipitation in 2024 but a negative

1022   anomaly in 2023. The former was contributed to by above-normal precipitation over the Asian and Australian

1023   monsoon region, likely associated with La Nina conditions, but was offset by dry conditions over South America and

1024   the southern part of Africa. The latter was driven by below normal precipitation over South Asia, Maritime Continents,

1025   the southern part of North America and the northern part of South America, due to El Niño conditions, with a

1026   corresponding increase in precipitation over the ocean (Adler and Gu, 2024).

1027
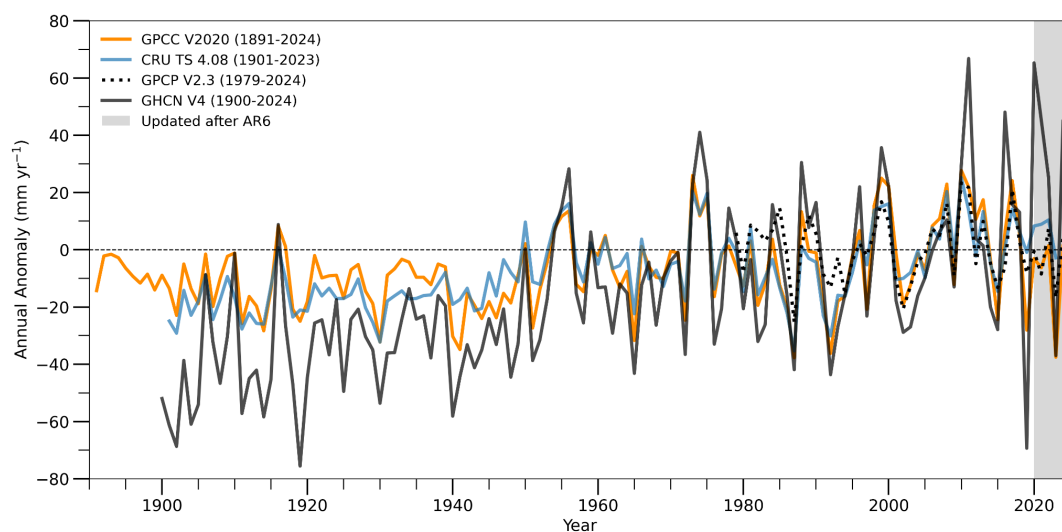
1028

1029

1030   **Figure 12 Time series of annual global land precipitation (mm yr⁻¹) from 1891 to date relative to a 1991-2020 climatology**

1031   **obtained from GPCP V2020, CRU TS 4.08, GPCP V2.3, and GHCN V4 (note that different products commence at distinct**

1032   **times). Annual global land precipitation for each observed data is estimated following the AR6 method except the period of**

1033   **climatology and updated from 2020 to 2024. In AR6, the reference period of the climatology was from 1981 to 2010.**

1034

1035   **12 Global mean sea-level rise**

1036   Global mean sea-level rise (GMSLR) is included in this annual update of AR6 for the first time. GMSLR is primarily

1037   driven by: (i) thermal expansion as the ocean warms; and (ii) increases in ocean mass associated with the addition of

1038   water or ice from land-based reservoirs, including glaciers and ice sheets (Fox-Kemper et al., 2021). Most of these

1039   processes are directly linked to changes in the global Earth energy inventory (Sect. 6). Sea-level rise can have large

1040   consequences for coastal ecosystems, safety and management, as it increases the baseline for sea-level extremes
1041   arising from short-term phenomena such as storm surges, waves and tides.
1042
1043   Observed GMSLR was assessed in IPCC AR6 WG1, in Chapter 2 (their Section 2.3.3.3, Gulev et al., 2021) and
1044   Chapter 9 (their Section 9.6.1 and Cross-Chapter Box 9.1, Fox-Kemper et al., 2021) on the basis of tide gauge
1045   reconstructions (up to 1993) and satellite altimeter observations (1993-2018). The assessment of GMSLR from tide
1046   gauge reconstructions used the ensemble approach presented by Palmer et al. (2021), which quantifies an ensemble
1047   and its uncertainties by combining an estimate of the structural uncertainty (informed by the ensemble spread) with
1048   an estimate of the internal uncertainty across the ensemble (i.e. the parametric uncertainty of each of the members in
1049   the ensemble). The members included in the tide gauge ensemble, which informed the total sea-level change estimate
1050   for the period 1901-1992, were reconstructions from Church and White (2011), Dangendorf et al (2019), Frederikse
1051   et al. (2020) and Hay et al. (2015). For the satellite period, from 1993 to 2018, AR6 used the estimate of the WCRP
1052   Global Sea Level Budget Group (2018), which was constructed from satellite-based GMSLR time series from six
1053   groups (AVISO/CNES, CSIRO, NASA/GSFC, NOAA, SL_cci/ESA and University of Colorado). Based on this
1054   information, AR6 concluded that GMSLR increased by 0.20 [0.15 to 0.25] m over the period 1901 to 2018, with a
1055   rate of 1.73 [1.28 to 2.17] mm yr^{-1} (*high confidence*). Periods closer to the present showed an accelerating GMSLR,
1056   with a rate of 2.3 [1.6 to 3.1] mm yr^{-1} over the period 1971–2018 increasing to 3.7 [3.2 to 4.2] mm yr^{-1} over the period
1057   2006–2018 (*high confidence*).
1058
1059   Here, we extend the AR6 GMSLR time series, which ended in 2018, closer to the present day. We use the same tide
1060   gauge-based ensemble estimate as in AR6 for the period up to 1993. We do note that two new reconstructions have
1061   been published recently, both providing rates in line with the AR6 assessment rates given above. The new GMSLR
1062   reconstruction by Dangendorf et al. (2024) uses a Kalman-smoother and adjusted estimates of the contributions of
1063   glacial isostatic adjustment, barystatic and sterodynamic changes to sea-level change and finds a trend of 1.50 ± 0.20
1064   mm/yr for the period 1900-2021. The new reconstruction by Wang et al. (2024) uses an updated vertical land motion
1065   correction and considers barystatic fingerprints and sterodynamic patterns from CMIP6 models and finds a trend of
1066   1.6 ± 0.2 mm/yr over 1900-2019.
1067
1068   The satellite record now provides observations up to the end of 2024, for three out of the six satellite data products
1069   used for the WCRP estimate used in AR6. The three records available to the end of 2024 are from NASA (2025),
1070   NOAA (2025) and AVISO (2025). All data was downloaded on 19 February 2025. We use the global mean time series
1071   based on the reference missions, with seasonal signals removed and corrected for glacial isostatic adjustment. We first
1072   compute annual averages and then an ensemble average time series, which is spliced to the AR6 GMSLR record
1073   ending in 2018. For consistency, we retain the uncertainties from the six-member WCRP ensemble and propagate
1074   them over the period 2019-2024. We note that reprocessing of the altimetry record is periodically required to account
1075   for new insights on instrument drift, retracking and geophysical corrections to the altimetry missions. This

1076   reprocessing may lead to small differences in the satellite altimeter record and the associated assessment of GMSLR

1077   in future iterations of IGCC.

1078

1079   Over the period 2019 to 2024 global mean sea level has increased by 26.1 [19.8 to 32.4] mm. When combining the

1080   AR6 estimate up to 2018 with the satellite time series for 2019-2024, we find a total GMSLR of 227.0 [176.4 to 229.6]

1081   mm for the period 1901-2024, which translates to an average rate of 1.85 [1.43 to 2.27] mm yr^{-1} (Table 10, Fig. 13).

1082   The rate increase associated with extending the time series by just 6 years, as well as the increasing rates over

1083   consecutive 20-yr periods (Fig. 13b), indicate a continuing acceleration of GMSLR. This is in line with the

1084   assessments of AR6 (Fox-Kemper et al., 2021), SROCC (Oppenheimer et al., 2019) and AR5 (Church et al., 2013)

1085   that sea-level change has been accelerating over course of the 20th and early 21st centuries, and consistent with the

1086   observed acceleration in some components of the Earth heat inventory (see Sect. 6).

1087

1088   **Table 10 Observed global mean sea-level rise (GMSLR) as presented in IPCC AR6, table 9.5 (Fox-Kemper et al., 2021)**
1089   **compared with the extended time series in this study. Values are expressed as the total change (Δ) in the annual mean**
1090   **over each period (mm) along with the equivalent rate calculated as the total change divided by the number of years (mm**
1091   **yr^{-1}). Uncertainties represent the *very likely* range.**

Observed GMSLR		IPCC AR6	This study
Start year		**End year 2018**	**End year 2024**
1901	Δ(mm)	201.9 [150.3 to 253.5]	227.0 [176.4 to 229.6]
	mm yr^{-1}	1.73 [1.28 to 2.17]	1.85 [1.43 to 2.27]
1971	Δ(mm)	109.6 [72.8 to 146.4]	135.8 [99.0 to 172.5]
	mm yr^{-1}	2.33 [1.55 to 3.12]	2.56 [1.87 to 3.26]
1993	Δ(mm)	81.2 [72.1 to 90.2]	107.3 [98.2 to 116.4]
	mm yr^{-1}	3.25 [2.88 to 3.61]	3.46 [3.17 to 3.75]
2006	Δ(mm)	44.3 [38.6 to 50.0]	70.4 [64.7 to 76.1]
	mm yr^{-1}	3.69 [3.21 to 4.17]	3.91 [3.59 to 4.23]

1092

1093
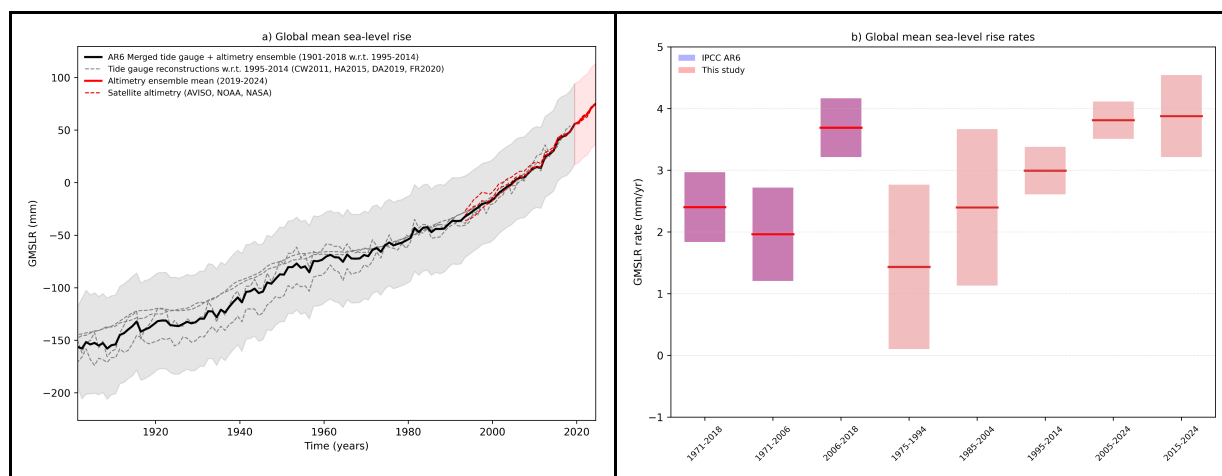
Figure 13 (a) Global mean sea-level rise time series 1901-2024 (mm). The GMSLR ensemble from AR6 in black, w.r.t. the period 1995-2014; the updated satellite altimetry ensemble in red, w.r.t. the AR6 ensemble in 2018. Individual time series are shown in dashed lines. (b) GMSLR rates (mm yr-1) for different periods. Uncertainties in a) show the *likely* range and in b) the *very likely* range, computed relative to 1901, including estimates of both structural uncertainty and parametric uncertainty (Palmer et al., 2021).

13 Code, data availability and visualisations

We publish a set of selected key indicators of global climate change via Climate Change Tracker (https://climatechangetracker.org/, Climate Change Tracker, 2025), a platform which aims to provide reliable, user-friendly, high-quality interactive dashboards, visualisations, data, and easily accessible insights of this paper.

With Climate Change Tracker we aim to reach a wider public audience, including policymakers involved in UNFCCC negotiations, and decision makers working in climate change mitigation and adaptation. Climate Change Tracker plans to update significant indicators multiple times throughout the year, providing an up-to-date picture of the indicators of climate change. Within the dashboards, all data is traceable to the underlying sources.

The carbon budget calculation is available from https://github.com/Rlamboll/AR6CarbonBudgetCalc/tree/v1.0.3 (Lamboll and Rogelj, 2025). The code and data used to produce other indicators are available in repositories under https://github.com/ClimateIndicator/data/releases/tag/v2025.04.30b (Smith et al., 2025b). All data are available from https://doi.org/10.5281/zenodo.15327155 (Smith et al., 2025a). Data are provided under the CC-BY 4.0 License.

HadEX3 [3.0.4] data were obtained from https://catalogue.ceda.ac.uk/uuid/115d5e4ebf7148ec941423ec86fa9f26 (Dunn et al., 2023) on 5 April 2023 and are © British Crown Copyright, Met Office, 2022, provided under an Open

1116   Government Licence; http://www.nationalarchives.gov.uk/doc/open-government-licence/version/2/ (last access: 2

1117   June 2023).

1118   **14 Discussion and conclusions**

1119   The third year of the Indicators of Global Climate Change (IGCC) initiative has built on previous years' efforts to

1120   provide a comprehensive update of the climate change indicators required to estimate the human-induced warming

1121   and the remaining carbon budget. Table 11 and Fig. 14 present a summary of the headline indicators from each section

1122   compared to those given in the AR6 assessment. Table 11 also summarises methodological updates.

1123

1124   **Table 11 Summary of headline results and methodological updates from the Indicators of Global Climate Change (IGCC)**
1125   **initiative.**

Climate Indicator	AR6 2021 assessment	This 2024 assessment	Explanation of changes	Methodological updates since AR6
GHG emissions **AR6 WGIII Chapter 2: Dhakal et al. (2022); see also Minx et al. (2021)**	**2010-2019 average:** **55.9 ± 6 GtCO₂e**	**2010-2019 average:** **52.9 ± 5.4 GtCO₂e** **2014-2023 average:** **53.6 ± 5.2 GtCO₂e**	**Average emissions in the past decade grew at a slower rate than in the previous decade. The change from AR6 is due to a systematic downward revision in CO₂-LULUCF and CH₄ estimates. Real-world emissions have slightly increased.**	**CO₂-LULUCF emissions revised down. CO₂ GCB Fossil Fuel and Industry emissions used instead of EDGAR. PRIMAP-hist TP used in place of EDGAR for CH₄ and N₂O emissions, atmospheric measurements taken for F-gas emissions. These changes reduce estimates by around 3 GtCO₂e (Sect. 2).**
GHG concentrations **AR6 WGI Chapter 2: Gulev et al. (2021)**	**2019:** **CO₂, 410.1 [± 0.36] ppm** **CH₄, 1866.3 [± 3.2] ppb** **N₂O, 332.1 [± 0.7] ppb**	**2024:** **CO₂, 422.8 [±0.4] ppm** **CH₄, 1929.8 [±3.3] ppb** **N₂O, 337.9 [±0.4] ppb**	**Increases caused by continued GHG anthropogenic emissions**	**Updates based on NOAA data and AGAGE (Sect. 3)**

Open Access Earth System Science Data Discussions

Effective radiative forcing change since 1750 **AR6 WGI Chapter 7: Forster et al. (2021)**	**2019:** **2.72 [1.96 to 3.48] W m^{-2}**	**2023:** **2.97 [2.05 to 3.76] W m^{-2}**	**Trend since 2019 is caused by increases in GHG concentrations and reductions in aerosol precursors.**	**Follows AR6 with minor update to aerosol precursor treatment and emissions dataset that revises 2019 ERF estimate relative to 1750 downwards (more negative) by 0.09 W m^{-2}. Added this year is a new method to estimate the ERF from land use surface reflection and irrigation to avoid scaling with cumulative emissions. This does not materially affect the ERF. (Sect. 5)**
Earth's energy imbalance **AR6 WGI Chapter 7: Forster et al. (2021)**	**2006-2018 average:** **0.79 [0.52 to 1.06] W m^{-2}**	**2012-2024 average:** **0.99 [0.70 to 1.28] W m^{-2}**	**A 25% increase in energy imbalance estimated based on increased rate of ocean heating.**	**Ocean heat content timeseries extended from 2018 to 2024 using all of the 5 AR6 datasets. Other heat inventory terms updated following von Schuckmann et al. (2023a). Ocean heat content uncertainty is used as a proxy for total uncertainty. Further details in Sect. 6.**
Global mean surface temperature change since 1850-1900 **AR6 WGI Chapter 2: Gulev et al. (2021)**	**2011-2020 average:** **1.09 [0.95 to 1.20] °C**	**2014-2023 average:** **1.24 [1.11 to 1.35] °C**	**An increase of 0.15 °C within four years, indicating a high decadal rate of change which may in part be internal variability.**	**Methods match four datasets used in AR6. Individual datasets have updated historical data, but these changes are not materially affecting results. (Sect. 7).**
Human induced global warming since preindustrial **AR6 WGI Chapter 3: Eyring et al. (2021)** **SR1.5 Chapter 1**	**2010-2019 decade average:** **1.07 [0.8 to 1.3] °C** **2017 single year: 1.0 [0.8 to 1.2] °C**	**2015-2024 decade average:** **1.22 [1.0 to 1.5] °C** **2024 single year: 1.36 [1.1 to 1.7] °C**	**An increase of 0.15 °C within five years, indicating a high decadal rate of change (broadly consistent with warming projections). The decadal warming rate increased slightly between 2019 and 2024. One of the three AR6 methods is diverging.**	**The three methods for the basis of the AR6 assessment are retained, but each has new input data (Sect. 8)**

Remaining carbon budget for 50% likelihood of limiting global warming to 1.5 °C AR6 WGI Chapter 5: Canadell et al. (2021)	From the start of 2020: 500 GtCO$_2$	From the start of 2025: 130 GtCO$_2$	The 1.5 °C budget is becoming very small. The RCB can exhaust before the 1.5 °C threshold is reached due to having to allow for future non-CO$_2$ warming.	Emulator and scenario change has reduced budget since 2020 by 100 GtCO$_2$ (Sect. 9)
Land average maximum temperature change compared to pre-industrial. AR6 WGI Chapter 11: Seneviratne et al., 2021	2009-2018 average: 1.55 °C	2015-2024 average: 1.90 °C	Rising at a substantially faster rate compared to global mean surface temperature	HadEX3 data used in AR6 replaced with ERA reanalysis data employed in this report which is more updatable going forward. Adds 0.01 °C to estimate (Sect. 10)
Global land precipitation compared to preindustrial (Douville et al., 2021)	Likely increased since the middle of the 20th century with a faster increase since the 1980s with large interannual variability	Large interannual variability associated with El Niño dominates the record in recent years, making long-term trend less clear	2023 exhibited a negative anomaly relative to preindustrial due El Niño conditions	The four datasets used in AR6 have been extended (Sect. 11)
Global mean sea-level rise since 1901 (Gulev et al., 2021; Fox-Kemper et al., 2021)	1901 to 2018 change 201.9 [150.3 to 253.5] mm at a rate of 1.73 [1.28 to 2.17] mm yr^{-1}	1901 to 2024 change 227.0 [176.4 to 229.6] mm at a rate of 1.85 [1.43 to 2.27] mm yr^{-1}	Sea-level rise continues to accelerate.	AR6 data extended with three of the six datasets from AR6, using latest satellite data (Sect. 12).

1126

1127

Key indicators of global climate change 2024: What's changed since AR6?

Human induced warming is increasing at the **unprecedented rate** of over 0.2°C per decade, the result of greenhouse gas emissions being at an all-time high over the last decade, as well as reductions in the strength of aerosol cooling.

Key greenhouse gas concentrations

	AR6	Now
CO_2	410.1 ppm	422.8 ppm
CH_4	1866.3 ppb	1929.8 ppb
N_2O	332.1 ppb	337.9 ppb

Effective radiative forcing
AR6: 2.72 W m^{-2}
Now: 2.97 W m^{-2}

Earth's energy imbalance
AR6: 0.79 W m^{-2}
Now: 0.99 W m^{-2}

Total greenhouse gas emissions
2010-2019 average: 53 GtCO$_2$e
2014-2023 average: 54 GtCO$_2$e

Remaining Carbon Budget for 1.5°C (50% likelihood)
AR6: 500 GtCO$_2$ (from start of 2020)
Now: 130 GtCO$_2$ (from start of 2025)

Human-induced warming
AR6: 1.07 °C
Now: 1.23 °C

Land average maximum temperature change
AR6: 1.55 °C
Now: 1.90 °C

Change in global mean surface temperature
AR6: 1.09 °C
Now: 1.24 °C

Global mean sea-level rise
1901-2018 change: 201.9mm at a rate of 1.73mm yr^{-1}
1901-2024 change: 227.0mm at a rate of 1.85mm yr^{-1}

1128

Figure 14 Infographic for the best estimate of headline indicators assessed in this paper.

Last year (2024) witnessed global surface temperatures likely exceeding 1.5 °C above preindustrial levels which has widely been reported in the press. Sects. 7 and 8. show that such high levels of global temperature anomalies are typical of what we expect from current best estimates of human induced warming, modulated by internal climate variability.

1134

1135   The overview of key indicators of the state of global climate indeed highlights the multiple fingerprints of the 2023-
1136   2024 El-Nino event regarding peak global surface temperature (Section 7.2), regional dry anomalies in land
1137   precipitation (Section 11), and their implications for reduced land carbon sinks and the record growth rate of
1138   atmospheric CO_2 concentrations in 2024 (Section 3).

1139   The overall increase in land maximum temperatures (Section 10), closely related to global warming levels, drives
1140   increasing trends in potential evapotranspiration, decreasing trends in soil moisture (Seo et al., 2025), contributing to
1141   the increased rate of global mean sea-level rise (Section 12).

1142   Methane and biomass emissions had a strong component of change related to climate feedbacks (Sects. 2 and 3). Such
1143   changes will become increasingly important over this century, even if the direct human influence declines. This year,
1144   we explored different inventory choices in Sect. 2. In future years a more consistent approach to attribution of
1145   atmospheric emissions, concentration change and radiative forcing should be developed, so it can be assessed in AR7.

1146   It is hoped that this update can support the science community in its collection and provision of reliable and timely
1147   global climate data. In future years we are particularly interested in improving SLCF updating methods to get a more
1148   accurate estimate of short-term ERF changes. The work also highlights the importance of high-quality metadata to
1149   document changes in methodological approaches over time. This year we have extended the datasets with land
1150   precipitation and global mean sealevel rise. In future years we hope to improve the robustness of the indicators
1151   presented here and could update other AR6 assessments. Parallel efforts could explore how we might update indicators
1152   of regional climate extremes and their attribution, which are particularly relevant for supporting actions on adaptation
1153   and loss and damage.

1154

1155   Generally, scientists and scientific organisations have an important role as "watchdogs" to critically inform evidence-
1156   based decision-making. This annual update traced to IPCC methods can provide a reliable, timely source of
1157   trustworthy information. It very much relies on continued support for high quality global monitoring networks of
1158   atmospheric and climate data, and also on open data sources that are regularly updated and easily accessed.

1159

1160   This is a critical decade: human-induced global warming rates are at their highest historical level, and 1.5 °C global
1161   warming might be expected to be reached or exceeded in around 5 years in the absence of cooling from major volcanic
1162   eruptions (Sects. 8 and 9). Yet this is also the decade when global GHG emissions could be expected to peak and
1163   begin to substantially decline. The indicators of global climate change presented here show that the Earth's energy
1164   imbalance has increased to around $1.0 \, \mathrm{W \, m^{-2}}$, averaged over the last 12 years (Sect. 5), which represents a 25%
1165   increase on the value assessed for 2006-2018 by AR6. This also has implications for the committed response of slow
1166   components in the climate system (glaciers, deep ocean, ice sheets) and committed long-term sea-level rise (through
1167   ocean thermal expansion and land-based ice melt/loss), to be addressed further in future updates. However, rapid and
1168   stringent GHG emission decreases such as those committed to at COP28 could halve warming rates over the next 20

Earth System
Science
Data

Open Access

Discussions

1169   years (McKenna et al., 2021). Table 1 shows that global GHG emissions are at a long-term high, yet there are signs

1170   that their rate of increase has slowed. Depending on the societal choices made in this critical decade, a continued series

1171   of these annual updates could track an improving trend for some of the indicators herein discussed.

1172   **Supplement**

1173   The supplement related to this article is available online.

1174   **Author contributions**

1175   PMF, CS, MA, PF, JR and AP developed the concept of an annual update in discussions with the wider IPCC

1176   community over many years. CS led the work of the data repositories. VMD, PZ, SS, CS, SIS, VN, AP, NPG, GPP,

1177   BT, MDP, KvS, JR, PF, MA, JCM, XZ, RAB, CB, CC, SB and PT provided important IPCC and UNFCCC framing.

1178   PMF coordinated the production of the manuscript with support from DR. WFL led Sect. 2 with contributions from

1179   PF, GPP, JG, JP, JCM and RA. CS led Sect. 3 with inputs from JM, PK, LW, PMF and MR. SS led Sect. 4 with inputs

1180   from VK, CS, GvdW, LAR and MG. CS led Sect. 5 with contributions from CW, TG, SS, VN and GvdW. KvS and

1181   MDP led Sect. 6 with contributions from LC, MI, JR, REK, AS, CMD, DPM and SEW. BT, CC and ZH led Sect. 7

1182   with contributions from PT, CM, CK, JK, RR, RV, AL and LC. TW led Sect. 8 with contributions and calculations

1183   from AR, NPG, SJ, CS and MA. RL led Sect. 9 with contributions from JR and HDM. Sect. 10 was led by MH, with

1184   contributions from SIS, and XZ. JYL, JEY, and RK led Sect. 11 with contributions from VMD, PT, and KvS. AS led

1185   Sect. 12 with contributions from MDP. All authors either edited or commented on the manuscript. DR, AB and JAB

1186   coordinated the data visualisation effort.

1187   **Competing interests**

1188   The contact author has declared that none of the authors has any competing interests.

1189   **Disclaimer**

1190   Publisher's note: Copernicus Publications remains neutral with regard to jurisdictional claims in published maps and

1191   institutional affiliations.

1192   **Acknowledgements**

References

1208   Acker, J. G. and Leptoukh, G.: Online analysis enhances use of NASA Earth science data, EoS Transactions, 88, 14–
1209   17, https://doi.org/10.1029/2007EO020003, 2007.

1210   Adler, R. F. and Gu, G.: Global precipitation for the year 2023 and how it relates to longer term variations and trends,
1211   Atmosphere, 15, 535, 2024.

1212   Adler, R. F., Sapiano, M. R. P., Huffman, J., Wang, J.-J., Gu G., Bolvin, D., Chiu, L., Schneider, U., Becker, A.,
1213   Nelkin, E., Xie, P., Ferrarok R., and Shin, D.-B.: The global precipitation climatology project (GPCP) monthly
1214   analysis (new version 2.3) and a review of 2017 global precipitation. Atmosphere, 9, 138,
1215   https://doi.org/10.3390/atmos9040138, 2018.

1216   Allen, M. R., O. P. Dube, W. Solecki, F. Aragón-Durand, W. Cramer, S. Humphreys, M. Kainuma, J. Kala, N.
1217   Mahowald, Y. Mulugetta, R. Perez, M. Wairiu, and K. Zickfeld, 2018: Framing and Context. In: Global Warming of
1218   1.5°C. An IPCC Special Report on the impacts of global warming of 1.5°C above pre-industrial levels and related
1219   global greenhouse gas emission pathways, in the context of strengthening the global response to the threat of climate
1220   change, sustainable development, and efforts to eradicate poverty [Masson-Delmotte, V., P. Zhai, H.-O. Pörtner, D.
1221   Roberts, J. Skea, P.R. Shukla, A. Pirani, W. Moufouma-Okia, C. Péan, R. Pidcock, S. Connors, J.B.R. Matthews, Y.
1222   Chen, X. Zhou, M.I. Gomis, E. Lonnoy, T. Maycock, M. Tignor, and T. Waterfield (eds.)], Cambridge University
1223   Press, Cambridge, UK and New York, NY, USA, 49-92, https://doi.org/10.1017/9781009157940.003, 2018.

1224   Allen, M. R., Frame, D. J., Friedlingstein, P., Gillett, N. P., Grassi, G., Gregory, J. M., Hare, W., House, J.,
1225   Huntingford, C., Jenkins, S., Jones, C. D., Knutti, R., Lowe, J. A., Matthews, H. D., Meinshausen, M., Meinshausen,
1226   N., Peters, G. P., Plattner, G.-K., Raper, S., Rogelj, J., Stott, P. A., Solomon, S., Stocker, T. F., Weaver, A. J., and
1227   Zickfeld, K.: Geological Net Zero and the need for disaggregated accounting for carbon sinks, Nature, 638, 343–350,
1228   https://doi.org/10.1038/s41586-024-08326-8, 2025.

1229   Allison, L. C., Palmer, M. D., Allan, R. P., Hermanson, L., Liu, C., and Smith, D. M.: Observations of planetary
1230   heating since the 1980s from multiple independent datasets, Environ. Res. Commun., 2, 101001,
1231   https://doi.org/10.1088/2515-7620/abbb39, 2020.

1232   AVISO: Mean sea-level product, https://www.aviso.altimetry.fr/en/data/products/ocean-indicators-products/mean-
1233   sea-level/data-acces.html, [data set], accessed 19 February 2025, 2025.

1234   Barnes, C., Boulanger, Y., Keeping, T., Gachon, P., Gillett, N., Haas, O., Wang, X., Roberge, F., Kew, S., Heinrich,
1235   D., Singh, R., Vahlberg, M., Van Aalst, M., Otto, F., Kimutai, J., Boucher, J., Kasoar, M., Zachariah, M., and Krikken,
1236   F.: Climate change more than doubled the likelihood of extreme fire weather conditions in Eastern Canada, Imperial
1237   College London, https://doi.org/10.25561/105981, 2023.

1238   Basu, S., Lan, X., Dlugokencky, E., Michel, S., Schwietzke, S., Miller, J. B., Bruhwiler, L., Oh, Y., Tans, P. P.,
1239   Apadula, F., Gatti, L. V., Jordan, A., Necki, J., Sasakawa, M., Morimoto, S., Di Iorio, T., Lee, H., Arduini, J., and
1240   Manca, G.: Estimating emissions of methane consistent with atmospheric measurements of methane and δ 13 C of
1241   methane, Atmos. Chem. Phys., 22, 15351–15377, https://doi.org/10.5194/acp-22-15351-2022, 2022.

1242   Bellouin, N., Davies, W., Shine, K. P., Quaas, J., Mülmenstädt, J., Forster, P. M., Smith, C., Lee, L., Regayre, L.,
1243   Brasseur, G., Sudarchikova, N., Bouarar, I., Boucher, O., and Myhre, G.: Radiative forcing of climate change from
1244   the Copernicus reanalysis of atmospheric composition, Earth Syst. Sci. Data, 12, 1649–1677,
1245   https://doi.org/10.5194/essd-12-1649-2020, 2020.

1246   Betts, R. A., Belcher, S. E., Hermanson, L., Klein Tank, A., Lowe, J. A., Jones, C. D., Morice, C. P., Rayner, N. A.,
1247   Scaife, A. A., and Stott, P. A.: Approaching 1.5 °C: how will we know we've reached this crucial warming mark?,
1248   Nature, 624, 33–35, https://doi.org/10.1038/d41586-023-03775-z, 2023.

1249   Bond, T. C., Doherty, S. J., Fahey, D. W., Forster, P. M., Berntsen, T., DeAngelo, B. J., Flanner, M. G., Ghan, S.,
1250   Kärcher, B., Koch, D., Kinne, S., Kondo, Y., Quinn, P. K., Sarofim, M. C., Schultz, M. G., Schulz, M., Venkataraman,
1251   C., Zhang, H., Zhang, S., Bellouin, N., Guttikunda, S. K., Hopke, P. K., Jacobson, M. Z., Kaiser, J. W., Klimont, Z.,
1252   Lohmann, U., Schwarz, J. P., Shindell, D., Storelvmo, T., Warren, S. G., and Zender, C. S.: Bounding the role of black
1253   carbon in the climate system: A scientific assessment, J. Geophys. Res.-Atmos., 118, 5380–5552,
1254   https://doi.org/10.1002/jgrd.50171, 2013.

1255   Bun, R., Marland, G., Oda, T., See, L., Puliafito, E., Nahorski, Z., Jonas, M., Kovalyshyn, V., Ialongo, I., Yashchun,
1256   O., and Romanchuk, Z.: Tracking unaccounted greenhouse gas emissions due to the war in Ukraine since 2022,
1257   Science of The Total Environment, 914, 169879, https://doi.org/10.1016/j.scitotenv.2024.169879, 2024.

1258   Burton, C., Lampe, S., Kelley, D. I., Thiery, W., Hantson, S., Christidis, N., Gudmundsson, L., Forrest, M., Burke,
1259   E., Chang, J., Huang, H., Ito, A., Kou-Giesbrecht, S., Lasslop, G., Li, W., Nieradzik, L., Li, F., Chen, Y., Randerson,
1260   J., Reyer, C. P. O., and Mengel, M.: Global burned area increasingly explained by climate change, Nat. Clim. Chang.,
1261   14, 1186–1192, https://doi.org/10.1038/s41558-024-02140-w, 2024.

1262   Canadell, J.G., P. M. S. Monteiro, M. H. Costa, L. Cotrim da Cunha, P. M. Cox, A.V. Eliseev, S. Henson, M. Ishii, S.
1263   Jaccard, C. Koven, A. Lohila, P. K. Patra, S. Piao, J. Rogelj, S. Syampungani, S. Zaehle, and K. Zickfeld: Global
1264   Carbon and other Biogeochemical Cycles and Feedbacks. In Climate Change 2021: The Physical Science Basis.
1265   Contribution of Working Group I to the Sixth Assessment Report of the Intergovernmental Panel on Climate Change
1266   [Masson-Delmotte, V., P. Zhai, A. Pirani, S.L. Connors, C. Péan, S. Berger, N. Caud, Y. Chen, L. Goldfarb, M.I.
1267   Gomis, M. Huang, K. Leitzell, E. Lonnoy, J.B.R. Matthews, T.K. Maycock, T. Waterfield, O. Yelekçi, R. Yu, and B.

1268 Zhou (eds.)]. Cambridge University Press, Cambridge, United Kingdom and New York, NY, USA, pp. 673–816,
1269 https://doi.org/10.1017/9781009157896.007, 2021.

1270 Cao, J., Wang, H., Wang, B., Zhao, H., Wang, C., and Zhu, X.: Higher sensitivity of Northern Hemisphere monsoon
1271 to anthropogenic aerosol than greenhouse gases, Geophys Res. Lett., 49, e2022GL100270.
1272 https://doi.org/10.1029/2022GL100270, 2022.

1273 Cattiaux, J., Ribes, A., and Cariou, E.: How Extreme Were Daily Global Temperatures in 2023 and Early 2024?,
1274 Geophysical Research Letters, 51, e2024GL110531, https://doi.org/10.1029/2024GL110531, 2024.

1275 Cheng, L., Abraham, J., Hausfather, Z., and Trenberth, K. E.: How fast are the oceans warming?, Science, 363, 128–
1276 129, https://doi.org/10.1126/science.aav7619, 2019.

1277 Cheng, L., Von Schuckmann, K., Abraham, J. P., Trenberth, K. E., Mann, M. E., Zanna, L., England, M. H., Zika, J.
1278 D., Fasullo, J. T., Yu, Y., Pan, Y., Zhu, J., Newsom, E. R., Bronselaer, B., and Lin, X.: Past and future ocean warming,
1279 Nat. Rev. Earth. Environ., 3, 776–794, https://doi.org/10.1038/s43017-022-00345-1, 2022.

1280 Church, J. A., White, N. J., Konikow, L. F., Domingues, C. M., Cogley, J. G., Rignot, E., Gregory, J. M., Van Den
1281 Broeke, M. R., Monaghan, A. J., and Velicogna, I.: Revisiting the Earth's sea-level and energy budgets from 1961 to
1282 2008: SEA-LEVEL AND ENERGY BUDGETS, Geophys. Res. Lett., 38, n/a-n/a,
1283 https://doi.org/10.1029/2011GL048794, 2011.

1284 Climate Change Tracker, https://climatechangetracker.org/igcc, accessed 20.05.2025, 2025.

1285 Collins, M., Knutti, R., Arblaster, J., Dufresne, J.-L., Fichefet, T., Friedlingstein, P., Gao, X., Gutowski, W.J., Johns,
1286 T., Krinner, G., Shongwe, M., Tebaldi, C., Weaver, A.J. & Wehner, M.: Long-term Climate Change: Projections,
1287 Commitments and Irreversibility. In: V.B. Stocker T.F., .D. Qin, G.K. Plattner, M. Tignor, S.K. Allen, J. Boschung,
1288 A. Nauels, Y. Xia & P.M. Midgley (eds.). Climate Change 2013: The Physical Science Basis. Contribution of Working
1289 Group I to the Fifth Assessment Report of the Intergovernmental Panel on Climate Change. Cambridge, United
1290 Kingdom and New York, NY, USA, Cambridge University Press. pp. 1029–1136, 2013.

1291 Crippa, M., Guizzardi, D., Schaaf, E., Monforti-Ferrario, F., Quadrelli, R., Risquez Martin, A., Rossi, S., Vignati, E.,
1292 Muntean, M., Brandao De Melo, J., Oom, D., Pagani, F., Banja, M., Taghavi-Moharamli, P., Köykkä, J., Grassi, G.,
1293 Branco, A., and San-Miguel, J.: GHG emissions of all world countries – 2023, Publications Office of the European
1294 Union, https://doi.org/doi/10.2760/953322, 2023.

1295 Cuesta-Valero, F. J., Beltrami, H., García-García, A., Krinner, G., Langer, M., MacDougall, A., Nitzbon, J., Peng, J.,
1296 von Schuckmann, K., Seneviratne, S., Thiery, W., Vanderkelen, I., Wu, T.: GCOS EHI 1960-2020 Continental Heat
1297 Content (Version 2), World Data Center for Climate (WDCC) at DKRZ,
1298 https://doi.org/10.26050/WDCC/GCOS_EHI_1960-2020_CoHC_v2, 2023.

1299 Dangendorf, S., Hay, C., Calafat, F. M., Marcos, M., Piecuch, C. G., Berk, K., and Jensen, J.: Persistent acceleration
1300 in global sea-level rise since the 1960s, Nat. Clim. Chang., 9, 705–710, https://doi.org/10.1038/s41558-019-0531-8,
1301 2019.

1302 Dangendorf, S., Sun, Q., Wahl, T., Thompson, P., Mitrovica, J. X., and Hamlington, B.: Probabilistic reconstruction
1303 of sea-level changes and their causes since 1900, Earth Syst. Sci. Data, 16, 3471–3494, https://doi.org/10.5194/essd-
1304 16-3471-2024, 2024.

1305 Deng, Z., Ciais, P., Tzompa-Sosa, Z. A., Saunois, M., Qiu, C., Tan, C., Sun, T., Ke, P., Cui, Y., Tanaka, K., Lin, X.,
1306 Thompson, R. L., Tian, H., Yao, Y., Huang, Y., Lauerwald, R., Jain, A. K., Xu, X., Bastos, A., Sitch, S., Palmer, P.
1307 I., Lauvaux, T., d'Aspremont, A., Giron, C., Benoit, A., Poulter, B., Chang, J., Petrescu, A. M. R., Davis, S. J., Liu,
1308 Z., Grassi, G., Albergel, C., Tubiello, F. N., Perugini, L., Peters, W., and Chevallier, F.: Comparing national
1309 greenhouse gas budgets reported in UNFCCC inventories against atmospheric inversions, Earth System Science Data,
1310 14, 1639–1675, https://doi.org/10.5194/essd-14-1639-2022, 2022.

1311 Deng, Z., Zhu, B., Davis, S. J., Ciais, P., Guan, D., Gong, P., and Liu, Z.: Global carbon emissions and decarbonization
1312 in 2024, Nat Rev Earth Environ, 6, 231–233, https://doi.org/10.1038/s43017-025-00658-x, 2025.

1313 Denier van der Gon, H., Gauss, M., Granier, C., Arellano, S., Benedictow, A., Darras, S., Dellaert, S., Guevara, M.,
1314 Jalkanen, J.-P., Krueger, K., Kuenen, J., Liaskoni, M., Liousse, C., Markova, J., Prieto Perez, A., Quack, B., Simpson,
1315 D., Sindelarova, K., and Soulie, A.: Documentation of CAMS emission inventory products,
1316 https://doi.org/10.24380/Q2SI-TI6I, 2023.

1317 Dhakal, S., J. C. Minx, F. L. Toth, A. Abdel-Aziz, M. J. Figueroa Meza, K. Hubacek, I. G. C. Jonckheere, Yong-Gun
1318 Kim, G. F. Nemet, S. Pachauri, X. C. Tan, T. Wiedmann: Emissions Trends and Drivers. In IPCC, 2022: Climate
1319 Change 2022: Mitigation of Climate Change. Contribution of Working Group III to the Sixth Assessment Report of
1320 the Intergovernmental Panel on Climate Change [P.R. Shukla, J. Skea, R. Slade, A. Al Khourdajie, R. van Diemen,
1321 D. McCollum, M. Pathak, S. Some, P. Vyas, R. Fradera, M. Belkacemi, A. Hasija, G. Lisboa, S. Luz, J. Malley,
1322 (eds.)]. Cambridge University Press, Cambridge, UK and New York, NY, USA,
1323 https://doi.org/10.1017/9781009157926.004, 2022.

1324 Douville, H., K. Raghavan, J. Renwick, R.P. Allan, P.A. Arias, M. Barlow, R. Cerezo-Mota, A. Cherchi, T.Y. Gan, J.
1325 Gergis, D. Jiang, A. Khan, W. Pokam Mba, D. Rosenfeld, J. Tierney, and O. Zolina: Water Cycle Changes. In Climate
1326 Change 2021: The Physical Science Basis. Contribution of Working Group I to the Sixth Assessment Report of the
1327 Intergovernmental Panel on Climate Change [Masson-Delmotte, V., P. Zhai, A. Pirani, S.L. Connors, C. Péan, S.
1328 Berger, N. Caud, Y. Chen, L. Goldfarb, M.I. Gomis, M. Huang, K. Leitzell, E. Lonnoy, J.B.R. Matthews, T.K.
1329 Maycock, T. Waterfield, O. Yelekçi, R. Yu, and B. Zhou (eds.)]. Cambridge University Press, Cambridge, United
1330 Kingdom and New York, NY, USA, pp. 1055–1210, https://doi.org/10.1017/9781009157896.010, 2021.

1331 Droste, E. S., Adcock, K. E., Ashfold, M. J., Chou, C., Fleming, Z., Fraser, P. J., Gooch, L. J., Hind, A. J., Langenfelds,
1332 R. L., Leedham Elvidge, E. C., Mohd Hanif, N., O'Doherty, S., Oram, D. E., Ou-Yang, C.-F., Panagi, M., Reeves, C.
1333 E., Sturges, W. T., and Laube, J. C.: Trends and emissions of six perfluorocarbons in the Northern Hemisphere and
1334 Southern Hemisphere, Atmos. Chem. Phys., 20, 4787–4807, https://doi.org/10.5194/acp-20-4787-2020, 2020.

1335 Dunn, R. J. H., Alexander, L. V., Donat, M. G., Zhang, X., Bador, M., Herold, N., Lippmann, T., Allan, R., Aguilar,
1336 E., Barry, A. A., Brunet, M., Caesar, J., Chagnaud, G., Cheng, V., Cinco, T., Durre, I., Guzman, R., Htay, T. M., Wan

Ibadullah, W. M., Bin Ibrahim, M. K. I., Khoshkam, M., Kruger, A., Kubota, H., Leng, T. W., Lim, G., Li-Sha, L., Marengo, J., Mbatha, S., McGree, S., Menne, M., Milagros Skansi, M., Ngwenya, S., Nkrumah, F., Oonariya, C., Pabon-Caicedo, J. D., Panthou, G., Pham, C., Rahimzadeh, F., Ramos, A., Salgado, E., Salinger, J., Sané, Y., Sopaheluwakan, A., Srivastava, A., Sun, Y., Timbal, B., Trachow, N., Trewin, B., Schrier, G., Vazquez-Aguirre, J., Vasquez, R., Villarroel, C., Vincent, L., Vischel, T., Vose, R., and Bin Hj Yussof, M. N.: Development of an updated global land in situ-based data set of temperature and precipitation extremes: HadEX3, J. Geophys. Res.-Atmos., 125, e2019JD032263, https://doi.org/10.1029/2019JD032263, 2020.

Dunn, R. J. H., Donat, M. G., and Alexander, L. V.: Comparing extremes indices in recent observational and reanalysis products, Front. Clim., 4, 98905, https://doi.org/10.3389/fclim.2022.989505, 2022.

Dunn, R.J.H., Alexander, L., Donat, M., Zhang, X., Bador, M., Herold, N., Lippmann, T., Allan, R.J., Aguilar, E., Aziz, A., Brunet, M., Caesar, J., Chagnaud, G., Cheng, V., Cinco, T., Durre, I., de Guzman, R., Htay, T.M., Wan Ibadullah, W.M., Bin Ibrahim, M.K.I., Khoshkam, M., Kruge, A., Kubota, H., Leng, T.W., Lim, G., Li-Sha, L., Marengo, J., Mbatha, S., McGree, S., Menne, M., de los Milagros Skansi, M., Ngwenya, S., Nkrumah, F., Oonariya, C., Pabon-Caicedo, J.D., Panthou, G., Pham, C., Rahimzadeh, F., Ramos, A., Salgado, E., Salinger, J., Sane, Y., Sopaheluwakan, A., Srivastava, A., Sun, Y., Trimbal, B., Trachow, N., Trewin, B., van der Schrier, G., Vazquez-Aguirre, J., Vasquez, R., Villarroel, C., Vincent, L., Vischel, T., Vose, R., Bin Hj Yussof, and M.N.A.: HadEX3: Global land-surface climate extremes indices v3.0.4 (1901-2018), NERC EDS Centre for Environmental Data Analysis [data set], https://dx.doi.org/10.5285/115d5e4ebf7148ec941423ec86fa9f26, 2023.

Dunn, R. J. H., Blannin, J., Gobron, N., Miller, J. B. and Willett, K. M. eds: Global climate [in "State of the Climate in 2023"]. Bull. Amer. Meteor. Soc., 105, S12-S155, https://doi.org/10.1175/BAMS-D-24-0116.1, 2024.

Dutton, G.S., B. D. Hall, S.A. Montzka, J. D. Nance, S. D. Clingan, K. M. Petersen, Combined Atmospheric Chloroflurocarbon-12 Dry Air Mole Fractions from the NOAA GML Halocarbons Sampling Network, 1977-2024, Version: 2024-03-07, https://doi.org/10.15138/PJ63-H440, 2024.

ECCAD: CAMS database version 6.2 (v6.2), https://permalink.aeris-data.fr/CAMS-GLOB-ANT, [data set], accessed 20 April 2025, 2025.

Eyring, V., N. P. Gillett, K.M. Achuta Rao, R. Barimalala, M. Barreiro Parrillo, N. Bellouin, C. Cassou, P. J. Durack, Y. Kosaka, S. McGregor, S. Min, O. Morgenstern, and Y. Sun: Human Influence on the Climate System. In Climate Change 2021: The Physical Science Basis. Contribution of Working Group I to the Sixth Assessment Report of the Intergovernmental Panel on Climate Change[Masson-Delmotte, V., P. Zhai, A. Pirani, S.L. Connors, C. Péan, S. Berger, N. Caud, Y. Chen, L. Goldfarb, M.I. Gomis, M. Huang, K. Leitzell, E. Lonnoy, J.B.R. Matthews, T.K. Maycock, T. Waterfield, O. Yelekçi, R. Yu, and B. Zhou (eds.)]. Cambridge University Press, Cambridge, United Kingdom and New York, NY, USA, pp. 423–552, http://doi:10.1017/9781009157896.005, 2021.

Feron, S., Malhotra, A., Bansal, S., Fluet-Chouinard, E., McNicol, G., Knox, S. H., Delwiche, K. B., Cordero, R. R., Ouyang, Z., Zhang, Z., Poulter, B., and Jackson, R. B.: Recent increases in annual, seasonal, and extreme methane

1371   fluxes driven by changes in climate and vegetation in boreal and temperate wetland ecosystems, Global Change

1372   Biology, 30, e17131, https://doi.org/10.1111/gcb.17131, 2024.

1373   Forster, P. M., Forster, H. I., Evans, M. J., Gidden, M. J., Jones, C. D., Keller, C. A., Lamboll, R. D., Le Quéré, C.,

1374   Rogelj, J., Rosen, D., Schleussner, C. F., Richardson, T. B., Smith, C. J. and Turnock, S. T.: Current and future global

1375   climate impacts resulting from COVID-19, Nature Clim. Chang, 10, 913–919, https://doi.org/10.1038/s41558-020-

1376   0883-0, 2020.

1377   Forster, P., T. Storelvmo, K. Armour, W. Collins, J.-L. Dufresne, D. Frame, D.J. Lunt, T. Mauritsen, M.D. Palmer,

1378   M. Watanabe, M. Wild, and H. Zhang, 2021: The Earth's Energy Budget, Climate Feedbacks, and Climate Sensitivity.

1379   In Climate Change 2021: The Physical Science Basis. Contribution of Working Group I to the Sixth Assessment

1380   Report of the Intergovernmental Panel on Climate Change [Masson-Delmotte, V., P. Zhai, A. Pirani, S.L. Connors,

1381   C. Péan, S. Berger, N. Caud, Y. Chen, L. Goldfarb, M.I. Gomis, M. Huang, K. Leitzell, E. Lonnoy, J.B.R. Matthews,

1382   T.K. Maycock, T. Waterfield, O. Yelekçi, R. Yu, and B. Zhou (eds.)]. Cambridge University Press, Cambridge, United

1383   Kingdom and New York, NY, USA, pp. 923–1054, https://doi.org/10.1017/9781009157896.009, 2021.

1384   Forster, P., Smith, C., Walsh, T., Lamb, W., Lamboll, R., Hauser, M., Ribes, A., Rosen, D., Gillett, N., Palmer, M.,

1385   Rogelj, J., von Schuckmann, K., Seneviratne, S., Trewin, B., Zhang, X., Allen, M., Andrew, R., Birt, A., Borger, A.,

1386   Boyer, T., Broersma, J., Cheng, L., Dentener, F., Friedlingstein, P., Gutiérrez, J., Gütschow, J., Hall, B., Ishii, M.,

1387   Jenkins, S., Lan, X., Lee, J.-Y., Morice, C., Kadow, C., Kennedy, J., Killick, R., Minx, J., Naik, V., Peters, G., Pirani,

1388   A., Pongratz, J., Schleussner, C.-F., Szopa, S., Thorne, P., Rohde, R., Rojas Corradi, M., Schumacher, D., Vose, R.,

1389   Zickfeld, K., Masson-Delmotte, V., and Zhai, P.: Indicators of Global Climate Change 2022: annual update of large-

1390   scale indicators of the state of the climate system and human influence, Earth System Science Data, 15, 2295–2327,

1391   https://doi.org/10.5194/essd-15-2295-2023, 2023.

1392   Forster, P. M., Smith, C., Walsh, T., Lamb, W. F., Lamboll, R., Hall, B., Hauser, M., Ribes, A., Rosen, D., Gillett, N.

1393   P., Palmer, M. D., Rogelj, J., Von Schuckmann, K., Trewin, B., Allen, M., Andrew, R., Betts, R. A., Borger, A.,

1394   Boyer, T., Broersma, J. A., Buontempo, C., Burgess, S., Cagnazzo, C., Cheng, L., Friedlingstein, P., Gettelman, A.,

1395   Gütschow, J., Ishii, M., Jenkins, S., Lan, X., Morice, C., Mühle, J., Kadow, C., Kennedy, J., Killick, R. E., Krummel,

1396   P. B., Minx, J. C., Myhre, G., Naik, V., Peters, G. P., Pirani, A., Pongratz, J., Schleussner, C.-F., Seneviratne, S. I.,

1397   Szopa, S., Thorne, P., Kovilakam, M. V. M., Majamäki, E., Jalkanen, J.-P., Van Marle, M., Hoesly, R. M., Rohde, R.,

1398   Schumacher, D., Van Der Werf, G., Vose, R., Zickfeld, K., Zhang, X., Masson-Delmotte, V., and Zhai, P.: Indicators

1399   of Global Climate Change 2023: annual update of key indicators of the state of the climate system and human

1400   influence, Earth Syst. Sci. Data, 16, 2625–2658, https://doi.org/10.5194/essd-16-2625-2024, 2024.

1401   Fox-Kemper, B.,Fox-Kemper, B., H. T. Hewitt, C. Xiao, G. Aðalgeirsdóttir, S.S. Drijfhout, T. L. Edwards, N. R.

1402   Golledge, M. Hemer, R. E. Kopp, G. Krinner, A. Mix, D. Notz, S. Nowicki, I. S. Nurhati, L. Ruiz, J.-B. Sallée, A. B.

1403   A. Slangen, and Y. Yu: Ocean, Cryosphere and Sea Level Change. In Climate Change 2021: The Physical Science

1404   Basis. Contribution of Working Group I to the Sixth Assessment Report of the Intergovernmental Panel on Climate

1405   Change [Masson-Delmotte, V., P. Zhai, A. Pirani, S.L. Connors, C. Péan, S. Berger, N. Caud, Y. Chen, L. Goldfarb,

1406   M.I. Gomis, M. Huang, K. Leitzell, E. Lonnoy, J. B. R. Matthews, T. K. Maycock, T. Waterfield, O. Yelekçi, R. Yu,

1407   and B. Zhou (eds.)]. Cambridge University Press, Cambridge, United Kingdom and New York, NY, USA, pp. 1211–

1408   1362, https://doi.org/10.1017/9781009157896.011, 2021.

1409   Francey, R.J., L.P. Steele, R.L. Langenfelds and B.C. Pak, High precision long-term monitoring of radiatively-active

1410   trace gases at surface sites and from ships and aircraft in the Southern Hemisphere atmosphere, J. Atmos. Science, 56,

1411   279-285 https://doi.org/10.1175/1520-0469(1999)056<0279:HPLTMO>2.0.CO;2, 1999.

1412   Frederikse, T., Landerer, F., Caron, L., Adhikari, S., Parkes, D., Humphrey, V. W., Dangendorf, S., Hogarth, P.,

1413   Zanna, L., Cheng, L., and Wu, Y.-H.: The causes of sea-level rise since 1900, Nature, 584, 393–397,

1414   https://doi.org/10.1038/s41586-020-2591-3, 2020.

1415   Friedlingstein, P., O'Sullivan, M., Jones, M. W., Andrew, R. M., Hauck, J., Olsen, A., Peters, G. P., Peters, W.,

1416   Pongratz, J., Sitch, S., Le Quéré, C., Canadell, J. G., Ciais, P., Jackson, R. B., Alin, S., Aragão, L. E. O. C., Arneth,

1417   A., Arora, V., Bates, N. R., Becker, M., Benoit-Cattin, A., Bittig, H. C., Bopp, L., Bultan, S., Chandra, N., Chevallier,

1418   F., Chini, L. P., Evans, W., Florentie, L., Forster, P. M., Gasser, T., Gehlen, M., Gilfillan, D., Gkritzalis, T., Gregor,

1419   L., Gruber, N., Harris, I., Hartung, K., Haverd, V., Houghton, R. A., Ilyina, T., Jain, A. K., Joetzjer, E., Kadono, K.,

1420   Kato, E., Kitidis, V., Korsbakken, J. I., Landschützer, P., Lefèvre, N., Lenton, A., Lienert, S., Liu, Z., Lombardozzi,

1421   D., Marland, G., Metzl, N., Munro, D. R., Nabel, J. E. M. S., Nakaoka, S.-I., Niwa, Y., O'Brien, K., Ono, T., Palmer,

1422   P. I., Pierrot, D., Poulter, B., Resplandy, L., Robertson, E., Rödenbeck, C., Schwinger, J., Séférian, R., Skjelvan, I.,

1423   Smith, A. J. P., Sutton, A. J., Tanhua, T., Tans, P. P., Tian, H., Tilbrook, B., van der Werf, G., Vuichard, N., Walker,

1424   A. P., Wanninkhof, R., Watson, A. J., Willis, D., Wiltshire, A. J., Yuan, W., Yue, X., and Zaehle, S.: Global carbon

1425   budget 2020, Earth Syst. Sci. Data, 12, 3269–3340, https://doi.org/10.5194/essd-12-3269-2020, 2020.

1426   Friedlingstein, P., O'Sullivan, M., Jones, M. W., Andrew, R. M., Gregor, L., Hauck, J., Le Quéré, C., Luijkx, I. T.,

1427   Olsen, A., Peters, G. P., Peters, W., Pongratz, J., Schwingshackl, C., Sitch, S., Canadell, J. G., Ciais, P., Jackson, R.

1428   B., Alin, S. R., Alkama, R., Arneth, A., Arora, V. K., Bates, N. R., Becker, M., Bellouin, N., Bittig, H. C., Bopp, L.,

1429   Chevallier, F., Chini, L. P., Cronin, M., Evans, W., Falk, S., Feely, R. A., Gasser, T., Gehlen, M., Gkritzalis, T.,

1430   Gloege, L., Grassi, G., Gruber, N., Gürses, Ö., Harris, I., Hefner, M., Houghton, R. A., Hurtt, G. C., Iida, Y., Ilyina,

1431   T., Jain, A. K., Jersild, A., Kadono, K., Kato, E., Kennedy, D., Klein Goldewijk, K., Knauer, J., Korsbakken, J. I.,

1432   Landschützer, P., Lefèvre, N., Lindsay, K., Liu, J., Liu, Z., Marland, G., Mayot, N., McGrath, M. J., Metzl, N.,

1433   Monacci, N. M., Munro, D. R., Nakaoka, S.-I., Niwa, Y., O'Brien, K., Ono, T., Palmer, P. I., Pan, N., Pierrot, D.,

1434   Pocock, K., Poulter, B., Resplandy, L., Robertson, E., Rödenbeck, C., Rodriguez, C., Rosan, T. M., Schwinger, J.,

1435   Séférian, R., Shutler, J. D., Skjelvan, I., Steinhoff, T., Sun, Q., Sutton, A. J., Sweeney, C., Takao, S., Tanhua, T., Tans,

1436   P. P., Tian, X., Tian, H., Tilbrook, B., Tsujino, H., Tubiello, F., van der Werf, G. R., Walker, A. P., Wanninkhof, R.,

1437   Whitehead, C., Willstrand Wranne, A., et al.: Global Carbon Budget 2022, Earth Syst. Sci. Data, 14, 4811–4900,

1438   https://doi.org/10.5194/essd-14-4811-2022, 2022.

1439   Friedlingstein, P., O'Sullivan, M., Jones, M. W., Andrew, R. M., Bakker, D. C. E., Hauck, J., Landschützer, P., Le

1440   Quéré, C., Luijkx, I. T., Peters, G. P., Peters, W., Pongratz, J., Schwingshackl, C., Sitch, S., Canadell, J. G., Ciais, P.,

1441   Jackson, R. B., Alin, S. R., Anthoni, P., Barbero, L., Bates, N. R., Becker, M., Bellouin, N., Decharme, B., Bopp, L.,

Brasika, I. B. M., Cadule, P., Chamberlain, M. A., Chandra, N., Chau, T.-T.-T., Chevallier, F., Chini, L. P., Cronin, M., Dou, X., Enyo, K., Evans, W., Falk, S., Feely, R. A., Feng, L., Ford, D. J., Gasser, T., Ghattas, J., Gkritzalis, T., Grassi, G., Gregor, L., Gruber, N., Gürses, Ö., Harris, I., Hefner, M., Heinke, J., Houghton, R. A., Hurtt, G. C., Iida, Y., Ilyina, T., Jacobson, A. R., Jain, A., Jarníková, T., Jersild, A., Jiang, F., Jin, Z., Joos, F., Kato, E., Keeling, R. F., Kennedy, D., Klein Goldewijk, K., Knauer, J., Korsbakken, J. I., Körtzinger, A., Lan, X., Lefèvre, N., Li, H., Liu, J., Liu, Z., Ma, L., Marland, G., Mayot, N., McGuire, P. C., McKinley, G. A., Meyer, G., Morgan, E. J., Munro, D. R., Nakaoka, S.-I., Niwa, Y., O'Brien, K. M., Olsen, A., Omar, A. M., Ono, T., Paulsen, M., Pierrot, D., Pocock, K., Poulter, B., Powis, C. M., Rehder, G., Resplandy, L., Robertson, E., Rödenbeck, C., Rosan, T. M., Schwinger, J., Séférian, R., et al.: Global Carbon Budget 2023, Earth System Science Data, 15, 5301–5369, https://doi.org/10.5194/essd-15-5301-2023, 2023.

Friedlingstein, P., O'Sullivan, M., Jones, M. W., Andrew, R. M., Hauck, J., Landschützer, P., Le Quéré, C., Li, H., Luijkx, I. T., Olsen, A., Peters, G. P., Peters, W., Pongratz, J., Schwingshackl, C., Sitch, S., Canadell, J. G., Ciais, P., Jackson, R. B., Alin, S. R., Arneth, A., Arora, V., Bates, N. R., Becker, M., Bellouin, N., Berghoff, C. F., Bittig, H. C., Bopp, L., Cadule, P., Campbell, K., Chamberlain, M. A., Chandra, N., Chevallier, F., Chini, L. P., Colligan, T., Decayeux, J., Djeutchouang, L. M., Dou, X., Duran Rojas, C., Enyo, K., Evans, W., Fay, A. R., Feely, R. A., Ford, D. J., Foster, A., Gasser, T., Gehlen, M., Gkritzalis, T., Grassi, G., Gregor, L., Gruber, N., Gürses, Ö., Harris, I., Hefner, M., Heinke, J., Hurtt, G. C., Iida, Y., Ilyina, T., Jacobson, A. R., Jain, A. K., Jarníková, T., Jersild, A., Jiang, F., Jin, Z., Kato, E., Keeling, R. F., Klein Goldewijk, K., Knauer, J., Korsbakken, J. I., Lan, X., Lauvset, S. K., Lefèvre, N., Liu, Z., Liu, J., Ma, L., Maksyutov, S., Marland, G., Mayot, N., McGuire, P. C., Metzl, N., Monacci, N. M., Morgan, E. J., Nakaoka, S.-I., Neill, C., Niwa, Y., Nützel, T., Olivier, L., Ono, T., Palmer, P. I., Pierrot, D., Qin, Z., Resplandy, L., Roobaert, A., Rosan, T. M., Rödenbeck, C., Schwinger, J., Smallman, T. L., Smith, S. M., Sospedra-Alfonso, R., Steinhoff, T., Sun, Q., Sutton, A. J., Séférian, R., Takao, S., Tatebe, H., Tian, H., Tilbrook, B., Torres, O., Tourigny, E., Tsujino, H., Tubiello, F., van der Werf, G., Wanninkhof, R., Wang, X., Yang, D., Yang, X., Yu, Z., Yuan, W., Yue, X., Zaehle, S., Zeng, N., and Zeng, J.: Global Carbon Budget 2024, Earth Syst. Sci. Data, 17, 965–1039, https://doi.org/10.5194/essd-17-965-2025, 2025.

Gasser, T., Crepin, L., Quilcaille, Y., Houghton, R. A., Ciais, P., and Obersteiner, M.: Historical CO2 emissions from land use and land cover change and their uncertainty, Biogeosciences, 17, 4075–4101, https://doi.org/10.5194/bg-17-4075-2020, 2020.

Gidden, M. J., Gasser, T., Grassi, G., Forsell, N., Janssens, I., Lamb, W. F., Minx, J., Nicholls, Z., Steinhauser, J., and Riahi, K.: Aligning climate scenarios to emissions inventories shifts global benchmarks, Nature, 624, 102–108, https://doi.org/10.1038/s41586-023-06724-y, 2023.

Gillett, N.P., Kirchmeier-Young, M., Ribes, A., Shiogama, H., Hegerl, G.C., Knutti, R., Gastineau, G., John, J.G., Li, L., Nazarenko, L., Rosenbloom, N., Seland, Ø., Wu, T., Yukimoto, S., and Ziehn, T.: Constraining human contributions to observed warming since the pre-industrial period, Nat. Clim. Chang., 11, 207–212, https://doi.org/10.1038/s41558-020-00965-9, 2021.

1478   Gleckler, P. J., Durack, P. J., Stouffer, R. J., Johnson, G. C., and Forest, C. E.: Industrial-era global ocean heat uptake
1479   doubles in recent decades, Nat. Clim. Chang., 6, 394–398, https://doi.org/10.1038/nclimate2915, 2016.

1480   Goessling, H. F., Rackow, T., and Jung, T.: Recent global temperature surge intensified by record-low planetary
1481   albedo, Science, 387, 68–73, https://doi.org/10.1126/science.adq7280, 2025.

1482   Grassi, G., Stehfest, E., Rogelj, J., Van Vuuren, D., Cescatti, A., House, J., Nabuurs, G.-J., Rossi, S., Alkama, R.,
1483   Viñas, R. A., Calvin, K., Ceccherini, G., Federici, S., Fujimori, S., Gusti, M., Hasegawa, T., Havlik, P., Humpenöder,
1484   F., Korosuo, A., Perugini, L., Tubiello, F. N., and Popp, A.: Critical adjustment of land mitigation pathways for
1485   assessing countries' climate progress, Nat. Clim. Chang., 11, 425–434, https://doi.org/10.1038/s41558-021-01033-6,
1486   2021.

1487   Grassi, G., Schwingshackl, C., Gasser, T., Houghton, R. A., Sitch, S., Canadell, J. G., Cescatti, A., Ciais, P., Federici,
1488   S., Friedlingstein, P., Kurz, W. A., Sanz Sanchez, M. J., Abad Viñas, R., Alkama, R., Bultan, S., Ceccherini, G., Falk,
1489   S., Kato, E., Kennedy, D., Knauer, J., Korosuo, A., Melo, J., McGrath, M. J., Nabel, J. E. M. S., Poulter, B.,
1490   Romanovskaya, A. A., Rossi, S., Tian, H., Walker, A. P., Yuan, W., Yue, X., and Pongratz, J.: Harmonising the land-
1491   use flux estimates of global models and national inventories for 2000–2020, Earth Syst. Sci. Data, 15, 1093–1114,
1492   https://doi.org/10.5194/essd-15-1093-2023, 2023.

1493   Guinaldo, T., Cassou, C., Sallée, J.-B., and Liné, A.: Internal variability effect doped by climate change drove the
1494   2023 marine heat extreme in the North Atlantic, Commun Earth Environ, 6, 291, https://doi.org/10.1038/s43247-025-
1495   02197-1, 2025.

1496   Gulev, S. K., P. W. Thorne, J. Ahn, F. J. Dentener, C. M. Domingues, S. Gerland, D. Gong, D. S. Kaufman, H. C.
1497   Nnamchi, J. Quaas, J.A. Rivera, S. Sathyendranath, S.L. Smith, B. Trewin, K. von Schuckmann, and R. S. Vose:
1498   Changing State of the Climate System. In Climate Change 2021: The Physical Science Basis. Contribution of Working
1499   Group I to the Sixth Assessment Report of the Intergovernmental Panel on Climate Change[Masson-Delmotte, V., P.
1500   Zhai, A. Pirani, S.L. Connors, C. Péan, S. Berger, N. Caud, Y. Chen, L. Goldfarb, M.I. Gomis, M. Huang, K. Leitzell,
1501   E. Lonnoy, J.B.R. Matthews, T.K. Maycock, T. Waterfield, O. Yelekçi, R. Yu, and B. Zhou (eds.)]. Cambridge
1502   University Press, Cambridge, United Kingdom and New York, NY, USA, pp. 287–422,
1503   https://doi.org/10.1017/9781009157896.004, 2021.

1504   Gupta, A. K., Mittal, T., Fauria, K. E., Bennartz, R., and Kok, J. F.: The January 2022 Hunga eruption cooled the
1505   southern hemisphere in 2022 and 2023, Commun Earth Environ, 6, 240, https://doi.org/10.1038/s43247-025-02181-
1506   9, 2025.

1507   Gütschow, J., Jeffery, M. L., Gieseke, R., Gebel, R., Stevens, D., Krapp, M., and Rocha, M.: The PRIMAP-hist
1508   national historical emissions time series, Earth Syst. Sci. Data, 8, 571–603, https://doi.org/10.5194/essd-8-571-2016,
1509   2016.

1510   Gütschow, J., and Busch, D., and Pflüger, M.: The PRIMAP-hist national historical emissions time series v2.6.1
1511   (1750-2023) (2.6.1), Zenodo [data set] https://doi.org/10.5281/zenodo.15016289, 2025.

Hardy, A., Palmer, P. I., and Oakes, G.: Satellite data reveal how Sudd wetland dynamics are linked with globally-significant methane emissions, Environ. Res. Lett., 18, 074044, https://doi.org/10.1088/1748-9326/ace272, 2023.

Hay, C. C., Morrow, E., Kopp, R. E., and Mitrovica, J. X.: Probabilistic reanalysis of twentieth-century sea-level rise, Nature, 517, 481–484, https://doi.org/10.1038/nature14093, 2015.

Hakuba, M. Z., Frederikse, T., and Landerer, F. W.: Earth's energy imbalance from the ocean perspective (2005–2019), Geophys Res Lett, 48, e2021GL093624, https://doi.org/10.1029/2021GL093624, 2021.

Hansen, J. E., Sato, M., Simons, L., Nazarenko, L. S., Sangha, I., Kharecha, P., Zachos, J. C., von Schuckmann, K., Loeb, N. G., Osman, M. B., Jin, Q., Tselioudis, G., Jeong, E., Lacis, A., Ruedy, R., Russell, G., Cao, J., and Li, J.: Global warming in the pipeline, Oxford Open Climate Change, 3, kgad008, https://doi.org/10.1093/oxfclm/kgad008, 2023.

Hansis, E., Davis, S. J., and Pongratz, J.: Relevance of methodological choices for accounting of land use change carbon fluxes, Global Biogeochem. Cy., 29, 1230–1246, https://doi.org/10.1002/2014GB004997, 2015.

Haustein, K., Allen, M. R., Forster, P. M., Otto, F. E. L., Mitchell, D. M., Matthews, H. D., and Frame, D. J.: A real-time Global Warming Index, Sci Rep, 7, 15417, https://doi.org/10.1038/s41598-017-14828-5, 2017.

Harris, I., Osborn, T. J., Jones, P., and Lister, D.: Version 4 of the CRU TS monthly high-resolution gridded multivariate climate dataset, Scientific data, 7, 109, https://doi.org/10.1038/s41597-020-045303, 2020

Hersbach, H., Bell, B., Berrisford, P., Hirahara, S., Horányi, A., Muñoz-Sabater, J., Nicolas, J., Peubey, C., Radu, R., Schepers, D., Simmons, A., Soci, C., Abdalla, S., Abellan, X., Balsamo, G., Bechtold, P., Biavati, G., Bidlot, J., Bonavita, M., De Chiara, G., Dahlgren, P., Dee, D., Diamantakis, M., Dragani, R., Flemming, J., Forbes, R., Fuentes, M., Geer, A., Haimberger, L., Healy, S., Hogan, R. J., Hólm, E., Janisková, M., Keeley, S., Laloyaux, P., Lopez, P., Lupu, C., Radnoti, G., de Rosnay, P., Rozum, I., Vamborg, F., Villaume, S., and Thépaut, J.-N.: The ERA5 global reanalysis, Q. J. R. Meteorol. Soc., 146, 1999–2049, https://doi.org/10.1002/qj.3803, 2020.

Hodnebrog, Ø., Aamaas, B., Fuglestvedt, J. S., Marston, G., Myhre, G., Nielsen, C. J., Sandstad, M., Shine, K. P., and Wallington, T. J.: Updated Global Warming Potentials and Radiative Efficiencies of Halocarbons and Other Weak Atmospheric Absorbers, Rev. Geophys., 58, e2019RG000691, https://doi.org/10.1029/2019RG000691, 2020.

Hodnebrog, Ø., Myhre, G., Jouan, C., Andrews, T., Forster, P. M., Jia, H., Loeb, N. G., Olivié, D. J. L., Paynter, D., Quaas, J., Raghuraman, S. P., and Schulz, M.: Recent reductions in aerosol emissions have increased Earth's energy imbalance, Communications Earth & Environment, 5, 166, https://doi.org/10.1038/s43247-024-01324-8, 2024.

Hoesly, R., Smith, S. J., Ahsan, H., Prime, N., O'Rourke, P., Crippa, M., Klimont, Z., Guizzardi, D., Feng, L., Harkins, C., MCDONALD, B., and Wang, S.: CEDS v_2025_03_18 Aggregate Data (v_2025_03_18), https://doi.org/10.5281/ZENODO.15059443, 2025.

Hoesly, R. M., Smith, S. J., Feng, L., Klimont, Z., Janssens-Maenhout, G., Pitkanen, T., Seibert, J. J., Vu, L., Andres, R. J., Bolt, R. M., Bond, T. C., Dawidowski, L., Kholod, N., Kurokawa, J.-I., Li, M., Liu, L., Lu, Z., Moura, M. C. P., O'Rourke, P. R., and Zhang, Q.: Historical (1750–2014) anthropogenic emissions of reactive gases and aerosols from

the Community Emissions Data System (CEDS), Geosci. Model. Dev., 11, 369–408, https://doi.org/10.5194/gmd-11-369-2018, 2018.

Hoesly, R., & Smith, S., CEDS v_2024_04_01 Release Emission Data (v_2024_04_01) [Data set], Zenodo. https://doi.org/10.5281/zenodo.10904361, 2024.

Houghton, R. A., and Nassikas, A. A.: Global and regional fluxes of carbon from land use and land cover change 1850–2015, Global Biogeochem. Cy., 31, 456– 472, https://doi.org/10.1002/2016GB005546, 2017.

Houghton, R. A. and Castanho, A.: Annual emissions of carbon from land use, land-use change, and forestry from 1850 to 2020, Earth System Science Data, 15, 2025–2054, https://doi.org/10.5194/essd-15-2025-2023, 2023.

Hu, Y., Yue, X., Tian, C., Zhou, H., Fu, W., Zhao, X., Zhao, Y., and Chen, Y.: Identifying the main drivers of the spatiotemporal variations in wetland methane emissions during 2001–2020, Frontiers in Environmental Science, 11, https://doi.org/10.3389/fenvs.2023.1275742, 2023.

Huang, B., Yin, X., Boyer, T., Liu, C., Menne, M., Rao, Y. D., Smith, T., Vose, R., and Zhang, H.-M.: Extended Reconstructed Sea Surface Temperature, Version 6 (ERSSTv6). Part I: An Artificial Neural Network Approach, Journal of Climate, 38, 1105–1121, https://doi.org/10.1175/JCLI-D-23-0707.1, 2025.

IATA: Air Passenger Monthly Analysis March 2024, https://www.iata.org/en/iata-repository/publications/economic-reports/air-passenger-market-analysis-march-2024/, accessed 20.05.2024, 2024.

IEA: CO2 Emissions in 2023. https://www.iea.org/reports/co2-emissions-in-2023, accessed 20.04.2024, 2024.

IPCC: Sixty-second Session of the IPCC (IPCC-62), Fifteenth Session of the IPCC Working Group I (WGI-15), Thirteenth Session of the IPCC Working Group II (WGII-13), and Fifteenth Session of the IPCC Working Group III (WGIII-15), https://www.ipcc.ch/meeting-doc/ipcc-62/, accessed 20 April 2025, 2025.

IPCC: Climate Change 2013: The Physical Science Basis. Contribution of Working Group I to the Fifth Assessment Report of the Intergovernmental Panel on Climate Change [Stocker, T.F., D. Qin, G.-K. Plattner, M. Tignor, S.K. Allen, J. Boschung, A. Nauels, Y. Xia, V. Bex and P.M. Midgley (eds.)]. Cambridge University Press, Cambridge, United Kingdom and New York, NY, USA, 1535 pp, https://doi:10.1017/CBO9781107415324, 2013.

IPCC: Summary for Policymakers. In: Global Warming of 1.5°C. An IPCC Special Report on the impacts of global warming of 1.5°C above pre-industrial levels and related global greenhouse gas emission pathways, in the context of strengthening the global response to the threat of climate change, sustainable development, and efforts to eradicate poverty [Masson-Delmotte, V., P. Zhai, H.-O. Pörtner, D. Roberts, J. Skea, P.R. Shukla, A. Pirani, W. Moufouma-Okia, C. Péan, R. Pidcock, S. Connors, J.B.R. Matthews, Y. Chen, X. Zhou, M.I. Gomis, E. Lonnoy, T. Maycock, M. Tignor, and T. Waterfield (eds.)]. Cambridge University Press, Cambridge, UK and New York, NY, USA, pp. 3-24, https://doi.org/10.1017/9781009157940.001, 2018.

IPCC: Climate Change 2021: The Physical Science Basis. Contribution of Working Group I to the Sixth Assessment Report of the Intergovernmental Panel on Climate Change, Cambridge University Press, Cambridge, United Kingdom and New York, NY, USA, https://doi.org/10.1017/9781009157896, 2021a.

1580   IPCC: Summary for Policymakers, in: Climate Change 2021: The Physical Science Basis. Contribution of Working
1581   Group I to the Sixth Assessment Report of the Intergovernmental Panel on Climate Change, edited by: Masson-
1582   Delmotte, V., Zhai, P., Pirani, A., Connors, S. L., Péan, C., Berger, S., Caud, N., Chen, Y., Goldfarb, L., Gomis, M.
1583   I., Huang, M., Leitzell, K., Lonnoy, E., Matthews, J. B. R., Maycock, T. K., Waterfield, T., Yelekçi, O., Yu, R., and
1584   Zhou, B., Cambridge University Press, Cambridge, United Kingdom and New York, NY, USA, pp.3−32
1585   https://doi.org/10.1017/9781009157896.001, 2021b.

1586   IPCC: Climate Change 2022: Impacts, Adaptation, and Vulnerability. Contribution of Working Group II to the Sixth
1587   Assessment Report of the Intergovernmental Panel on Climate Change [H.-O. Pörtner, D.C. Roberts, M. Tignor, E.S.
1588   Poloczanska, K. Mintenbeck, A. Alegría, M. Craig, S. Langsdorf, S. Löschke, V. Möller, A. Okem, B. Rama (eds.)].
1589   Cambridge University Press. Cambridge University Press, Cambridge, UK and New York, NY, USA, 3056 pp.,
1590   https://doi:10.1017/9781009325844, 2022.

1591   IPCC, 2023: Climate Change 2023: Synthesis Report. Contribution of Working Groups I, II and III to the Sixth
1592   Assessment Report of the Intergovernmental Panel on Climate Change [Core Writing Team, H. Lee and J. Romero
1593   (eds.)].   IPCC,   Geneva,   Switzerland.,   Intergovernmental   Panel   on   Climate   Change   (IPCC),
1594   https://doi.org/10.59327/IPCC/AR6-9789291691647, 2023a.

1595   IPCC, 2023: Climate Change 2023: Summary for Policy Makers. Contribution of Working Groups I, II and III to the
1596   Sixth Assessment Report of the Intergovernmental Panel on Climate Change [Core Writing Team, H. Lee and J.
1597   Romero   (eds.)].   IPCC,   Geneva,   Switzerland.,   Intergovernmental   Panel   on   Climate   Change   (IPCC),
1598   https://doi.org/10.59327/IPCC/AR6-9789291691647, 2023b.

1599   Iturbide, M., Fernández, J., Gutiérrez, J. M., Pirani, A., Huard, D., Al Khourdajie, A., Baño-Medina, J., Bedia, J.,
1600   Casanueva, A., Cimadevilla, E., Cofiño, A. S., De Felice, M., Diez-Sierra, J., García-Díez, M., Goldie, J., Herrera, D.
1601   A., Herrera, S., Manzanas, R., Milovac, J., Radhakrishnan, A., San-Martín, D., Spinuso, A., Thyng, K. M., Trenham,
1602   C., and Yelekçi, Ö.: Implementation of FAIR principles in the IPCC: the WGI AR6 Atlas repository, Sci Data, 9, 629,
1603   https://doi.org/10.1038/s41597-022-01739-y, 2022.

1604   Janardanan, R., Maksyutov, S., Wang, F., Nayagam, L., Sahu, S. K., Mangaraj, P., Saunois, M., Lan, X., and
1605   Matsunaga, T.: Country-level methane emissions and their sectoral trends during 2009–2020 estimated by high-
1606   resolution   inversion   of   GOSAT   and   surface   observations,   Environ.   Res.   Lett.,   19,   034007,
1607   https://doi.org/10.1088/1748-9326/ad2436, 2024.

1608   Jenkins, S., Povey, A., Gettelman, A., Grainger, R., Stier, P., and Allen, M.: Is Anthropogenic Global Warming
1609   Accelerating?, Journal of Climate, 35, 7873–7890, https://doi.org/10.1175/JCLI-D-22-0081.1, 2022.

1610   Jenkins, S., Smith, C., Allen, M., and Grainger, R.: Tonga eruption increases chance of temporary surface temperature
1611   anomaly above 1.5 °C, Nature Clim. Chang., 13, 127–129, https://doi.org/10.1038/s41558-022-01568-2, 2023.

1612   Kirchengast, G., Gorfer, M., Mayer, M., Steiner, A. K., and Haimberger, L.: GCOS EHI 1960-2020 Atmospheric Heat
1613   Content, https://doi.org/10.26050/WDCC/GCOS_EHI_1960-2020_AHC, 2022.

Kramer, R. J., He, H., Soden, B. J., Oreopoulos, L., Myhre, G., Forster, P. M., and Smith, C. J., Observational evidence of increasing global radiative forcing, Geophys. Res. Lett., 48, e2020GL091585, https://doi.org/10.1029/2020GL091585, 2021.

Lamb, W., Andrew, R., Jones, M., Nicholls, Z., Peters, G., Smith, C., Saunois, M., Grassi, G., Pongratz, J., Smith, S., Tubiello, F., Crippa, M., Gidden, M., Friedlingstein, P., Minx, J., and Forster, P.: Differences in anthropogenic greenhouse gas emissions estimates explained, https://doi.org/10.5194/essd-2025-188, 24 April 2025.

Lamboll, R. D., Jones, C. D., Skeie, R. B., Fiedler, S., Samset, B. H., Gillett, N. P., Rogelj, J., and Forster, P. M.: Modifying emissions scenario projections to account for the effects of COVID-19: protocol for CovidMIP, Geoscientific Model Development, 14, 3683–3695, https://doi.org/10.5194/gmd-14-3683-2021, 2021.

Lamboll, R. D. and Rogelj, J.: Code for estimation of remaining carbon budget in IPCC AR6 WGI, Zenodo [code], https://doi.org/10.5281/zenodo.6373365, 2022.

Lamboll, R. and Rogelj, J.: Carbon Budget Calculator, 2025, Github [code], https://github.com/Rlamboll/AR6CarbonBudgetCalc/tree/v1.0.1, last access: 25 April 2025, 2025.

Lamboll, R. D., Nicholls, Z. R. J., Smith, C. J., Kikstra, J. S., Byers, E., and Rogelj, J.: Assessing the size and uncertainty of remaining carbon budgets, Nature Climate Change, 13, 1360–1367, https://doi.org/10.1038/s41558-023-01848-5, 2023.

Lan, X., Tans, P. and Thoning, K.W.: Trends in globally-averaged CO_2 determined from NOAA Global Monitoring Laboratory measurements, Version Monday, 14-Apr-2025 09:08:57 MDT https://doi.org/10.15138/9N0H-ZH07, 2025.

Lan, X., Thoning, K. W., and Dlugokencky, E.J.: Trends in globally-averaged CH4 N2O, and SF6 determined from NOAA Global Monitoring Laboratory measurements, Version 2023-04, https://doi.org/10.15138/P8XG-AA10, 2023b.

Laube, J., Newland, M., Hogan, C., Brenninkmeijer, A.M., Fraser, P.J., Martinerie, P., Oram, D.E., Reeves, C.E., Röckmann, T., Schwander, J., Witrant, E., Sturges, W.T.: Newly detected ozone-depleting substances in the atmosphere. Nature Geosci., 7, 266–269, https://doi.org/10.1038/ngeo2109, 2014.

Lee, J.-Y., J. Marotzke, G. Bala, L. Cao, S. Corti, J.P. Dunne, F. Engelbrecht, E. Fischer, J.C. Fyfe, C. Jones, A. Maycock, J. Mutemi, O. Ndiaye, S. Panickal, and T. Zhou: Future Global Climate: Scenario-Based Projections and Near-Term Information. In Climate Change 2021: The Physical Science Basis. Contribution of Working Group I to the Sixth Assessment Report of the Intergovernmental Panel on Climate Change[Masson-Delmotte, V., P. Zhai, A. Pirani, S.L. Connors, C. Péan, S. Berger, N. Caud, Y. Chen, L. Goldfarb, M.I. Gomis, M. Huang, K. Leitzell, E. Lonnoy, J.B.R. Matthews, T.K. Maycock, T. Waterfield, O. Yelekçi, R. Yu, and B. Zhou (eds.)]. Cambridge University Press, Cambridge, United Kingdom and New York, NY, USA, pp. 553–672,https://doi.org/10.1017/9781009157896.006, 2021.

Lee, H., K. Calvin, D. Dasgupta, G. Krinner, A. Mukherji, P. Thorne, C. Trisos, J. Romero, P. Aldunce, K. Barrett, G. Blanco, W.W.L. Cheung, S.L. Connors, F. Denton, A. Diongue-Niang, D. Dodman, M. Garschagen, O. Geden, B.

Earth System
Science
Data
Open Access
Discussions

1649   Hayward, C. Jones, F. Jotzo, T. Krug, R. Lasco, J.-Y. Lee, V. Masson-Delmotte, M. Meinshausen, K. Mintenbeck, A.
1650   Mokssit, F.E.L. Otto, M. Pathak, A. Pirani, E. Poloczanska, H.-O. Pörtner, A. Revi, D.C. Roberts, J. Roy, A.C. Ruane,
1651   J. Skea, P.R. Shukla, R. Slade, A. Slangen, Y. Sokona, A.A. Sörensson, M. Tignor, D. van Vuuren, Y.-M. Wei, H.
1652   Winkler, P. Zhai, and Z. Zommers: Synthesis Report of the IPCC Sixth Assessment Report (AR6): Summary for
1653   Policymakers.   Intergovernmental   Panel   on   Climate   Change   [accepted],   available   at
1654   https://www.ipcc.ch/report/ar6/syr/, 2023.

1655   Liu, Z., Deng, Z., Davis, S. J., and Ciais, P.: Global carbon emissions in 2023, Nature Reviews Earth & Environment,
1656   5, 253–254, https://doi.org/10.1038/s43017-024-00532-2, 2024.

1657   Loeb, N. G., Johnson, G. C., Thorsen, T. J., Lyman, J. M., Rose, F. G., Kato, S.: Satellite and ocean data reveal marked
1658   increase in Earth's heating rate. Geophys. Res. Lett., 48, e2021GL093047, https://doi.org/10.1029/2021GL093047,
1659   2021.

1660   van Marle, M. J. E., Kloster, S., Magi, B. I., Marlon, J. R., Daniau, A.-L., Field, R. D., Arneth, A., Forrest, M.,
1661   Hantson, S., Kehrwald, N. M., Knorr, W., Lasslop, G., Li, F., Mangeon, S., Yue, C., Kaiser, J. W., and van der Werf,
1662   G. R.: Historic global biomass burning emissions for CMIP6 (BB4CMIP) based on merging satellite observations
1663   with proxies and fire models (1750–2015), Geosci. Model Dev., 10, 3329–3357, https://doi.org/10.5194/gmd-10-
1664   3329-2017, 2017.

1665   McKenna, C. M., Maycock, A. C., Forster, P. M., Smith, C. J., and Tokarska, K. B.: Stringent mitigation substantially
1666   reduces   risk   of   unprecedented   near-term   warming   rates,   Nature   Climate   Change,   11,   126–131,
1667   https://doi.org/10.1038/s41558-020-00957-9, 2021.

1668   Menne, M. J., Williams, C. N., Gleason, B. E., Rennie, J. J., and Lawrimore, J. H.: The global historical climatology
1669   network monthly temperature dataset, version 4, J. Climate, 31, 9835-9854, https://doi.org/10.1175/JCLI-D-18-
1670   0094.1, 2018.

1671   Minière, A., von Schuckmann, K., Sallée, J.-B., and Vogt, L.: Robust acceleration of Earth system heating observed
1672   over the past six decades, Scientific Reports, 13, 22975, https://doi.org/10.1038/s41598-023-49353-1, 2023.

1673   Minobe, S., Behrens, E., Findell, K. L., Loeb, N. G., Meyssignac, B., and Sutton, R.: Global and regional drivers for
1674   exceptional climate extremes in 2023-2024: beyond the new normal, npj Clim Atmos Sci, 8, 138,
1675   https://doi.org/10.1038/s41612-025-00996-z, 2025.

1676   Minx, J. C., Lamb, W. F., Andrew, R. M., Canadell, J. G., Crippa, M., Döbbeling, N., Forster, P. M., Guizzardi, D.,
1677   Olivier, J., Peters, G. P., Pongratz, J., Reisinger, A., Rigby, M., Saunois, M., Smith, S. J., Solazzo, E., and Tian, H.:
1678   A comprehensive and synthetic dataset for global, regional, and national greenhouse gas emissions by sector 1970–
1679   2018 with an extension to 2019, Earth Syst. Sci. Data, 13, 5213–5252, https://doi.org/10.5194/essd-13-5213-2021,
1680   2021.

1681   NASA: Satellite sea level observations, [data set], https://sealevel.nasa.gov/understanding-sea-level/key-
1682   indicators/global-mean-sea-level/, accessed 19 February 2025, 2025.

1683   Nickolay A. Krotkov, Lok N. Lamsal, Sergey V. Marchenko, Edward A. Celarier, Eric J.Bucsela, William H. Swartz,

1684   Joanna Joiner and the OMI core team, OMI/Aura NO2 Cloud-Screened Total and Tropospheric Column L3 Global

1685   Gridded 0.25 degree x 0.25 degree V3, NASA Goddard Space Flight Center, Goddard Earth Sciences Data and

1686   Information   Services   Center   (GES   DISC),   Accessed: [Data   Access   22   April   2024],

1687   https://doi.org/10.5067/Aura/OMI/DATA3007, 2019. Nisbet, E. G., Manning, M. R., Dlugokencky, E. J., Michel, S.

1688   E., Lan, X., Roeckmann, T., Gon, H. A. D. V. D., Palmer, P., Oh, Y., Fisher, R., Lowry, D., France, J. L., and White,

1689   J. W. C.: Atmospheric methane: Comparison between methane's record in 2006-2022 and during glacial terminations,

1690   Preprints, https://doi.org/10.22541/essoar.167689502.25042797/v1, 2023.

1691   Nitzbon, J., Krinner, G., Langer, M.: GCOS EHI 1960-2020 Permafrost Heat Content, World Data Center for Climate

1692   (WDCC) at DKRZ, https://doi.org/10.26050/WDCC/GCOS_EHI_1960-2020_PHC, 2022.

1693   NOAA: Global   sea   level   timeseries,

1694   https://www.star.nesdis.noaa.gov/socd/lsa/SeaLevelRise/LSA_SLR_timeseries.php , [data set], accessed 19 February

1695   2025, 2025.

1696   Palmer, M. D. and McNeall, D. J.: Internal variability of Earth's energy budget simulated by CMIP5 climate models,

1697   Environ. Res. Lett., 9, 034016, https://doi.org/10.1088/1748-9326/9/3/034016, 2014.

1698   Palmer, M. D., Domingues, C. M., Slangen, A. B. A., and Boeira Dias, F.: An ensemble approach to quantify global

1699   mean sea-level rise over the 20th century from tide gauge reconstructions, Environ. Res. Lett., 16, 044043,

1700   https://doi.org/10.1088/1748-9326/abdaec, 2021.

1701   Peng, S., Lin, X., Thompson, R. L., Xi, Y., Liu, G., Hauglustaine, D., Lan, X., Poulter, B., Ramonet, M., Saunois, M.,

1702   Yin, Y., Zhang, Z., Zheng, B., and Ciais, P.: Wetland emission and atmospheric sink changes explain methane growth

1703   in 2020, Nature, 612, 477–482, https://doi.org/10.1038/s41586-022-05447-w, 2022.

1704   Pelz, S., Ganti, G., Lamboll, R., Grant, L., Smith, C., Pachauri, S., Rogelj, J., Riahi, K., Thiery, W., and Gidden, M.

1705   J.: Using net-zero carbon debt to track climate overshoot responsibility, Proc. Natl. Acad. Sci. U.S.A., 122,

1706   e2409316122, https://doi.org/10.1073/pnas.2409316122, 2025.

1707   Pirani, A., Alegria, A., Khourdajie, A. A., Gunawan, W., Gutiérrez, J. M., Holsman, K., Huard, D., Juckes, M.,

1708   Kawamiya, M., Klutse, N., Krey, V., Matthews, R., Milward, A., Pascoe, C., Van Der Shrier, G., Spinuso, A.,

1709   Stockhause, M., and Xiaoshi Xing: The implementation of FAIR data principles in the IPCC AR6 assessment process,

1710   https://doi.org/10.5281/ZENODO.6504469, 2022.

1711   Pongratz, J., Schwingshackl, C., Bultan, S., Obermeier, W., Havermann, F., and Guo, S.: Land Use Effects on Climate:

1712   Current   State,   Recent   Progress,   and   Emerging   Topics,   Curr.   Clim.   Change   Rep.,   7,   99–120,

1713   https://doi.org/10.1007/s40641-021-00178-y, 2021.

1714   Prinn, R. G., Weiss, R. F., Arduini, J., Arnold, T., DeWitt, H. L., Fraser, P. J., Ganesan, A. L., Gasore, J., Harth, C.

1715   M., Hermansen, O., Kim, J., Krummel, P. B., Li, S., Loh, Z. M., Lunder, C. R., Maione, M., Manning, A. J., Miller,

1716   B. R., Mitrevski, B., Mühle, J., O'Doherty, S., Park, S., Reimann, S., Rigby, M., Saito, T., Salameh, P. K., Schmidt,

1717   R., Simmonds, P. G., Steele, L. P., Vollmer, M. K., Wang, R. H., Yao, B., Yokouchi, Y., Young, D., and Zhou, L.:

History of chemically and radiatively important atmospheric gases from the Advanced Global Atmospheric Gases Experiment (AGAGE), Earth Syst. Sci. Data, 10, 985–1018, https://doi.org/10.5194/essd-10-985-2018, 2018.

Purich, A. and Doddridge, E. W.: Record low Antarctic sea ice coverage indicates a new sea ice state, Commun Earth Environ, 4, 314, https://doi.org/10.1038/s43247-023-00961-9, 2023.

Quaas, J., Jia, H., Smith, C., Albright, A. L., Aas, W., Bellouin, N., Boucher, O., Doutriaux-Boucher, M., Forster, P. M., Grosvenor, D., Jenkins, S., Klimont, Z., Loeb, N. G., Ma, X., Naik, V., Paulot, F., Stier, P., Wild, M., Myhre, G., and Schulz, M.: Robust evidence for reversal of the trend in aerosol effective climate forcing, Atmos. Chem. Phys., 22, 12221–12239, https://doi.org/10.5194/acp-22-12221-2022, 2022.

Qin, Z., Zhu, Y., Canadell, J. G., Chen, M., Li, T., Mishra, U., and Yuan, W.: Global spatially explicit carbon emissions from land-use change over the past six decades (1961–2020), One Earth, 7, 835–847, https://doi.org/10.1016/j.oneear.2024.04.002, 2024.

Raghuraman, S.P., Paynter, D. and Ramaswamy, V.: Anthropogenic forcing and response yield observed positive trend in Earth's energy imbalance, Nat. Commun. 12, 4577, https://doi.org/10.1038/s41467-021-24544-4, 2021.

Raghuraman, S. P., Soden, B., Clement, A., Vecchi, G., Menemenlis, S., and Yang, W.: The 2023 global warming spike was driven by the El Niño–Southern Oscillation, Atmos. Chem. Phys., 24, 11275–11283, https://doi.org/10.5194/acp-24-11275-2024, 2024.

Ribes, A., Qasmi, S., and Gillett, N. P.: Making climate projections conditional on historical observations, Sci. Adv., 7, eabc0671, https://doi.org/10.1126/sciadv.abc0671, 2021.

Rogelj, J., D. Shindell, K. Jiang, S. Fifita, P. Forster, V. Ginzburg, C. Handa, H. Kheshgi, S. Kobayashi, E. Kriegler, L. Mundaca, R. Séférian, and M. V. Vilariño: Mitigation Pathways Compatible with 1.5°C in the Context of Sustainable Development. In: Global Warming of 1.5°C. An IPCC Special Report on the impacts of global warming of 1.5°C above pre-industrial levels and related global greenhouse gas emission pathways, in the context of strengthening the global response to the threat of climate change, sustainable development, and efforts to eradicate poverty [Masson-Delmotte, V., P. Zhai, H.-O. Pörtner, D. Roberts, J. Skea, P.R. Shukla, A. Pirani, W. Moufouma-Okia, C. Péan, R. Pidcock, S. Connors, J. B. R. Matthews, Y. Chen, X. Zhou, M. I. Gomis, E. Lonnoy, T. Maycock, M. Tignor, and T. Waterfield (eds.)]. Cambridge University Press, Cambridge, UK and New York, NY, USA, pp. 93-174, https://doi.org/10.1017/9781009157940.004, 2018.

Rogelj, J., Forster, P. M., Kriegler, E., Smith, C. J., and Séférian, R.: Estimating and tracking the remaining carbon budget for stringent climate targets, Nature, 571, 335–342, https://doi.org/10.1038/s41586-019-1368-z, 2019.

Rogelj, J., Lamboll, R.D.: Substantial reductions in non-CO2 greenhouse gas emissions reductions implied by IPCC estimates of the remaining carbon budget. Communications Earth Environ 5, 35. https://doi.org/10.1038/s43247-023-01168-8, 2024.

Rogelj, J., Rao, S., McCollum, D. L., Pachauri, S., Klimont, Z., Krey, V., and Riahi, K: Air-pollution emission ranges consistent with the representative concentration pathways, Nature Clim. Chang., 4 (6), 446–450, https://doi.org/10.1038/nclimate2178, 2014.

Rohde, R., Muller, R., Jacobsen, R., Perlmutter, S., Rosenfeld, A. et al.: Berkeley Earth Temperature Averaging Process, Geoinfor. Geostat.: An Overview 1:2., http://dx.doi.org/10.4172/gigs.1000103, 2013.

Saunois, M., Stavert, A. R., Poulter, B., Bousquet, P., Canadell, J. G., Jackson, R. B., Raymond, P. A., Dlugokencky, E. J., Houweling, S., Patra, P. K., Ciais, P., Arora, V. K., Bastviken, D., Bergamaschi, P., Blake, D. R., Brailsford, G., Bruhwiler, L., Carlson, K. M., Carrol, M., Castaldi, S., Chandra, N., Crevoisier, C., Crill, P. M., Covey, K., Curry, C. L., Etiope, G., Frankenberg, C., Gedney, N., Hegglin, M. I., Höglund-Isaksson, L., Hugelius, G., Ishizawa, M., Ito, A., Janssens-Maenhout, G., Jensen, K. M., Joos, F., Kleinen, T., Krummel, P. B., Langenfelds, R. L., Laruelle, G. G., Liu, L., Machida, T., Maksyutov, S., McDonald, K. C., McNorton, J., Miller, P. A., Melton, J. R., Morino, I., Müller, J., Murguia-Flores, F., Naik, V., Niwa, Y., Noce, S., O'Doherty, S., Parker, R. J., Peng, C., Peng, S., Peters, G. P., Prigent, C., Prinn, R., Ramonet, M., Regnier, P., Riley, W. J., Rosentreter, J. A., Segers, A., Simpson, I. J., Shi, H., Smith, S. J., Steele, L. P., Thornton, B. F., Tian, H., Tohjima, Y., Tubiello, F. N., Tsuruta, A., Viovy, N., Voulgarakis, A., Weber, T. S., Van Weele, M., Van Der Werf, G. R., Weiss, R. F., Worthy, D., Wunch, D., Yin, Y., Yoshida, Y., Zhang, W., Zhang, Z., Zhao, Y., Zheng, B., Zhu, Q., Zhu, Q., and Zhuang, Q.: The Global Methane Budget 2000–2017, Earth Syst. Sci. Data, 12, 1561–1623, https://doi.org/10.5194/essd-12-1561-2020, 2020.

Sato, K., Sato, K., Savita, A., Schweiger, A., Shepherd, A., Seneviratne, S. I., Simons, L., Slater, D. A., Slater, T., Steiner, A. K., Suga, T., Szekely, T., Thiery, W., Timmermans, M.-L., Vanderkelen, I., Wjiffels, S. E., Wu, T., and Zemp, M.: GCOS EHI 1960-2020 Earth Heat Inventory Ocean Heat Content (Version 2), https://doi.org/10.26050/WDCC/GCOS_EHI_1960-2020_OHC_v2, 2023b.

Scarpelli, T. R., Jacob, D. J., Grossman, S., Lu, X., Qu, Z., Sulprizio, M. P., Zhang, Y., Reuland, F., Gordon, D., and Worden, J. R.: Updated Global Fuel Exploitation Inventory (GFEI) for methane emissions from the oil, gas, and coal sectors: evaluation with inversions of atmospheric methane observations, Atmos. Chem. Phys., 22, 3235–3249, https://doi.org/10.5194/acp-22-3235-2022, 2022.

Schamm, K., Ziese, M., Becker A., Finger, P., Meyer-Christoffer, A., Schneider, U., Schroder, M., and Stender, P.: Global gridded precipitation over land: a description of the new GPCC First Guess Daily product, Earth Syst. Sci. Data, 6, 49-60. https://doi.org/10.5194/essd-6-49-2014, 2014.

Schmidt, G.: Climate models can't explain 2023's huge heat anomaly — we could be in uncharted territory, Nature, 627, 467–467, https://doi.org/10.1038/d41586-024-00816-z, 2024.

von Schuckmann, K., Cheng, L., Palmer, M. D., Hansen, J., Tassone, C., Aich, V., Adusumilli, S., Beltrami, H., Boyer, T., Cuesta-Valero, F. J., Desbruyères, D., Domingues, C., García-García, A., Gentine, P., Gilson, J., Gorfer, M., Haimberger, L., Ishii, M., Johnson, G. C., Killick, R., King, B. A., Kirchengast, G., Kolodziejczyk, N., Lyman, J., Marzeion, B., Mayer, M., Monier, M., Monselesan, D. P., Purkey, S., Roemmich, D., Schweiger, A., Seneviratne, S. I., Shepherd, A., Slater, D. A., Steiner, A. K., Straneo, F., Timmermans, M.-L., and Wijffels, S. E.: Heat stored in the Earth system: where does the energy go?, Earth Syst. Sci. Data, 12, 2013–2041, https://doi.org/10.5194/essd-12-2013-2020, 2020.

1787 von Schuckmann, K., Minière, A., Gues, F., Cuesta-Valero, F. J., Kirchengast, G., Adusumilli, S., Straneo, F., Ablain,
1788 M., Allan, R. P., Barker, P. M., Beltrami, H., Blazquez, A., Boyer, T., Cheng, L., Church, J., Desbruyeres, D., Dolman,
1789 H., Domingues, C. M., García-García, A., Giglio, D., Gilson, J. E., Gorfer, M., Haimberger, L., Hakuba, M. Z.,
1790 Hendricks, S., Hosoda, S., Johnson, G. C., Killick, R., King, B., Kolodziejczyk, N., Korosov, A., Krinner, G., Kuusela,
1791 M., Landerer, F. W., Langer, M., Lavergne, T., Lawrence, I., Li, Y., Lyman, J., Marti, F., Marzeion, B., Mayer, M.,
1792 MacDougall, A. H., McDougall, T., Monselesan, D. P., Nitzbon, J., Otosaka, I., Peng, J., Purkey, S., Roemmich, D.,
1793 Sato, K., Sato, K., Savita, A., Schweiger, A., Shepherd, A., Seneviratne, S. I., Simons, L., Slater, D. A., Slater, T.,
1794 Steiner, A. K., Suga, T., Szekely, T., Thiery, W., Timmermans, M.-L., Vanderkelen, I., Wjiffels, S. E., Wu, T., and
1795 Zemp, M.: Heat stored in the Earth system 1960–2020: where does the energy go?, Earth System Science Data, 15,
1796 1675–1709, https://doi.org/10.5194/essd-15-1675-2023, 2023a.

1797 von Schuckmann, K., Minière, A., Gues, F., Cuesta-Valero, F. J., Kirchengast, G., Adusumilli, S., Straneo, F., Ablain,
1798 M., Allan, R. P., Barker, P. M., Beltrami, H., Blazquez, A., Boyer, T., Cheng, L., Church, J., Desbruyeres, D., Dolman,
1799 H., Domingues, C. M., García-García, A., Giglio, D., Gilson, J. E., Gorfer, M., Haimberger, L., Hakuba, M. Z.,
1800 Hendricks, S., Hosoda, S., Johnson, G. C., Killick, R., King, B., Kolodziejczyk, N., Korosov, A., Krinner, G., Kuusela,
1801 M., Landerer, F. W., Langer, M., Lavergne, T., Lawrence, I., Li, Y., Lyman, J., Marti, F., Marzeion, B., Mayer, M.,
1802 MacDougall, A. H., McDougall, T., Monselesan, D. P., Nitzbon, J., Otosaka, I., Peng, J., Purkey, S., Roemmich, D.,

1803 Schoeberl, M. R., Wang, Y., Taha, G., Zawada, D. J., Ueyama, R., and Dessler, A.: Evolution of the Climate Forcing
1804 During the Two Years After the Hunga Tonga-Hunga Ha'apai Eruption, JGR Atmospheres, 129, e2024JD041296,
1805 https://doi.org/10.1029/2024JD041296, 2024.

1806 Schwingshackl, C., Obermeier, W. A., Bultan, S., Grassi, G., Canadell, J. G., Friedlingstein, P., Gasser, T., Houghton,
1807 R. A., Kurz, W. A., Sitch, S., and Pongratz, J.: Differences in land-based mitigation estimates reconciled by separating
1808 natural and land-use CO2 fluxes at the country level, One Earth, 5, 1367–1376,
1809 https://doi.org/10.1016/j.oneear.2022.11.009, 2022.

1810 Seneviratne, S.I., X. Zhang, M. Adnan, W. Badi, C. Dereczynski, A. Di Luca, S. Ghosh, I. Iskandar, J. Kossin, S.
1811 Lewis, F. Otto, I. Pinto, M. Satoh, S. M. Vicente-Serrano, M. Wehner, and B. Zhou: Weather and Climate Extreme
1812 Events in a Changing Climate. In Climate Change 2021: The Physical Science Basis. Contribution of Working Group
1813 I to the Sixth Assessment Report of the Intergovernmental Panel on Climate Change [Masson-Delmotte, V., P. Zhai,
1814 A. Pirani, S.L. Connors, C. Péan, S. Berger, N. Caud, Y. Chen, L. Goldfarb, M.I. Gomis, M. Huang, K. Leitzell, E.
1815 Lonnoy, J.B.R. Matthews, T.K. Maycock, T. Waterfield, O. Yelekçi, R. Yu, and B. Zhou (eds.)]. Cambridge
1816 University Press, Cambridge, United Kingdom and New York, NY, USA, pp. 1513–1766,
1817 doi:10.1017/9781009157896.013.1513–1766, https://doi.org/10.1017/9781009157896.013, 2021.

1818 Seo, K.-W., Ryu, D., Jeon, T., Youm, K., Kim, J.-S., Oh, E. H., Chen, J., Famiglietti, J. S., and Wilson, C. R.: Abrupt
1819 sea level rise and Earth's gradual pole shift reveal permanent hydrological regime changes in the 21st century, Science,
1820 387, 1408–1413, https://doi.org/10.1126/science.adq6529, 2025.

1821 Sherwin, E. D., Rutherford, J. S., Zhang, Z., Chen, Y., Wetherley, E. B., Yakovlev, P. V., Berman, E. S. F., Jones, B.
1822 B., Cusworth, D. H., Thorpe, A. K., Ayasse, A. K., Duren, R. M., and Brandt, A. R.: US oil and gas system emissions

from nearly one million aerial site measurements, Nature, 627, 328–334, https://doi.org/10.1038/s41586-024-07117-5, 2024.

Simmonds, P. G., Rigby, M., McCulloch, A., O'Doherty, S., Young, D., Mühle, J., Krummel, P. B., Steele, P., Fraser, P. J., Manning, A. J., Weiss, R. F., Salameh, P. K., Harth, C. M., Wang, R. H. J., and Prinn, R. G.: Changing trends and emissions of hydrochlorofluorocarbons (HCFCs) and their hydrofluorocarbon (HFCs) replacements, Atmos. Chem. Phys., 17, 4641–4655, https://doi.org/10.5194/acp-17-4641-2017, 2017.

Sippel, S., Zscheischler, J., Heimann, M., Otto, F. E. L., Peters, J., and Mahecha, M. D.: Quantifying changes in climate variability and extremes: Pitfalls and their overcoming, Geophys. .Res. Lett., 42, 9990–9998, https://doi.org/10.1002/2015GL066307, 2015.

Smith, C., Walsh, T., Gillett, N., Hall, B., Hauser, M., Krummel, P., Lamb, W., Lamboll, R., Muhle, J., Palmer, M., Ribes, A., Seneviratne, S., Trewin, B., von Schuckmann, K., and Forster, P.: ClimateIndicator/data: Indicators of Global Climate Change 2024 submission (v2025.05.02), [Data set], https://doi.org/10.5281/zenodo.15327155, 2025a.

Smith, C., Walsh, T., Gillett, N., Hall, B., Hauser, M., Krummel, P., Lamb, W., Lamboll, R., X., Muhle, J., Palmer, M., Ribes, A., Seneviratne, S., Trewin, B., von Schuckmann, K., and Forster, P.: Data repository for Indicators of Global Climate Change, Github [code], https://github.com/ClimateIndicator/data/tree/v2025.05.02, last access: 2 May 2025, 2025b

Smith, C., Nicholls, Z. R. J., Armour, K., Collins, W., Forster, P., Meinshausen, M., Palmer, M. D., and Watanabe, M.: The Earth's Energy Budget, Climate Feedbacks, and Climate Sensitivity Supplementary Material, in: Climate Change 2021: The Physical Science Basis. Contribution of Working Group I to the Sixth Assessment Report of the Intergovernmental Panel on Climate Change, edited by: Masson-Delmotte, V., Zhai, P., Pirani, A., Connors, S. L., Péan, C., Berger, S., Caud, N., Chen, Y., Goldfarb, L., Gomis, M. I., Huang, M., Leitzell, K., Lonnoy, E., Matthews, J. B. R., Maycock, T. K., Waterfield, T., Yelekçi, O., Yu, R., and Zhou, B., 2021.

Smith, S. J., van Aardenne, J., Klimont, Z., Andres, R. J., Volke, A., and Delgado Arias, S.: Anthropogenic sulfur dioxide emissions: 1850–2005, Atmos. Chem. and Phys., 11, 1101–1116, https://doi.org/10.5194/acp-11-1101-2011, 2011.

Soulie, A., C. Granier, S. Darras, N. Zilbermann, T. Doumbia, M. Guevara, J.-P. Jalkanen, S. Keita, C. Liousse, M. Crippa, D. Guizzardi, R. Hoesly, S. J. Smith Global Anthropogenic Emissions (CAMS-GLOB-ANT) for the Copernicus Atmosphere Monitoring Service Simulations of Air Quality Forecasts and Reanalyses Earth Syst. Sci. Data, 2023.

Storto, A. and Yang, C.: Acceleration of the ocean warming from 1961 to 2022 unveiled by large-ensemble reanalyses, Nature Communications, 15, 545, https://doi.org/10.1038/s41467-024-44749-7, 2024.

Szopa, S., V. Naik, B. Adhikary, P. Artaxo, T. Berntsen, W.D. Collins, S. Fuzzi, L. Gallardo, A. Kiendler-Scharr, Z. Klimont, H. Liao, N. Unger, and P. Zanis: Short-Lived Climate Forcers. In Climate Change 2021: The Physical Science Basis. Contribution of Working Group I to the Sixth Assessment Report of the Intergovernmental Panel on

Climate Change [Masson-Delmotte, V., P. Zhai, A. Pirani, S.L. Connors, C. Péan, S. Berger, N. Caud, Y. Chen, L. Goldfarb, M.I. Gomis, M. Huang, K. Leitzell, E. Lonnoy, J.B.R. Matthews, T.K. Maycock, T. Waterfield, O. Yelekçi, R. Yu, and B. Zhou (eds.)]. Cambridge University Press, Cambridge, United Kingdom and New York, NY, USA, pp. 817–922, https://doi:10.1017/9781009157896.008, 2021.

Terhaar, J., Vogt, L., and Foukal, N. P.: Atlantic overturning inferred from air-sea heat fluxes indicates no decline since the 1960s, Nat Commun, 16, 222, https://doi.org/10.1038/s41467-024-55297-5, 2025.

Trewin, B.: Assessing Internal Variability of Global Mean Surface Temperature From Observational Data and Implications for Reaching Key Thresholds, JGR Atmospheres, 127, e2022JD036747, https://doi.org/10.1029/2022JD036747, 2022.

Tibrewal, K., Ciais, P., Saunois, M., Martinez, A., Lin, X., Thanwerdas, J., Deng, Z., Chevallier, F., Giron, C., Albergel, C., Tanaka, K., Patra, P., Tsuruta, A., Zheng, B., Belikov, D., Niwa, Y., Janardanan, R., Maksyutov, S., Segers, A., Tzompa-Sosa, Z. A., Bousquet, P., and Sciare, J.: Assessment of methane emissions from oil, gas and coal sectors across inventories and atmospheric inversions, Communications Earth & Environment, 5, 26, https://doi.org/10.1038/s43247-023-01190-w, 2024.

Vakilifard, N., Williams, R. G., Holden, P. B., Turner, K., Edwards, N. R., and Beerling, D. J.: Impact of negative and positive CO_2 emissions on global warming metrics using an ensemble of Earth system model simulations, Biogeosciences, 19, 4249–4265, https://doi.org/10.5194/bg-19-4249-2022, 2022.

Vanderkelen, I. and Thiery, W.: GCOS EHI 1960-2020 Inland Water Heat Content, https://doi.org/10.26050/WDCC/GCOS_EHI_1960-2020_IWHC, 2022.

Vimont, I. J, B. D. Hall, G. Dutton, S. A. Montzka, J. Mühle, M. Crotwell, K. Petersen, S. Clingan, and D. Nance, [in "State of the Climate in 2022"]. Bull. Amer. Meteor. Soc., 104 , 9, S76–S78, https://doi.org/10.1175/BAMS-D-23-0090.1., 2022.

Vollmer, M. K., Young, D., Trudinger, C. M., Mühle, J., Henne, S., Rigby, M., Park, S., Li, S., Guillevic, M., Mitrevski, B., Harth, C. M., Miller, B. R., Reimann, S., Yao, B., Steele, L. P., Wyss, S. A., Lunder, C. R., Arduini, J., McCulloch, A., Wu, S., Rhee, T. S., Wang, R. H. J., Salameh, P. K., Hermansen, O., Hill, M., Langenfelds, R. L., Ivy, D., O'Doherty, S., Krummel, P. B., Maione, M., Etheridge, D. M., Zhou, L., Fraser, P. J., Prinn, R. G., Weiss, R. F., and Simmonds, P. G.: Atmospheric histories and emissions of chlorofluorocarbons CFC-13 (CClF3), ΣCFC-114 (C2Cl2F4), and CFC-115 (C2ClF5), Atmos. Chem. Phys., 18, 979–1002, https://doi.org/10.5194/acp-18-979-2018, 2018.

Watson-Parris, D., Christensen, M. W., Laurenson, A., Clewley, D., Gryspeerdt, E., and Stier, P.: Shipping regulations lead to large reduction in cloud perturbations, Proc. Natl. Acad. Sci. U.S.A., 119, e2206885119, https://doi.org/10.1073/pnas.2206885119, 2022.

WCRP Global Sea Level Budget Group: Global sea-level budget 1993–present, Earth Syst. Sci. Data, 10, 1551–1590, https://doi.org/10.5194/essd-10-1551-2018, 2018.

1891 Western, L. M., Vollmer, M. K., Krummel, P. B., Adcock, K. E., Fraser, P. J., Harth, C. M., Langenfelds, R. L.,
1892 Montzka, S. A., Mühle, J., O'Doherty, S., Oram, D. E., Reimann, S., Rigby, M., Vimont, I., Weiss, R. F., Young, D.,
1893 and Laube, J. C.: Global increase of ozone-depleting chlorofluorocarbons from 2010 to 2020, Nat. Geosci., 16, 309–
1894 313, https://doi.org/10.1038/s41561-023-01147-w, 2023.

1895 Western, L. M., Daniel, J. S., Vollmer, M. K., Clingan, S., Crotwell, M., Fraser, P. J., Ganesan, A. L., Hall, B., Harth,
1896 C. M., Krummel, P. B., Mühle, J., O'Doherty, S., Salameh, P. K., Stanley, K. M., Reimann, S., Vimont, I., Young,
1897 D., Rigby, M., Weiss, R. F., Prinn, R. G., and Montzka, S. A.: A decrease in radiative forcing and equivalent effective
1898 chlorine from hydrochlorofluorocarbons, Nat. Clim. Chang., 14, 805–807, https://doi.org/10.1038/s41558-024-02038-
1899 7, 2024.

1900 van der Werf, G. R., Randerson, J. T., Giglio, L., van Leeuwen, T. T., Chen, Y., Rogers, B. M., Mu, M., van Marle,
1901 M. J. E., Morton, D. C., Collatz, G. J., Yokelson, R. J., and Kasibhatla, P. S.: Global fire emissions estimates during
1902 1997–2016, Earth System Science Data, 9, 697–720, https://doi.org/10.5194/essd-9-697-2017, 2017.

1903 Wild, M., Gilgen, H., Roesch, A., Ohmura, A., Long, C. N., Dutton, E. G., Forgan, B., Kallis, A., Russak, V., and
1904 Tsvetkov, A.: From Dimming to Brightening: Decadal Changes in Solar Radiation at Earth's Surface, Science, 308,
1905 847–850, https://doi.org/10.1126/science.1103215, 2005.

1906 World Meteorological Organization (WMO). State of the Global Climate 2024. WMO-No. 1368. 2025. ISBN: 978-
1907 92-63-11368-5.

1908 Xu, Q., Wei, S., Li, Z., and Li, Q.: A New Evaluation of Observed Changes in Diurnal Temperature Range,
1909 Geophysical Research Letters, 52, e2024GL113406, https://doi.org/10.1029/2024GL113406, 2025.

1910 Zickfeld, K., Azevedo, D., Mathesius, S., and Matthews, H. D.: Asymmetry in the climate–carbon cycle response to
1911 positive and negative CO2 emissions, Nat. Clim. Chang., 11, 613–617, https://doi.org/10.1038/s41558-021-01061-2,
1912 2021.

1913 Zhang, Z., Poulter, B., Feldman, A.F., Ying, Q., Ciais, P., Peng, S. and Xin, L.: Recent intensification of wetland
1914 methane feedback, Nat. Clim. Chang. 13, 430–433, https://doi.org/10.1038/s41558-023-01629-0, 2023.

1915